RUNOFF SIMULATION IN THE CANAGAGIGUE CREEK WATERSHED USING THE MIKE SHE MODEL

by

Shalini Oogathoo

Department of Bioresource Engineering
Faculty of Agricultural and Environmental Sciences
McGill University
Montreal, Canada

August, 2006

A thesis submitted to McGill University
in partial fulfillment of the requirements for the degree of

Master of Science

Your file Votre référence
ISBN: 978-0-494-32766-1
Our file Notre référence
ISBN: 978-0-494-32766-1

ABSTRACT

The Canagagigue Creek watershed, located in the Grand River Basin, is one of the fastest developing areas in Ontario. The watershed hydrology has changed considerably due to the increased anthropogenic activities, producing frequent floods and droughts as well as water quality problems. MIKE SHE, a watershed-scale model, was used to simulate surface runoff from the Canagagigue Creek watershed. Various management scenarios affecting the surface hydrology were also evaluated. The model was calibrated for four years (1994-95 to 1997-98) and validated for another four years (1990-91 to 1993-94). For the calibration period, the correlation between the observed and simulated daily runoff was satisfactory, as shown by the coefficient of determination value of 0.59. The coefficient of determination was 0.44 for the validation period. The Nash-Sutcliffe coefficients obtained were 59% and 40% for the calibration and validation period, respectively. Use of daily input data together with a simplistic snowmelt routine, was found to affect model performance during the winter/spring period. Henceforth, model performance can be greatly improved by adopting a more comprehensive method for simulating snowmelt and incorporating the frozen soil conditions. Overall, the model was able to simulate surface runoff reasonably well on annual, seasonal, monthly, and daily intervals, representing all the hydrological components adequately.

With the various management scenarios simulated, it was found that the deforestation scenario considerably increased the total flow (11%). On the other hand, the high runoff peaks were decreased and low flows were increased considerably in the application of the tile drainage scenario. It was also observed that surface flow increased in wet years and decreased in normal and dry years in the climate change scenario. Though impacts of certain scenarios were almost negligible, their effects were significant when associated with the percentage area under transformation. Hence, it was concluded that the model can be used to simulate various management scenarios to solve hydrologic problems in the Southern Ontario climatic condition.

RÉSUMÉ

Le basin versant du Ruisseau Canagagigue, situé dans celui la rivière Grande, est parmi les régions le plus développées en Ontario, Canada. Dû à l'intervention humaine, l'état hydrologique de ce basin versant a changé considérablement, produisant plus inondations et sécheresses, aussi que de problèmes de qualité d'eau. Le modèle hydrologigue, MIKE SHE, servit à simuler le ruissellement de surface provenant du bassin versant du Ruisseau Canagagigue. De plus, l'impact sur le procès hydrologigue de divers scénarios de gestion fut évalué. Le modèle fut calibré sur quatre ans (1994-95 à 1997-98) et validé sur quatre ans (1990-91 à 1993-94). Une bonne corrélation entre les ruissellements de surface observés et ceux simulés par le modèle exista pour la période de calibration, tel qu'indiqué par le coefficient de détermination de 0.59. Pour la période de validation, ce coefficient fut de 0.44. Les coefficients Nash-Sutcliffe obtenus pendant les périodes de calibration et validation furent de 59% et 40%, respectivement. L'utilisation de données quotidiennes et d'un mode de simulation de la fonde de neige simplifié limitèrent la performance du modèle. Donc, la performance du modèle serait amélioré par l'utilisation d'une méthode plus robuste de simulation de la fonde des neiges et l'incorporation des propriétés de sols gelés. En général, le modèle a su simuler convenablement le ruissellement de surface au niveau annuel, saisonnier, mensuel et quotidien, en représentant tous les procès hydrologiques adéquatement.

Parmi les divers scénarios simulés par le modèle MIKE SHE, celui du déboisement produit une importante (11%) augmentation du ruissellement de surface. Dans le scénario visant l'implantation de drainage souterrain, les écoulements de pointe élevés furent réduits tandis que les moins élevés augmentèrent considérablement. Sous le scénario de changement climatique, les ruissellements de surface augmentèrent durant l'année humide pour ensuite diminuer durant l'année sèche. Malgré que certains scénarios n'eussent qu'un impact insignifiant, celui-ci fut toutefois important étant donné l'importante superficie transformée. Dorénavant, le modèle pourra servir à simuler divers scénarios afin de résoudre des problèmes hydrologiques dans la région sud de l'Ontario.

ACKNOWLEDGEMENTS

I would like to express my genuine gratitude and appreciation to my thesis supervisor, Dr. Shiv O. Prasher, James McGill professor of McGill University. In spite of his tight schedule, he was able to provide proper guidance, advice and help in this research project. I also really appreciate the confidence he showed in me for launching into a research area which was completely new to me. I am indebted to his understanding and kindness for helping me throughout this study, from beginning to submission of this thesis.

I would also like extend my sincere gratitude to Dr. Ramesh P. Rudra, Professor in School of Engineering at the University of Guelph, Ontario, for the providing the data and giving advice and good suggestions throughout this research work. Also, I would like to thank Dr. Samaresh Das, Post Doctoral fellow in the School of Engineering at the University of Guelph, Ontario. He was a great help in providing data and assisting in sorting out all the problems encountered during this study. I would also like to thank Mrs Maria Loinaz and Mr Patrick Delaney, DHI officials, for providing constant help.

My special thanks go to Dr. R.M. Patel, Research Associate at McGill University, for his major contribution to this research study. He was a great help throughout, always providing good suggestions, advice, proper guidance and showed great patience. My thanks go as well to Dr. Yousef Karimi, Research Associate at McGill University, for helping me at the very beginning of this study. I sincerely thank Dr. Georges T. Dodds, Research Associate at McGill University, for proofreading the thesis.

Finally, I would like to thank all the professors, staff and other individuals in the Bioresource Engineering department who made my stay at the Macdonald Campus a memorable period of my life. Also, I thank all my friends who were with me during these two years, Dr. Marc David Andrade, Yuying Chen, Shadi Dayyani, Dr. Sadia Ehsan, Apurva Gollamudi, Aynur Gunenc, Yaqiong Hu, Hsin-Hui Huang, Azfar Syed Hussain, Jamshid Jazestani, Harjinder Kumar, Dr. Sobha Kunjikutty, Laura Mesones, Mariana Monroy, Abdel Moneim Osman, Fahmida Nilufar, Hossein Saadat, Vidisha Somashekar, Tahir Waheed, and Charlotte Yates. In case I forgot someone, please forgive me.

I would also like to extend my gratitude to the Ministry of Agriculture of Mauritius, for allowing me to do this Master's degree. Also my heartfelt gratitude goes to Dr Manta Nowbuth, Senior Lecturer in Civil Engineering Department, University of Mauritius, for her great advice and inspiration for pursuing this Master's degree. I would also like to thank Mr B. Lalljee, Lecturer in Faculty of Agriculture, University of Mauritius and Dr. Driver, Lecturer in Faculty of Agriculture, University of Mauritius, for supporting me in doing this study. Also my thanks go to my superiors at my previous job, Mr. Chinnappen, Mrs Leckraz, Mr. Sobun and Mr Mungur in the Plant Pathology Division, Ministry of Agriculture, Mauritius.

Last, but not the least, my deepest gratitude and appreciation go to my dearest mum and dad, Mr Preshram Oogathoo and Mrs Dayamanee Oogathoo, for their love and proper guidance in life. Also, I would like to thank my lovely sisters Devika Rani Utchanah, Priya Devi Appadoo and Soma Devi L.Appanah, for always caring for me. Finally, my deepest thanks go to my future husband, Mr Ravin Ramsamy, for his great comprehension, love, and support during this study.

TABLE OF CONTENT

LIST OF FIGURES

LIST OF FIGURES (CONT'D)

LIST OF TABLES

LIST OF SYMBOLS AND ABBREVIATIONS

α :	Curve shape factor in Rosetta Model
l :	Empirical pore tortuosity/connectivity parameter
AD:	Mean deviation
K_s :	Saturated hydraulic conductivity
BF:	Baseflow
D.O.G:	Days of Growth
d:	Day
DD:	Drainage depth
EF%:	Nash and Sutcliffe coefficient
ET:	Actual evapotranspiration
FAO:	Food and Agriculture Organisation
GIS:	Geographic Information System
Kc:	Crop coefficient
LAI:	Leaf area index
M:	Mannings' M, reciprocal of surface roughness coefficient
m:	Month
n:	Curve shape factor in Rosetta Model
n*:	Surface roughness coefficient
O_RO:	Observed runoff
OC:	Overland flow component
P:	Runoff peak
pF_{fc}:	Pressure head at field capacity
pF_w:	Pressure head at wilting point
PPT:	Precipitation
PRC:	Paved runoff coefficient
R^2:	Coefficient of determination
RD:	Rooting depth
Re:	Recharge
RMSE:	Root mean square error

LIST OF SYMBOLS AND ABBREVIATIONS (CONT'D)

RO:	Runoff
S_RO:	Simulated runoff
SZ:	Saturated zone
tc:	Time constant
UZ:	Unsaturated zone
WGS:	World Geographic System
y:	Year
θ_r:	Residual moisture content on volume basis
θ_{sat}:	Saturated moisture content on volume basis

CHAPTER I - INTRODUCTION

1.1 Background

Interacting in a complex manner to influence human lives and activities, soil and water are among the major resources impacting upon the Earth's hydrogeological and biological systems (Singh, 1995). The wide range of land use activities (agriculture, forestry, industrial, commercial, residential and recreational) existing or implemented in watersheds around the world, generate environmental or more localized ecosystem-level imbalances. To cope with the rising food demand under a rapidly increasing world population, the need to develop land and water resources is gaining momentum at an alarming rate. Indeed, in recent decades, the extensive use of these resources has led to dramatic and irreversible changes in the planet's natural cycles and biota. At the watershed level, an efficient, equitable and, most importantly, sustainable development of such resources is a very demanding task.

The Canagagigue Creek, situated in the Grand River basin of south-western Ontario, Canada, has undergone many changes over the centuries, from pristine and productive in late 1700s to sluggish and shallow in early 1900s (Boyd et al., 2000). The acceleration of settlements and development over the Grand River basin has led to both flood and drought problems, and deterioration of water quality (Boyd et al., 2000). Though the basin is naturally rich in nutrients, due to the till plains and clay soils, intensive agricultural activities have resulted in an increased nutrient loads in rivers, leading to eutrophication and low levels of dissolved oxygen (GRCA, 2003; GRCA, 2004). Agricultural non-point source pollution and urbanization have become critical issues regarding water quality, adversely affecting environmental conditions in this and other Ontario watersheds. Presently, the main concern is to sustain the watershed's ability to meet growing demands for water, and maintain water quality for human and wildlife consumption (Boyd et al., 2000; GRCA, 2003; GRCA, 2004).

Singh (1995) mentioned that although agricultural activities are field-based, remedial management practices should be integrated at a watershed scale to attain the ultimate goal of sustainable resource utilization. Before launching new activities within a

watershed or incorporating any remedial measures, it is vital for decision-makers and planners to evaluate the consequences of these acts. The impact of any given set of activities can be investigated by conducting field experiments; however, such experiments tend to be laborious, time-consuming, and expensive. Technological and scientific advances have enabled with some degree of accuracy the assessment and prediction of effects of alternative land use activities on watersheds through computer modeling techniques.

Modeling is a potentially efficient tool, widely used in the soil and water management field. Thompson et al. (2004) stated that "it is fast and less expensive for the evaluation of different management strategies, avoiding undesirable outcomes and targeting the often-limited resources available to watershed management authorities and conservation practitioners". Such models allow the consideration and holistic analysis of different kinds of information in the study of very complex problems (Sorooshian and Gupta, 1995). However, even the simpler hydrological models (e.g., rainfall-runoff models) used in the last few decades, are quite demanding in terms of hydro-meteorological data. These models are effective mostly at a smaller scale, and do not incorporate the option for evaluating the impacts of different land use scenarios (Abbott et al., 1986a). Given the high cost of water resource development, a novel approach to hydrological modeling arose to optimize watershed management planning.

Shrestha et al. (2005) mentioned that "in addressing non-point source pollution, watershed-scale models are considered cost-effective and time-efficient tools for the simulation of watershed processes, assessment of pollutant loads and management practices". These models are becoming a valued tool in developing environmental regulations (e.g. total maximum daily loads), generating development options, and assessing which potential environment impacts need to be most rigorously evaluated for an optimally sustainable exploitation of water resources (Abbott et al., 1986b; Johnson et al., 2003).

Compared to other empirical model types, physically-based models do not require long hydro-meteorological records for their calibration since their input parameters are directly related to the watershed's physical characteristics (i.e., topography, soil types,

vegetation and geology; Abbott et al., 1986a). Physically-based distributed models allow the inclusion of spatial variability of physical characteristics and meteorological conditions compared to lumped models (Sahoo et al., 2006). Accurate information on hydrological parameters is a basic requirement for efficient modeling of watershed hydrologic response and pollutant or sediment transport. Of the many models available, most are field-scale models, which function either for a single precipitation/runoff event (AGNPS, ANSWERS, etc.) or allow continuous simulation (SWAT and HSPF, etc.). Moreover, some models are empirical (AnnAGNPS) and others lumped (HSPF; Borah and Bera, 2003).

MIKE SHE is a watershed model that is physically-based, fully distributed and incorporates both single-event and continuous simulation. The model's flexible structure, distributed nature and ability to employ physical laws (*vs.* an empirical relationship) in the interpretation of hydrological processes, provides significant advantages over existing hydrological models, over a wide range of applications (Abbott et al.,1986a). MIKE SHE is also unique, in that it is the only watershed model that integrates surface, subsurface and groundwater flow, something which other models do not. Furthermore, baseflow, an important component of streamflow during the dry season, is simulated by MIKE SHE, whereas other models either ignore it, or employ simplistic methods to estimate it. Consequently, in order to model watershed hydrologic response and assess the impacts of different management practices in south-western Ontario's Canagagigue Creek watershed, the MIKE SHE model was chosen.

1.2 OBJECTIVES

The aims of this study were:

1. To evaluate the ability and applicability of MIKE SHE, a physically-based, watershed-scale model, for simulating hydrology in the Canagagigue Creek watershed in Ontario, Canada;
2. To assess the impact of different land use practices on the hydrologic response of the watershed.

1.3 SCOPE OF STUDY

The MIKE SHE model has the ability to simulate the total streamflow that includes direct flow and baseflow. Many models either do not simulate, or use simplistic methods, to determine the baseflow. The model also considers various land uses and soil types in the simulation, allowing evaluation of different management scenarios. Besides, MIKE SHE considers all other major hydrological components as well. Since this study was directed to the simulation of surface runoff including baseflow, MIKE SHE appeared to be suitable model.

Due to non-availability of river data (such as river cross-section and river bed elevation at different points in a river/channel), the MIKE 11 model was not used. In addition, very simple and fuzzy logic is used for simulating macropore flow and the subsurface drainage; hence these options were not used.

MIKE SHE model was used to simulate overland flow from Canagagigue Creek watershed in Southern Ontario. The climate data was obtained from one station, Waterloo Wellington A station, which was located near the watershed. Due to unavailability of field data, the Rosetta model was used to determine soil parameters based on percentage of sand, silt and clay. The land cover information (leaf area index, rooting depth and crop coefficient) were obtained from literature. In addition, the initial water table depth and the depth to impermeable layer were chosen at an arbitrary level due to lack of information. Overall, the study was limited to only one watershed in the Canadian climate. Thus, before drawing any concrete conclusions about the model's applicability in broader terms, it should be tested on other watersheds in Central Canada as well.

CHAPTER II - LITERATURE REVIEW

This chapter provides a review of the literature on hydrologic modeling, particularly with regards to the hydrologic cycle, watershed hydrology, watershed modeling, and watershed models. The review on watershed models is more exhaustive because this is the main topic of this research project.

2.1 HYDROLOGIC CYCLE

The schematic diagram of the hydrologic processes is presented in Figure 2.1. As mentioned in Schwab et al. (1993), precipitation falls upon the Earth's surface as rain, snow, sleet or hail. Part of the precipitation evaporates to some extent or totally before reaching the soil surface, particularly in the case of water intercepted by vegetation. Water reaching the soil surface may infiltrate into the soil, evaporate or flow over the surface as runoff. Evaporation can occur at the soil surface, free water bodies or within the stomata's of leaves (via transpiration process). Part of the water in the soil percolates to the saturated zone as recharge, where it seeps back to streams and rivers as base flow and eventually to the ocean (Schwab et al., 1993).

2.2 WATERSHED HYDROLOGY

Different components of water balance in a watershed are shown in Figure 2.2. A watershed, delineated by a topographic or groundwater divide, is defined as the land area contributing surface runoff into a stream or to any point of interest (Chow et al., 1988; Dingman, 2002; Warren and Gary, 2003). Usually, one watershed can consists of several sub-watersheds or can be a part of a larger watershed or river basin. The characteristics of a watershed (topography, geology and land cover) play an important role in determining the quantity, quality and timing of stream flow at its outlet as well as of groundwater outflow. Theoretical representation of watershed hydrology is mostly based on physical laws, particularly those of conservation of mass, Newton's laws of motion and the law of thermodynamics. The assumption is that the amount of water

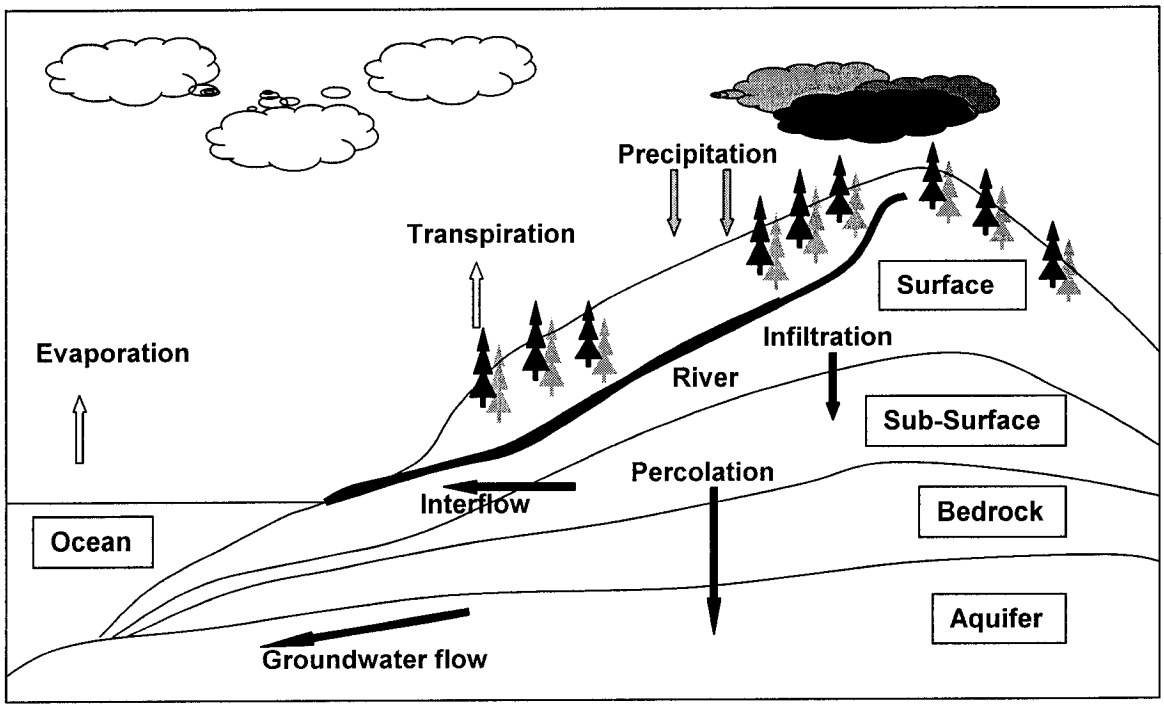

Figure 2.1 Schematic representation of the hydrologic cycle (Adopted from Ward and Trimble, 1995)

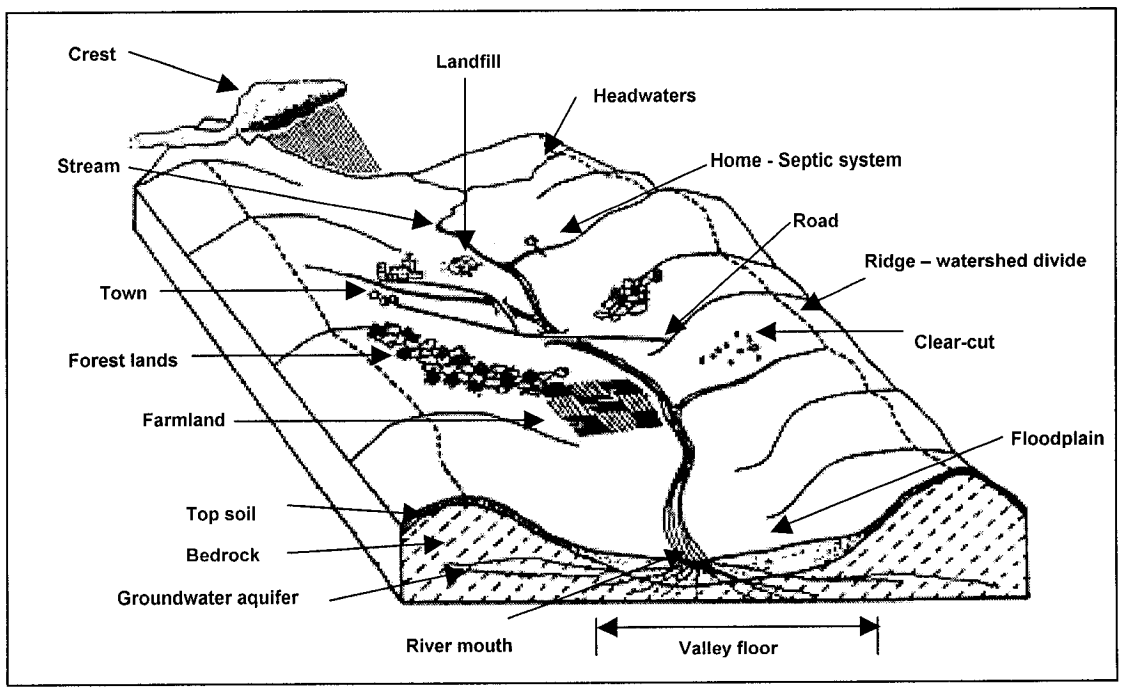

Figure 2.2 Schematic representation of a watershed system (Adopted from AGWA. 2004)

entering a watershed is equal to the amount of water leaving the watershed plus the net change in storage in the watershed that is:

Input – Output = Net Change in Storage (2.1)

2.2.1 Water Resource Problems

Figure 2.3 shows the global hydrological cycle and how water is distributed on the Earth. Clarke (1993) stated that "Besides coal, water is the most fundamental substance making life possible on our planet". Existing virtually everywhere, from the global hydrological system to the biological cell, water is the only resource that does not have any substitute.

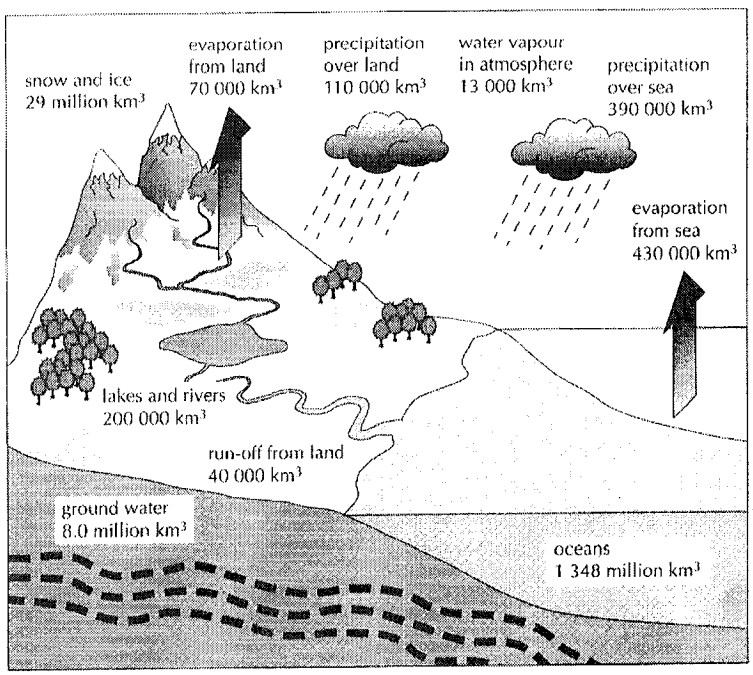

Figure 2.3 The global hydrological cycle (Clarke, 1993)

Though the world's estimated runoff (4×10^{13} m^3) is sufficient to support ten times the world's current population, localized water shortages exist due to the uneven distribution of water over the Earth's landmasses (Clarke, 1993). Given that it is a fragile and increasingly scarce resource in many parts of the world, its efficient and optimal use is crucial to human survival. While most water shortages are related to climate, shortages can also be caused or exacerbated by anthropogenic activities such as deforestation, intensive agriculture, over-grazing and increased population relying on a finite resource (Clarke, 1993). Besides water shortage problems, human activities can result in problems of excess water (flooding) and/or poor water quality. Overall, whether it is droughts or

floods, anthropogenic interventions have tended to worsen the impacts of these natural calamities (Clarke, 1993).

2.2.1.1 Water Shortage - Drought

Clarke (1993) stated that drought mostly occurs in low-rainfall areas or semi-arid regions of the world. However, through the degradation of the natural environments, anthropogenic activities can alter the climate, which can, in turn, cause drought in certain areas. For example, deforestation reduces the on-site rainfall depth, number of rainfall events, and ground water recharge, while concomitantly increasing surface runoff. Similarly, increased dust suspended in the atmosphere will reduce rainfall. Greenhouse gases released into the atmosphere are affecting atmospheric temperature, eventually increasing rainfall intensities in some places, changing storm patterns and raising sea levels. Many countries, such as Indonesia (1982-1983), the eastern half of Australia, California (1976-1977), India (1982-1983), southern and eastern Africa, and some parts of Europe (1989-1990), have recently faced severe drought problems. Proper allocation of water for different uses is becoming an issue in regions facing water shortages. In many countries, to meet water demands, groundwater is being exploited for domestic, industrial and irrigation purposes in a non-rational manner, where usage exceeds water replenishment through precipitation and/or groundwater recharge. Irrigated croplands represent 17% of the world's agricultural lands. In the United States, where 20% of irrigated croplands are fed by groundwater, the abstraction rate generally exceed that of replenishment. Such practices led to 0.15 m yr^{-1} lowering of water tables during the early 1980s, ultimately reducing the area of irrigated land by roughly 30% (Clarke, 1993).

2.2.1.2 Excess Water - Flooding

Among all natural calamities, floods account for the greatest percentage of deaths: roughly 40% (Clarke, 1993). Over recent decades, flooding, ascribed to a number of factors, including rising sea levels and high intensity storms linked to climatic changes, has become a critical issue in many parts of the world, particularly low-lying areas (Clarke, 1993). It is estimated that by the end of next century, a third of Bangladesh, a

quarter of Egypt's habitable land, and about 300 Pacific islands will be submerged. Anthropogenic actions such as deforestation and urban development also greatly influence the flooding events. While deforestation reduces the time taken by the precipitation-derived surface runoff to infiltrate and urbanization reduces the amount of pervious areas available for infiltration, both processes lead to an upward shift in the runoff-rainfall ratio, which in turn, causes greater detachment and carrying of sediment to rivers and lakes. In a watershed in North Carolina, streamflow rose 70% in the year after all woody vegetation was removed (Clarke, 1993). A study carried out in United States showed that urban development in a watershed increases the potential of flooding (Rogers and DeFee, 2005).

2.2.1.3 Water Quality – Water Pollution

Pollution, arising from soil-erosion enhanced sedimentation in surface water bodies, transport of nutrients and organic materials from livestock wastes and agricultural lands, and increased storm water flow from urban areas, constitute serious problems in a number of watersheds' waterways. Karakoc et al. (2003) showed lakes Eymir and Mogan in Turkey to be seriously threatened by anthropogenic activities (domestic, agricultural and industrial), which led to eutrophication. Similarly, Yuan et al. (2002) stated that agricultural areas' productivity and surface water bodies' quality, within the Mississippi River Delta (U.S.A), were adversely affected by soil erosion problems.

The rising worldwide occurrence of natural disasters and pollution are symptomatic of a larger and more basic problem of environmental imbalance. Since the incitant problems exist and interact with one another, they cannot be solved individually. Measures which holistically consider the economic, environmental, social and cultural factors are crucial to the mitigation of such problems. Given financial, human resource, and time constraints, devising an appropriate management strategy by conducting large-scale experiments over an extended period of time is impractical. In such cases, the need arises for modeling to assist in the management of the environment (Singh, 1995).

2.3 MODELING

As stated in Dingman (2002), "a model is a representation of a portion of the natural or human-constructed world", which can initially be classified as physical, analog, or mathematical (Figure 2.4). A physical model is a scaled-down version of a real system (Brooks et al., 1991). In an analog model, the observations of one process are used to simulate another physically analogous natural process. The mathematical model consists of explicit sequential set of equations and numerical and logical steps, which converts numerical inputs into numerical outputs (Dingman, 2002). Rapid advances in computer technology have led to the replacement of physical and analog models by mathematical ones.

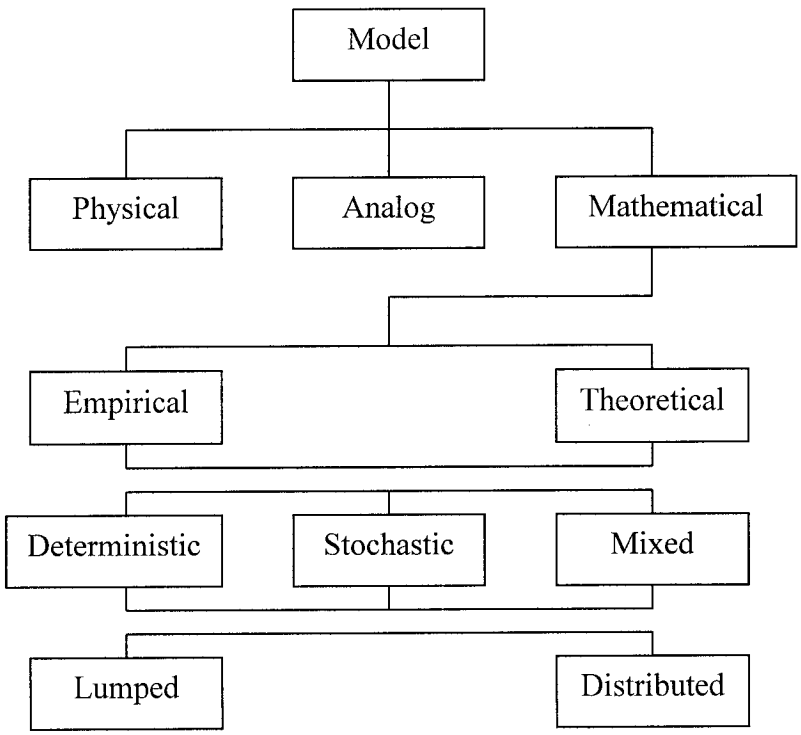

Figure 2.4 Classification of Hydrologic models

Mathematical models are further subdivided into several classes (Figure 2.4). Empirical models derived from experiments or observed input-output relationships, and theoretical (physically-based) models based on physical laws and theoretical principles (Brooks et al., 1991). In a deterministic model, every parameter is fully determined by governing equations, whereas in a stochastic (probabilistic) model, the model parameters

or input variables are totally or partially described by probability equations. Warren and Gary (2003) mentioned that a distributed model considers the spatial variability of input parameters in contrast to a lumped model. Event-based or single-event models simulate a particular event or process for a short time period, whereas a continuous model can simulate the phenomenon for several years. In an analytical model, the governing equations are solved by mathematical analysis, whereas in numerical model, the governing equations are solved approximately using arithmetic operations.

Hydrologic models, simplified representations of actual hydrologic systems, predict hydrologic responses and allow one to study the function and interaction of various inputs, and in so doing gain a better understanding of hydrologic events (Brooks et al., 1991). The goal of hydrologic modeling is to estimate the distribution and movement of water over land, underground, and in-stream, as well as the quantity of water stored in the soil and/or in natural bodies of water and their exchange; they can also estimate changes in rates and quantities over time. Hydrologic models have arisen as a result of the complexity, variability and limited availability of spatiotemporally distributed hydrological, climatic, soil and land-use data (Dingman, 2002). These models can be categorized into five main components: (1) system geometry, (2) input, (3) governing laws, (4) initial and boundary conditions, and (5) output. These components vary depending on the model type (Singh, 1995).

2.4 WATERSHED MODELS

A watershed model simulates hydrological processes in a watershed-scale compared to many other models which simulates mostly at the relatively small, field-scale. The first watershed model was the Stanford Watershed Model, developed in 1966 by Crawford and Linsley (Singh, 1995). Since then, numerous watershed models have been developed. Currently, the better-known watershed models include ADAPT, AnnAGNPS, ANSWERS-2000, APEX, BASINS, CANWET, CASC2D, CREAMS, DWSM, EPIC, HBV, HEC-1, HSPF, the Institute of Hydrology Distributed model, KINEROS, MIKE 11, MIKE SHE, NTRM, NWSRFS, PRMS, RORB, SIMPLE, SLURP, SPUR-91, SRM, SSARR, SWAT, SWMM, SWRRB, the Tank model,

THALES, TOPMODEL, the UBC Watershed model, and the Xinanjiang model (Parsons, 2004; Singh, 1995). However for this study, only the more commonly used watershed models, HEC-1, ANSWER-2000, HSPF, CREAMS, AnnAGNPS, EPIC, MIKE SHE and SWAT are reviewed.

2.4.1 HEC-1 Model

HEC-1 (Hydrologic Engineering Center) model was developed by US Corps of Engineers in 1968 to simulate hydrologic processes, as mentioned in Feldman (1995). This deterministic, rainfall-runoff model was evolved from a series of small programs simulating several parts of the precipitation-runoff process. It models watersheds, ranging in size from 1 km^2 to 100,000 km^2, and operates on a one-minute minimum time-step. The semi-distributed, single-event model develops hydrographs for both gauged and hypothetical rainfall events at one or more locations in the watershed. The model has the ability to simulate precipitation, losses, baseflow, runoff transformation and routing for each sub-basin. The baseflow is simulated using a simple method, which consists of a starting flow, a recession threshold, and a logarithmic decay recession rate. The loss component includes the infiltration, interception, and detention storage. There are two methods for determining runoff: (1) the unit hydrograph or SCS curve number method, and (2) kinematic wave methods. The model can thus be physically-based or empirical, depending on the method used for simulation. The Muskingum-Cunge method is used for channel routing of flow hydrographs (Feldman, 1995).

Duru and Hjelmfelt (1994), using the model's kinematic wave method, found that even with limited calibration, runoff prediction for ungauged catchments was good, and impacts of land use on the hydrologic cycle could be evaluated accurately. A study conducted in northern Ontario showed that HEC-1 model could be used for runoff simulation in an ungauged watershed (Sui, 2005).

Though HEC-1 has been used widely, it excludes certain important features. The model is constrained to a constant time step, which may not be suitable for components requiring detailed analysis. Since it is semi-distributed, the model assumes hydrologic processes to occur uniformly within each sub-basin. Also, as the primary purpose of the

model is to determine flood hydrographs, a simple method is used for the baseflow simulation. The loss component of the model is not tracked down in absence of precipitation, that is, the soil does not dry out and recover its loss potential.

2.4.2 ANSWERS-2000 Model - Areal Non-point Source Watershed Environment Response Simulation

ANSWERS-2000, the current version of the ANSWERS model developed by Beasley and Huggins in the late 1970s in the United States, is a physically-based, distributed parameter, continuous simulation, watershed-scale model (Dillaha et al., 2004). The model has Arc-Info-based user interface, which allows easy input and output data manipulation. This model was designed for ungauged watersheds where calibration is not possible, as well as for evaluating the effectiveness of agricultural and urban watershed best management practices in decreasing sediment and nutrient transport to streams during surface runoff events. The model is limited to medium-size watersheds (500 to 3000 ha) where surface hydrologic processes dominate. The watershed is divided into uniform grid squares of one hectare or less, based on homogeneous soil properties, land use, slopes, crops, nutrients, and management practices. The model uses breakpoint rainfall data and simulates on a 30-second time step during runoff events and on a daily time step between runoff events. The hydrology portion of ANSWERS-2000 addresses interception, surface retention/detention, infiltration, percolation, surface runoff (overland and channel flow), and evapotranspiration. A surface runoff hydrograph is provided at both the watershed outlet and any other point within the watershed (Dillaha et al., 2004).

Connolly et al. (1997), using ANSWERS to simulate runoff at a catchment outlet, showed that the model could accurately simulate different surface cover conditions; however, runoff prediction for low intensity rainfall events was less accurate than for high intensity events. They concluded that the model could be used for complex watersheds, without calibration. Bai et al. (2004) reported that ANSWERS-2000 was able to adequately simulate runoff during non-snow seasons, and suggested that the model should be improved to allow simulation of winter conditions.

Despite being a physically-based, distributed and watershed-scale model, ANSWERS-2000 is unable to simulate interflow and groundwater contributions to base flow, snow pack, and snowmelt. Hence, the model is not suitable for areas where base flow contribution, and winter snow accumulation and snow melt are high.

2.4.3 HSPF Model – Hydrological Simulation Program Fortran

As mentioned in Donigian et al. (1995), the HSPF is a widely used watershed model, developed by the United States Environmental Protection Agency (USEPA) in the late 1970s. Based on the original Stanford Watershed Model IV, it is an extension of three models (ARM, NPS and HSP). It was specifically developed to evaluate the impact of land use changes on water, sediment and pollutant movement. This mathematical, continuous-simulation, lumped-catchments, conceptual model is used to simulate water movement as overland flow, interflow and groundwater flow. The overland flow consists of an infiltration-excess mechanism (Johnson et al., 2003). The semi-distributed model employs HRUs (hydrological response unit) based on uniform climate and storage capacity factors. The flow from each HRU is routed downstream using the storage routing kinematic wave method. The model provides a water budget and considers snow accumulation and melt. The HSPF model is included in the USGS's water quality assessment tool, BASINS (Donigian et al., 1995).

Albek et al. (2004) conducted a study on a Turkish watershed, where they examined the effects of land use and climate change on watershed response, showed the model to agree fairly well with the observed data. Johnson et al. (2003), comparing the performance of the HSPF and SMR models on a watershed in the United States, found them to simulate stream flow with almost equal accuracy. The HSPF model gave better simulation of winter stream flow than SMR as the former includes a complex snowmelt routine with rigorous energy-balance equations. Brun and Band (2000) also used HSPF to evaluate the effect of land use changes on watershed behaviour in the United States, as well as analyzed the relationships of runoff ratio and base flow to percent of impervious cover and soil saturation. The study showed that observed runoff increases dramatically and base flow decreased when the percent impervious cover exceeds a threshold value of

roughly 20%. However, the model did not adequately represent the watershed processes, relying largely on calibration. In addition, the model showed transient model initialization effects, requiring three years of model initiation before calibration and validation.

The limitation of HSPF model is that it is not fully distributed, and it lumps the watershed characteristics and climatic parameters into several units. Also, it is not entirely physically-based as it uses both empirical and physical equations to simulate the water flow.

2.4.4 CREAMS Model – Chemicals, Runoff, and Erosion from Agricultural Management Systems

The CREAMS model, designed specifically for evaluating edge-of-field non-point source pollutant loadings under different management practices, was developed in 1978 by the USDA-ARS (Knisel and Williams, 1995). The major hydrologic processes considered by the model are precipitation, snowmelt, infiltration, soil water redistribution, percolation, evaporation, transpiration and surface runoff. This long-term, daily simulation model provides two methods for calculating runoff: (i) an SCS curve number method which uses daily rainfall data to estimates instantaneous peak runoff rates, and (ii) a modified Green and Ampt infiltration method where breakpoint or hourly rainfall input data is required. For the Green Ampt infiltration method, the runoff is summed at each time interval and routed to the field outlet to give runoff volume and peak runoff rate. The snowmelt option estimates snow accumulation and melt based on mean daily air temperature, but sublimation is not included. Frozen soil conditions are simulated using the modified SCS curve number method. Potential evaporation is estimated using the Priestly-Taylor method, while evaporation and transpiration are estimated using Ritchie's method (Knisel and Williams, 1995).

Rudra et al. (1985) applied a modified version of the CREAMS model, which considers temporal variability in soil hydraulic conductivity and soil erodibility, in a southern Ontario watershed to evaluate both the water quantity and quality. The results obtained were better as compared to the original version of CREAMS. Heatwole et al.

(1987) used a modified version of the CREAMS model (CREAMS-WT) to simulate shallow water tables in a South Florida watershed. The modified version of the model gave an improved prediction of runoff, evapotranspiration, percolation and soil water content.

The CREAMS model does not account for baseflow and sublimation of snow. Also, the model is lumped based on homogeneous soil, a single crop cover and management practice, and uniform rainfall over the entire watershed area.

2.4.5 AnnAGNPS Model - ANNualized AGricultural Non-Point Source model

Developed in 1980 by the USDA Agricultural Research Service (USDA-ARS), Minnesota Pollution Control Agency and U.S. Soil Conservation Service (SCS), the AnnAGNPS model, an updated version of AGNPS, was designed to evaluate runoff water quality from an agricultural watershed, ranging in size from a few hectares up to 300,000 hectares (Bosch et al., 2001; Young et al., 1995). It also assists in the management of runoff, erosion and nutrient movement and performs risk and cost/benefit analysis. It is semi-empirical, distributed-parameter, continuous simulation, and watershed-scale model. The runoff volume and rate are calculated using the SCS-Curve number method and TR-55 method, respectively, where the simulated direct runoff is due to storm events only. The input data is on a daily basis, while the model output is on an event, monthly, or annual basis (Bosch et al., 2001; Young et al., 1995).

While AnnAGNPS was shown to adequately predict long-term monthly and annual runoff, the model's overland flow did not properly represent the riparian areas, overestimating predicted nutrients and sediment loads (Suttles et al., 2003; Yuan et al., 2001). They suggested that proper cell discretization should be done to improve runoff estimates. Baginska et al. (2003) tested the AnnAGNPS model under Australian conditions and found event flow predictions to be satisfactory. Similarly, Das et al. (2004) showed the model to simulate runoff with acceptable accuracy in the Canagagigue Creek watershed of south-western Ontario. However, a study undertaken in Nepal (Shrestha et al., 2005), showed event-based peak flows to be over predicted.

The model simulates neither baseflow nor frozen soil conditions. The mass balance calculation for water inflow and outflow is not provided and model does not account for spatially varying rainfall over the watershed. Also, the runoff simulation is not entirely based on physical laws.

2.4.6 EPIC Model - Erosion-Productivity Impact Calculator

The EPIC model, a continuous simulation model, was developed to study the impact of soil erosion on soil productivity (Williams, 1995). The model consists of several components, such as weather simulation, hydrology, erosion-sedimentation, nutrient cycling, pesticide fate, plant growth, soil temperature, tillage, economics and plant environmental control. It is mostly used for agricultural management problems. Precipitation, air temperature and solar radiation are required as input data for weather simulation. The hydrology component determines surface runoff, percolation, lateral subsurface flow, evapotranspiration, snowmelt, and water table dynamics. The SCS curve number method is used for the determination of surface runoff volume. The model provides two methods (modified rational formula and the SCS TR-55) for the peak runoff rate computation. The percolation component simulates flow through soil layers using a storage routing technique, where flow occurs when soil water content exceeds field capacity. The model has four methods for determining potential evaporation; these are (1) Hargreaves and Samani, (2) Penman, (3) Priestley-Taylor, and (4) Penman-Monteith. The EPIC model has the potential to be used for irrigation planning based on the level of plant water stress, and is also able to compute crop yield reduction due to excess soil moisture (Williams, 1995).

Costantini et al. (2002) used daily soil water content, simulated by EPIC, to classify soil moisture regimes and showed EPIC-generated pedo-climatic classifications to match fairly closely to those obtained by traditional methods. The EPIC model has also been used, together with other models (such as a hydrologic model, economics model, and dynamic programming model), for decision-making and irrigation management for water release policies in a watershed in Oklahoma, United States (Evers et al., 1998).

The EPIC model does not simulate baseflow, and uses empirical equations for the determination of runoff. The model is limited to a 100 ha area, and is lumped assuming weather, soil, and management systems to be homogeneous.

2.4.7 SWAT Model - Soil and Water Assessment Tool

SWAT is a conceptual, physically-based, continuous simulation, watershed model, developed in the early 1990s (Arnold et al., 1993). It originated from the SWRRB model - Simulator for Water Resources in Rural Basin. The model was developed to predict the long-term impact of land management practices on water, sediment, pesticide and nutrient yields in watersheds with varying soils and land cover. The model components include weather, hydrology, erosion/sedimentation, plant growth, nutrients, pesticides, agricultural management, stream routing, and pond/reservoir routing. This semi-distributed model divides the watershed into several sub-basins termed hydrological response units (HRUs). It operates on a daily time step. The hydrology component of model consists of surface runoff, including runoff over frozen soils, percolation, lateral subsurface flow, groundwater flow, snowmelt, evapotranspiration, transmission losses, irrigation water transfer, and ponds. A modified SCS curve number method or the Green Ampt infiltration method is used to determine the runoff volume. The peak runoff rate is calculated using the modified Rational Formula or the SCS TR-55 method. The lateral subsurface flow is calculated together with percolation using a kinematic storage routine. The model considers base flow contribution to total stream flow by routing a shallow aquifer storage component to the stream. Potential evapotranspiration is estimated using either: (1) Hargreaves, (2) Priestley-Taylor or (3) Penman-Monteith equations. Snowmelt occurs depending on the snowpack temperature and the melted snow is considered as uniformly distributed rainfall with zero energy. The model output consists of evapotranspiration, soil water storage and water yield (sum of surface runoff and subsurface flow). The new version of the model, AVSWAT, includes a graphical user interface (Arnold et al., 1993; Chu and Shirmohammadi, 2004; Du et al., 2005; Kang et al., 2005; Spruill et al., 2000).

A study on a watershed situated in Georgia, United States, showed the model to provide good results on a monthly basis, but less accurate estimates on a daily basis (Bosch et al., 2004). In addition, the model did not provide baseflow estimations adequately. Other studies (Chu and Shirmohammadi, 2004; Spruill et al., 2000) corroborated the fact that the SWAT model failed to give reasonable runoff predictions on a daily basis. However, King et al. (1999), using a sub-daily time step for routing stream flow, showed a close correlation between the measured and simulated hydrographs. However, the authors concluded that use of sub-daily time steps and breakpoint rainfall was not advantageous for large basin simulations. Kang et al. (2005) demonstrated that AVSWAT was a useful tool for predicting and evaluating the total maximum daily load (TMDL) of total nitrogen, total phosphorus and suspended solid for a small watershed containing rice paddies, located in Korea. Gebremeskel et al. (2005) stated that the SWAT model performed very well for stream flow prediction in the Canagagigue creek watershed of south-western Ontario. Du et al. (2005) used a modified version of the SWAT model to simulate surface and subsurface flows, water table dynamics, tile flow, potholes, surface tile inlets, and aeration stress on plants, for large flat landscapes. The model results were reasonable with respect to patterns and amounts of monthly flows. Muttiah and Wurbs (2002) reported that the mean and variance of water balance components varied with geographic scale, thus exhibiting the scale-dependent water balance 'uncertainty' laws. These mean and variance of water balance components are very sensitive to a wet climate, soil heterogeneity within the watershed, land use, and uniformity of rainfall pattern.

The only drawback of the SWAT model is that it is semi-distributed, where it divides the watershed into sub-basins having homogeneous climate, soil, land cover and management practices.

2.4.8 MIKE SHE Model

The MIKE SHE model is a fully integrated watershed model that simulates all the major processes occurring in the land phase of the hydrologic cycle. Developed by three European organizations (Danish Hydraulic Institute, British Institute of Hydrology and

the French consulting company SOGREAH) and sponsored by the Commission of the European Communities, it was originally named SHE (Système Hydrologique Européen) model. This deterministic, fully distributed, and physically-based model is used mostly at the watershed scale and from a single soil profile to several sub-watersheds with different soil types (DHI, 2004; Refsgaard and Storm, 1995). The model's distributed nature allows a spatial distribution of watershed parameters, climate variables, and hydrological response through an orthogonal grid network and column of horizontal layers at each grid square in the horizontal and vertical, respectively (Abbott et al., 1986b). Being physically-based, the topography along with watershed characteristics (vegetation and soil properties) is included into the model. The MIKE SHE model has a modular structure, enabling data exchange between components as well as addition of new components. The flexible operating structure of MIKE SHE allows the use of as many or as few components of the model, based on availability of data (Abbott et al., 1986a). Since the MIKE SHE model was selected to be evaluated in this study, more detailed explanation of the model is provided in the next chapter.

Several studies have been conducted using the MIKE SHE model in different regions and under diverse soil and climatic conditions. Thompson et al. (2004), using the coupled MIKE SHE/MIKE 11 model for a wetland in England, showed the model's results consistently matched with the observed data, reproducing the seasonal dynamics of groundwater and ditch water levels. They concluded that the coupled model has the capacity to handle wetland situations. The model was also used in a mountainous region of Hawaii (Sahoo et al., 2006) to study watershed response to storm events. While a comparison of observed and predicted streamflow gave correlation coefficients greater than 0.7, the model underpredicted streamflow for large storm events. Demetriou and Punthakey (1999) applied MIKE SHE to an Australian watershed with a complex hydrogeological regime to evaluate the groundwater management options for dealing with rising water table levels and land salinisation problems. The model was accurate in spatially and temporally predicting water movement from aquifers, drainage and supply systems, and land surfaces as well as simulating various scenarios. Jaber and Shukla (2005) employed two approaches to model impoundment water dynamics with the coupled MIKE SHE/MIKE 11 models. The approach where the entire impoundment was

considered as a canal of wide cross section gave satisfactory and better agreement between observed and simulated water levels than one which represented the impoundment as flooding from a canal to a floodplain.

Many investigators have evaluated the MIKE SHE model in irrigated areas (Jayatilaka et al., 1998; Mishra et al., 2005; Punthakey et al., 1993; Singh et al., 1997; Singh et al., 1999). Punthakey et al. (1993) found the model to perform satisfactorily when they employed it to evaluate several management strategies in terms of the impact of irrigation on water-logging and soil salinisation arising from rising water tables in the Berriquin irrigation district in Australia. Singh et al. (1997), using the coupled MIKE SHE/MIKE 11 models for hydraulic simulation of a canal system and hydrological simulation of an irrigated command area in India, showed the versatility of the model in the planning and operation of large irrigation projects, and its contribution to greater water use efficiency and improved crop production. Jayatilaka et al. (1998) used MIKE SHE for quantifying the processes influencing surface drainage and groundwater levels, and their role in transporting salts to waterways. The study showed the inadequacy of the model to represent the complex behaviour of the physical system, the suitability of the adopted spatial and temporal scales to represent the dynamic flow processes, and the degree to which the model parameter values are representative of the physical conditions. Singh et al. (1999) similarly applied the model to plan and analyze crop irrigation requirements, based on water balance analyses. They showed that the hydrological model could be used effectively for irrigation planning and management of water resources for agricultural purposes. Mishra et al. (2005) used MIKE SHE/MIKE 11 with an optimization routine to improve irrigation system management by implementing optimal canal water release in India. They concluded that the overall deficit of the irrigated areas could be reduced by minimizing the gap between supply and demand, and enhancing the spatial distribution of the irrigation water in the canal system with the aid of an integrated optimization simulation model.

In this research project, the applicability and predictive capacity of the MIKE SHE model is tested under Canadian climate conditions. Compared to other watershed models, the MIKE SHE model used the fully-dynamic Saint Venant equations to determine surface runoff, rather than the SCS-CN method. Also, this model simulates all

the processes in the hydrologic cycle by fully integrating the surface, subsurface and groundwater flow. Snowmelt is also incorporated in the model. Model also includes river flow simulation via the MIKE 11 model. The literature has shown MIKE SHE to have been used effectively in several water resources studies, where conventional rainfall-runoff model or lumped catchment model do not meet the criteria. These studies investigated impacts of land use and climate change, irrigation planning, conjunctive use of groundwater and surface water, effects of localized river and groundwater abstractions and recharge, groundwater management, river basin management and planning, floodplain studies, and modeling of ungauged catchments with short hydro meteorological record, etc.. Overall, the unique feature of MIKE SHE hydrology component is the integration of various hydrological processes in the model, at different time scales. Besides, the model is user friendly. To the best of my knowledge, this model has not been used in Canada.

CHAPTER III – METHODOLOGY

In this section, the workings of the MIKE SHE model are described and its mathematical formulation is outlined. The details of the study watershed, from which the data was collected for evaluation of the model performance, are given. The procedure of model development, calibration and validation, and the thereafter simulation of various management scenarios on the watershed are also provided.

3.1 THE MIKE SHE MODEL

In this section, the hydrological components of the model used in this study are described and their mathematical basis is presented.

3.1.1 Hydrological Description

MIKE SHE simulates all the processes in the land phase of the hydrologic cycle, as stated in DHI (2004). Precipitation, falling from the atmosphere as snowfall or rainfall, is partly intercepted by vegetation and building structures. The intercepted precipitation is stored and later evaporated or passed to the soil surface. A significant amount of rainfall, reaching the soil surface, evaporates back to the atmosphere. Depending on the air temperature, the snow accumulates on the soil surface at temperature below $0^{o}C$, while rainfall infiltrates through the unsaturated zone. When the top layer of the unsaturated zone becomes saturated, there is surface ponding and eventually overland flow begins when all the surface depressions are filled. The infiltrated water in the unsaturated zone can be stored, evaporated, taken up by plant roots and transpired through the leaves, or percolated down to the saturated zone. The overland water flows along the surface topography, evaporates and infiltrates on the way, eventually reaching streams, rivers and other surface water bodies. The groundwater also contributes to streams and rivers as a base flow, while water in rivers and streams infiltrates back into the saturated zone as recharge (DHI, 2004).

3.1.2 Mathematical Description

Figure 3.1 gives a schematic representation of the MIKE SHE model. The MIKE SHE model has a modular structure consisting of several modules: a Water Movement module for hydrology (WM), an Advection/Dispersion of Solutes (AD) module for water quality, a Soil Erosion (SE) module for sediment transport, as well as others such as Dual Porosity (DP), Geochemical Processes (GC), Crop growth and Nitrogen processes in the root zone (CN), and IRrigation (IR). The Water Movement module of MIKE SHE has several components, each describing a specific physical process. These include evapotranspiration/interception, overland/channel flow (OC), unsaturated zone (UZ), saturated zone (SZ), snowmelt, and exchange between aquifer and rivers.

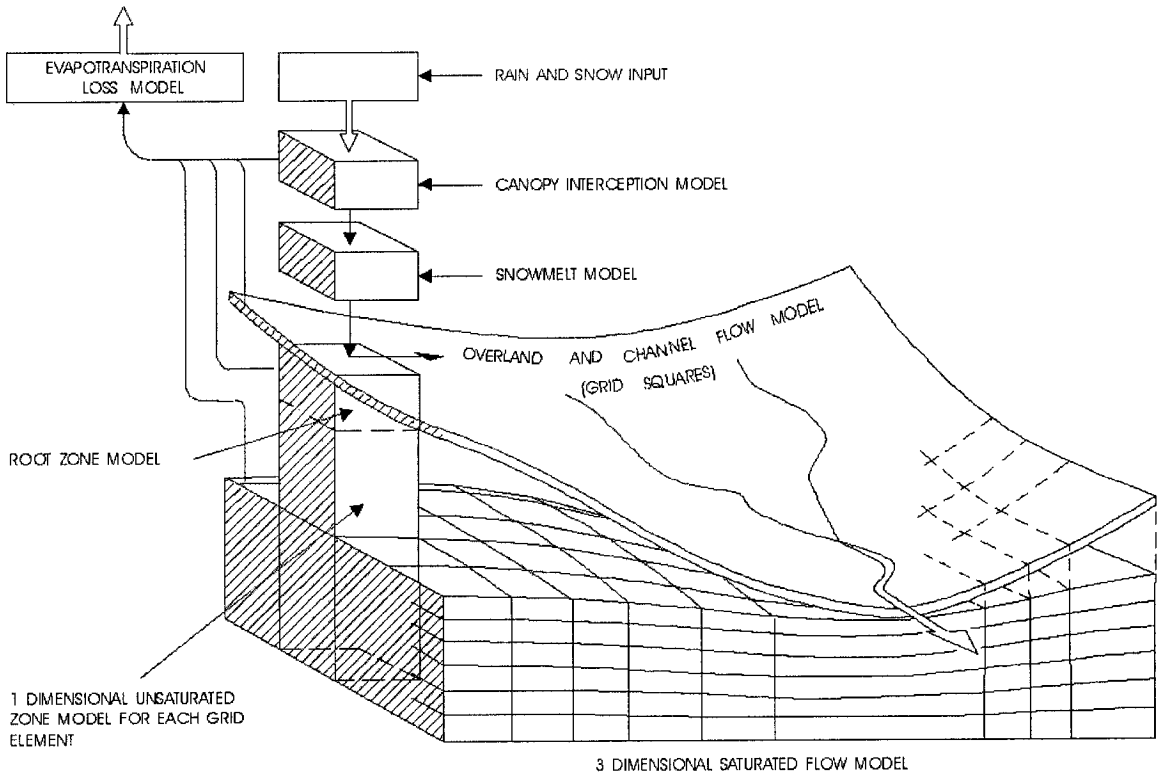

Figure 3.1 Schematic representation of MIKE SHE model (Refsgaard and Storm, 1995)

The hydrological processes are described mostly by physical laws (laws of conservation of mass, momentum and energy). The 1-D and 2-D diffusive wave Saint Venant equations describe channel and overland flow, respectively. The Kristensen and Jensen methods are used for evapotranspiration, the 1-D Richards's equation for

unsaturated zone flow, and a 3-D Boussinesq equation for saturated zone flow. These partial differential equations are solved by finite difference methods, while other methods (interception/evapotranspiration and snowmelt) in the model are empirical equations obtained from independent experimental research (DHI, 2004). The FRAME component enables components having different time steps to run in parallel and to exchange information (Abbott et al., 1986b).

3.1.2.1 Interception and Evapotranspiration Components

The interception component determines the net amount of rainfall reaching the ground, the canopy storage and evaporation from the canopy. The interception storage capacity depends on the vegetation type, its stage of development and density, rainfall intensity as well as other climatic conditions (Abbott et al., 1986b). The evapotranspiration component calculates the amount of water that evaporates from the soil and water surfaces, and that transpires through the leaves. The latter is controlled by root zone water availability, aerodynamic transport conditions and plant physiological factors, and it varies both spatially and temporally. The processes in the interception/evapotranspiration component are shown in Figure 3.2. The model provides two methods for determining interception and evapotranspiration: (i) the Kristensen-Jensen method and (ii) the Rutter model/Penman-Monteith equation. In this study, the first method was used.

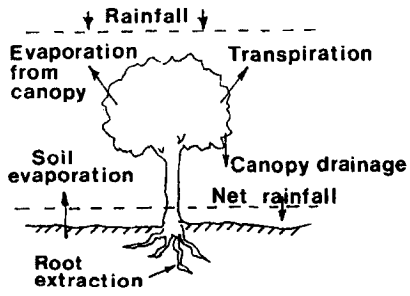

Figure 3.2 Schematic Diagram of Interception/Evapotranspiration (Abbott et al., 1986a)

i. Kristensen and Jensen Method

Based on empirical equations, derived by Kristensen and Jensen in 1975 at the Royal Veterinary and Agricultural University in Denmark, the actual evapotranspiration and actual soil moisture status in the root zone are calculated, assuming that temperature is always above 0°C. The maximum interception storage capacity of vegetation, I_{max} (mm), is defined as:

$$I_{max} = C_{int}\, LAI \tag{3.1}$$

where

C_{int} is the interception coefficient, defining the interception storage capacity of the vegetation (mm) with the typical value of 0.05 mm, and

LAI is the leaf area index ($m^2\ m^{-2}$).

Evaporation from the canopy storage, E_{can} (mm), for a sufficient amount of intercepted water, is given by:

$$E_{can} = \min (I_{max}, E_p \Delta t) \tag{3.2}$$

where

E_p is the potential evapotranspiration rate (mm hr^{-1}), and

Δt is the time step duration for the simulation (hr).

Actual Plant transpiration, E_{at} (mm) is determined as

$$Eat = f1(LAI) \cdot f2(\theta) \cdot RDF \cdot Ep \tag{3.3}$$

where

$f_1(LAI)$ is a function based on the leaf area index,

$f_2(\theta)$ is a function based on the soil moisture content, and

RDF is a root distribution function.

The LAI function is given by:

$$f_1(LAI) = C_2 + C_1 \cdot LAI \tag{3.4}$$

where

C_1 and C_2 are empirical parameters with usual values of 0.3 and 0.2, respectively.

The soil moisture function is given by:

$$f_2(\theta) = 1 - \left(\frac{\theta_{FC} - \theta}{\theta_{FC} - \theta_W} \right)^{\frac{C_3}{E_p}} \tag{3.5}$$

where

θ_{FC} is the volumetric moisture content at field capacity ($m^3\ m^{-3}$),

θ_W is the volumetric moisture content at the wilting point ($m^3\ m^{-3}$),

θ is the actual volumetric moisture content ($m^3\ m^{-3}$), and

C_3 is an empirical parameter (mm day^{-1}), based on soil type and root density where a value of 20 mmday^{-1} is used in MIKE SHE.

The root distribution function is given as:

$$RDF_i = \int_{z1}^{z2} R(z)\partial z \Big/ \int_0^{L_R} R(z)\partial z \tag{3.6}$$

where

$R(z)$ is the root extraction, calculated as:

$$\log R(z) = \log R_o - AROOT \cdot z \tag{3.7}$$

where

R_o is the root extraction at soil surface (m),

AROOT is a parameter describing root mass distribution (m^{-1}), where the typical value used is 0.25 m^{-1},

z is depth below the ground surface (m).

Soil evaporation, E_s (mm), is given by:

$$E_s = E_p \cdot f_3(\theta) + (E_p - E_{at} - E_p \cdot f3(\theta)) \cdot f4(\theta) \cdot (1 - f_1(LAI)) \tag{3.8}$$

where

f_3 and f_4 are a function of soil moisture content.

$$f_3(\theta)=\begin{cases} C_2 & \theta \geq \theta_w \\ C_2 \dfrac{\theta}{\theta_w} & \theta_r \leq \theta \leq \theta_w \\ 0 & \theta \leq \theta_w \end{cases} \tag{3.9}$$

$$f_4(\theta)=\begin{cases} \dfrac{\theta - \dfrac{\theta_W + \theta_{FC}}{2}}{\theta_{FC} - \dfrac{\theta_W + \theta_{FC}}{2}} & \theta \geq \dfrac{(\theta_W + \theta_F)}{2} \\ 0 & \theta < \dfrac{(\theta_W + \theta_F)}{2} \end{cases} \tag{3.10}$$

where

C_2 is the empirical parameter with typical value of 0.2.

The f_l(LAI) function and E_{at} are zero in the absence of vegetation, and evaporation from the soil occurs only from the upper node of the unsaturated zone.

3.1.2.2 Overland and Channel Flow Component

Overland flow, influenced by topography, flow resistance, evaporation and infiltration along the path, occurs when the rainfall rate exceeds the infiltration rate, resulting in surface ponding and eventually surface water flow. The model allows interaction with other processes, such as evaporation, infiltration, tile drains, and drainage into the channel network. There are two methods for determining the overland flow: (i) the diffusive wave approximation of the Saint Venant equations and (ii) simplified overland flow routing, where the first method was used.

i. Diffusive Wave Approximation of St Venant Equations

Diffusive wave approximations of the St Venant equations is derived from the fully dynamic St Venant equations, wherein the last three terms of the momentum equations are neglected in order to reduce the fully dynamic equations' complexity. The continuity equation (Eq. 3.11) and momentum equations (Eqs. 3.12 and 3.13) allow the simulation of significant variation in overland flow depth between neighbouring cells as well as that of backwater conditions.

$$\frac{\partial h}{\partial t}+\frac{\partial(uh)}{\partial x}+\frac{\partial(vh)}{\partial y}=i \tag{3.11}$$

where

h is the flow depth above ground surface (m);

u is the velocity (m s^{-1}) in the x-direction,

v is the velocity (m s^{-1}) in the y-direction, and

i is the net input over overland flow (m s^{-1}).

The momentum equations are:

$$S_{fx}=S_{ox}-\frac{\partial h}{\partial x} \tag{3.12}$$

$$S_{fy}=S_{oy}-\frac{\partial h}{\partial y} \tag{3.13}$$

where

S_f are the friction slopes (-) in the x and y directions, and

S_o are the slopes of the ground surface (–) in the x and y directions.

Using the diffusive wave approximations of the St Venant equations and Manning's equations, one obtains:

$$uh=k_x\left(-\frac{\partial z}{\partial x}\right)^{1/2}h^{5/3} \tag{3.14}$$

$$vh=k_y\left(-\frac{\partial z}{\partial y}\right)^{1/2}h^{5/3} \tag{3.15}$$

where

uh and vh represent discharge per unit length along the cell boundary in x- and y-directions respectively [$m^2 s^{-1}$], and

k_x and k_y are Manning M or Stickler coefficient in x- and y- directions, respectively.

Flow across any boundary between grids, from equations (3.14) and (3.15), is given by:

$$Q = \frac{k\Delta x}{\Delta x^{1/2}}(Z_u - Z_D)^{1/2} h_u^{5/3} \qquad \{3.16\}$$

where

h_u is the depth of water that can freely flow into the next cell (actual water depth minus detention storage, mm), and

Z_u and Z_D are the maximum and minimum water levels, respectively (mm).

The modified Gauss Seidel method is used for the numerical solution. Water is added or removed (due to infiltration, recharge or evaporation) to the ponded water in the model grid at the beginning of every overland flow time step. During iteration, since the flow equations are explicitly defined, overland flows are reduced in some situations to avoid internal water balance errors and divergence of the solution scheme. Henceforth, outflow should be:

$$\sum |Q_{out}| \le \sum Q_{in} + I + \frac{\Delta x^2 h(t)}{\Delta t} \qquad \{3.17\}$$

where

$\sum Q_{in}$ is the sum of inflows rates ($m^3 s^{-1}$), and

$I = i\Delta x^2$ is the net input into overland flow in each grid ($m^3 s^{-1}$).

3.1.2.3 Unsaturated Zone Components

The flow in the unsaturated zone is assumed to be vertical. The model provides three options to calculate flow: (i) full Richard's equation, (ii) a simplified gravity flow and (iii) a simple two-layer water balance method for shallow water tables. The full Richard's equation was used in this study.

(i) Richards Equation

The pressure head-based Richards equation, based on Darcy's law and continuity equation, assumes the soil matrix to be incompressible and soil water to be at constant density:

$$C\frac{\partial \psi}{\partial t} = \frac{\partial}{\partial z}\left(K\frac{\partial \psi}{\partial z} \right) + \frac{\partial K}{\partial z} - S \qquad \{3.18\}$$

where

C is the soil water capacity (mm^{-1}),

ψ is the pressure head (mm),

K is the saturated hydraulic conductivity ($mm\ s^{-1}$),

Z is the gravitational head (mm), and

S is the root extraction sink term (s^{-1}).

The Richard's equation is solved numerically using the finite difference implicit approximation method, associated with the Gauss-Seidal iteration formula, thus removing the stability and convergence problems due to heterogeneous soil properties. The unsaturated zone is defined by an upper boundary (ground surface) and a lower boundary (groundwater table). The upper boundary is considered as a Neuman boundary when there is a constant flux, such as rainfall, applied to the surface, or a Dirichlet boundary when there is a constant head on the surface, such as ponded water. The lower boundary is generally a pressure boundary, but is a zero flux boundary when the watertable falls below the impermeable bed, such that there is an upward flux in the lower part of the profile. The initial conditions set up by the model are hydrostatic conditions, defined by an equilibrium soil moisture-pressure profile, with no flow. The sink term in the Richards' equation is the root extraction due to transpiration in the upper part of the unsaturated zone, which is the actual transpiration for the entire root zone.

(ii) Coupling of Unsaturated Zone to the Saturated Zone

Coupling is required to enable water table fluctuation, especially in shallow soils. The unsaturated zone (UZ) and saturated zone (SZ) are explicitly coupled to optimize the time steps used. The explicit interaction is solved by an iterative mass balance procedure that conserves mass for the entire column by considering outflows and source/sink terms in the saturated zone. Mass balance errors normally occur when (1) water table level is kept constant during the unsaturated zone time step, (2) an incorrect specific yield, S_y, is used in the saturated zone. The coupling is limited to the entire unsaturated zone and the uppermost calculation layer of the saturated zone. If the water table is below the bottom of the first SZ calculation layer, the UZ module treats the bottom of SZ calculation layer one as a free drainage boundary or a zero-flux boundary (Richard's equation). However, several geological layers can be specified within calculation layer number one if the lower levels of the SZ calculation layers are explicitly defined.

3.1.2.4 Saturated Zone Components

There are two methods for determining the flow in the saturated zone: (i) 3-D finite difference method and, (ii) linear reservoir method, where the first method was applied in the model set-up.

(i) 3-D Finite Difference Method

In this method, the saturated flow is defined by the 3-dimensional Darcy equation and equation of continuity, and it is solved by an iterative implicit finite difference technique. The two solvers provided by this method are preconditioned conjugate gradient and successive over-relaxation solution techniques, which differ somewhat in the formulation of potential flow and sink/source terms. The preconditioned conjugate gradient was chosen as the solution technique in this model simulation. The SZ interacts with other components of MIKE SHE using their boundary flows implicitly or explicitly, as sources and sinks. The governing 3-D partial differential equation is given as:

$$\frac{\partial}{\partial x}\left(K_{xx}\frac{\partial h}{\partial x}\right)+\frac{\partial}{\partial y}\left(K_{yy}\frac{\partial h}{\partial y}\right)+\frac{\partial}{\partial z}\left(K_{zz}\frac{\partial h}{\partial z}\right)-Q=S\frac{\partial h}{\partial t} \qquad \{3.19\}$$

where

K_{xx}, K_{yy}, and K_{zz} are the hydraulic conductivity along the x, y and z axes [mm s^{-1}],

h is the hydraulic head (mm),

Q is the source/sink term (s^{-1}), and

S is the specific storage coefficient (m^{-1}).

The peculiarities of the equation are that: (1) it is non-linear for unconfined flow and (2) the storage coefficient is not constant and changes from a specific storage coefficient for confined conditions to a specific yield for unconfined conditions.

a. The PCG (Preconditioned Conjugate gradient) solver

The potential flow terms, based on Darcy's law, are given as:

$$Q = \Delta hC \qquad \{3.20\}$$

where

Δh is the piezometric head difference (mm), and

C is the conductance ($m^2 s^{-1}$).

The horizontal conductance is calculated from the harmonic mean of the horizontal conductivity and the geometric mean of the layer thickness, while the vertical conductance is the weighted serial connection of the hydraulic conductivity, calculated from the middle of one layer to the middle of another layer. For dewatering conditions in SZ cells, where the bottom cell becomes dewatered, a correction term is added to the right-hand side of the finite difference equation, using the last computed head. The correction term is

$$q_c = Cv_{k+½}(h_{k+1} - z_{top,\, k+1}) \qquad \{3.21\}$$

where

C_v is the vertical conductance ($m^2 s^{-1}$),

z layer thickness (m), and

k+1 number of node.

The storage capacity is calculated by

$$\frac{\Delta w}{\Delta t} = \frac{S2\left(h^n - z_{top}\right) + S1\left(z_{top} - h^{n-1}\right)}{\Delta t} \qquad \{3.22\}$$

where

n is time step,

S1 is the storage capacity at the start of the iteration at time step n, and

S2 is the storage capacity at the last iteration.

The boundary conditions of the saturated zone can be subject to (1) Dirichlet's conditions based on hydraulic head, (2) Neumann's conditions based on gradient of hydraulic head, or (3) Fourier's conditions based on head dependent flux.

In MIKE SHE, the drainage flow is calculated as a linear reservoir and is controlled by the height of water table above the drain depth and the specified time constant. However, drainage flow occurs only in the top layer of the saturated zone layer and when water table is above the drain depth. With the PCG solver, the drain flow is added directly in the matrix calculations as a head dependent boundary, and is solved implicitly as

$$q = (h - Z_{dr})C_{dr} \qquad \{3.23\}$$

where

h is head in the drain cell (m),

Z_{dr} is the drainage level (m), and

C_{dr} is the drain conductance or time constant (m^2s^{-1}).

The exchange of saturated zone flow and overland flow is calculated implicitly using the Darcy equation, with continuously updating of the overland water depth:

$$Q = \Delta h C_{½} \qquad \{3.24\}$$

where

$C_{½}$ is the conductance from surface level to the middle of the top calculation layer ($m^2 s^{-1}$).

In case of full contact or reduced contact between overland and saturated zones, the conductance used in the Darcy equation is different for each case. The initial conditions applied for the saturated zone can be constant or distributed over the model domain, while the initial conditions in the boundary cells are kept constant during the simulation (DHI, 2004).

3.2 DESCRIPTION OF STUDY AREA

The Grand River flows from its headwaters near Dundalk, Ontario, Canada, to Port Maitland where it empties into Lake Erie. The Canagagigue Creek is a sub-watershed, located in the north western part of the Grand River Basin (Figure 3.3). It is located between 43^{o} 36' N and 43^{o} 42' N latitude and 80^{o} 33' W and 80^{o} 38' W longitude. The Grand River Basin, housing a human population of 750,000, is the largest Canadian tributary contributing to Lake Erie, with a total area of 7000 km^2 and a length of 300 km. The sub-watershed is 19 km long and 10 km wide, with a total drainage area of 143 km^2. It begins from the Waterloo hills in Peel Township and extends to the flatter Guelph drumlin fields in the south easterly section of Woolwich Township (Carey et al., 1983).

The upper part of the Canagagigue Creek watershed study area, has elevations ranging from 368 m to 465 m. It is flat to gently undulating with a mean slope of 1.5 %. Loam is the predominant soil type. The watershed has 80% agricultural land and about 10% woodlots (Carey et al., 1983). Agricultural activities include mixed farming, predominantly dairy farming, and cropping of silage corn (*Zea mays* L.), small grains (soybean - *Glycine max* Merr.) and hay (alfalfa — *Medicago sativa* L.). They are grown mainly for livestock feed, with a very small part of the watershed under cash crop cultivation (Das et al., 2004). The woodlots are mainly comprised of boreal forest and coniferous species which dominate the headwater of Canagagigue Creek (GRCA, 1997). The rest of the sub-watershed is occupied by urban areas, fallow land, and rivers and lakes. Climatic conditions vary across the Grand River Watershed, covering four different climatic zones. In the Grand River basin, July and August are the warmest months of the year, and have the greatest precipitation. Evapotranspiration occurs mainly in the summer months, and represents 65% of the annual precipitation. The months of

January and February are the coldest and driest months of the year. The mean annual precipitation ranges from 750-1000 mm, including 100-200 mm of snowfall (Das et al., 2004).

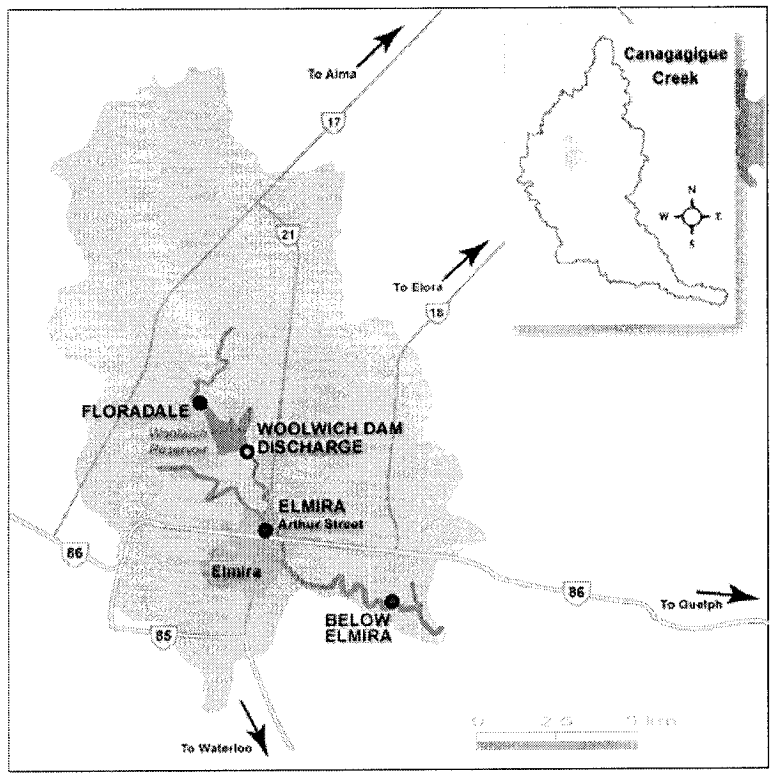

Figure 3.3 Location of Canagagigue Creek in Grand River Basin (GRCA, 2005)

Based on the availability and credibility of observed flow data at the Floradale gauge station (Figure 3.3), the study only targeted the upstream portion of the Canagagigue Creek, roughly 53 km^2. The watershed climate can be classified as humid continental with warm summers and moderate winters, according to the Koppen-Geiger climatic classification system (Bai et al., 2004).

3.3 INPUT DATA

3.3.1 Hydro-Meteorological Data

The model required precipitation, air temperature and potential evapotranspiration as climatic input data. The precipitation data required was the total rainfall and rainfall-

equivalent of the snowfall. Potential Evapotranspiration (PET) was calculated using the FAO modified Penman method (Doorenbos and Pruitt, 1977). Vazquez and Feyen (2001) reported that the FAO Penman method is as capable as the Penman Monteith equation, also a better model performance was obtained with the first method. Daily minimum and maximum temperature, relative humidity, wind speed and percentage cloud cover are used for the computation of PET. These data, together with daily precipitation, were obtained from the closest weather station – Waterloo Wellington A (ENV CAN, 2005). Though the MIKE SHE model enables these climatic data to be entered in hourly, minutes and seconds, daily data was used, given its availability from the weather station.

The FAO Modified Penman equation is given by:

$$ET_0 = c[W \cdot Rn + (1-W)f(u)(e_a - e_d)] \quad \{3.25\}$$

where

ET_0 is the reference crop evapotranspiration (mm/day),

W is a weighting factor (-),

Rn is net radiation in equivalent evaporation (mm/day),

$f(u)$ is the wind function (-),

(e_a-e_d) is vapour pressure (mbar), and

c is an adjustment factor (-).

The adjustment factor was taken as 1 (one) in this study.

The model simulation started at the beginning of water year (1st October), when the initial water table depth was set as 1 m below the surface and was assumed to be uniform over the watershed.

3.3.2 Hydro-geological Data - Surface and Subsurface Geology

The topography of the study area was obtained from the Grand River Conservation Authority as a digital elevation model (DEM) with a 100 m x 100 m spatial resolution. The DEM was converted into a point shape file to be imported into the model.

The soil and land use classification across the watershed was defined by polygon shape files, provided by the Ontario Ministry of Agriculture and Food. Figures 3.4, 3.5 and 3.6 show the topography, soil and land use maps of the study area, respectively.

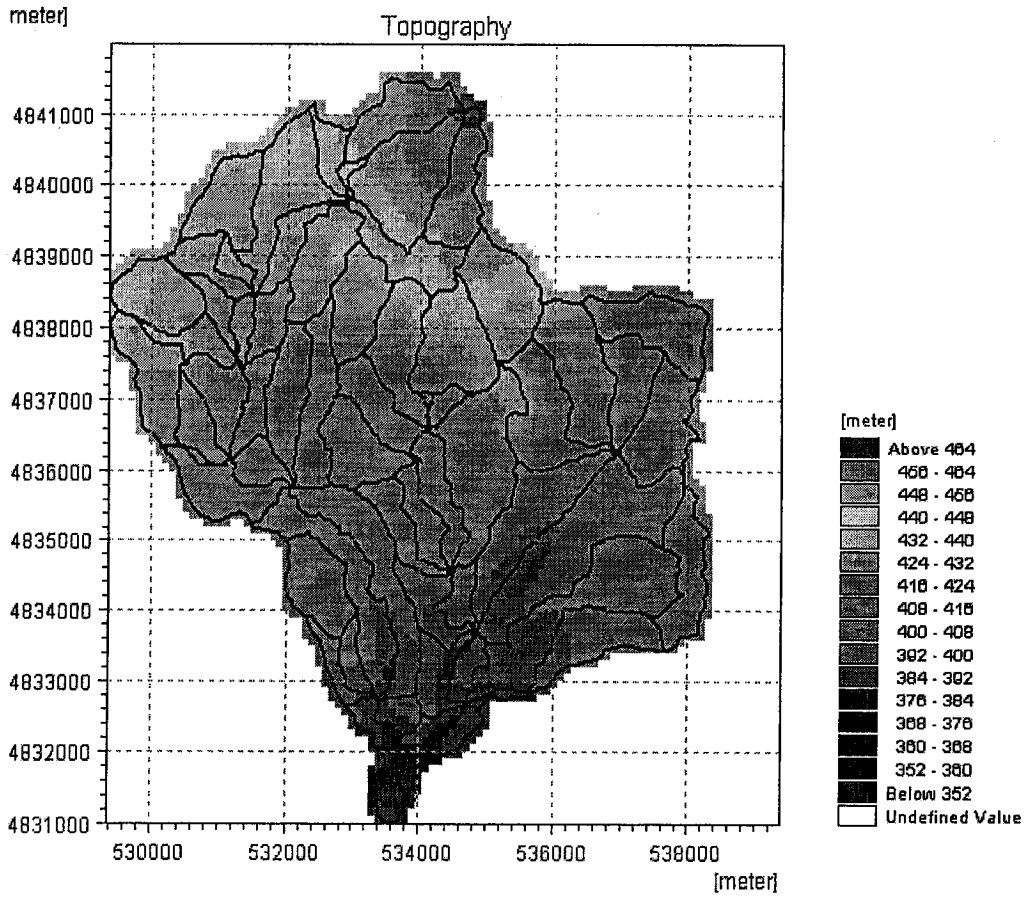

Figure 3.4 Topography map of Canagagigue Creek watershed in UTM Coordinate - zone 17N

Christiaens and Feyen (2001) stated that there is less uncertainty associated with the neural network approach (Rosetta model) for the determination of soil parameters. Thus for the van Genuchten equations used, the model required soil properties for each soil series, describing the retention curve and hydraulic conductivity. The van Genuchten parameters were obtained from the Rosetta model, using the percentage sand, silt and clay as primary input data, except for the Burford and Freeport soil series where the textural classes were used directly. The Rosetta output parameters are: saturated moisture content

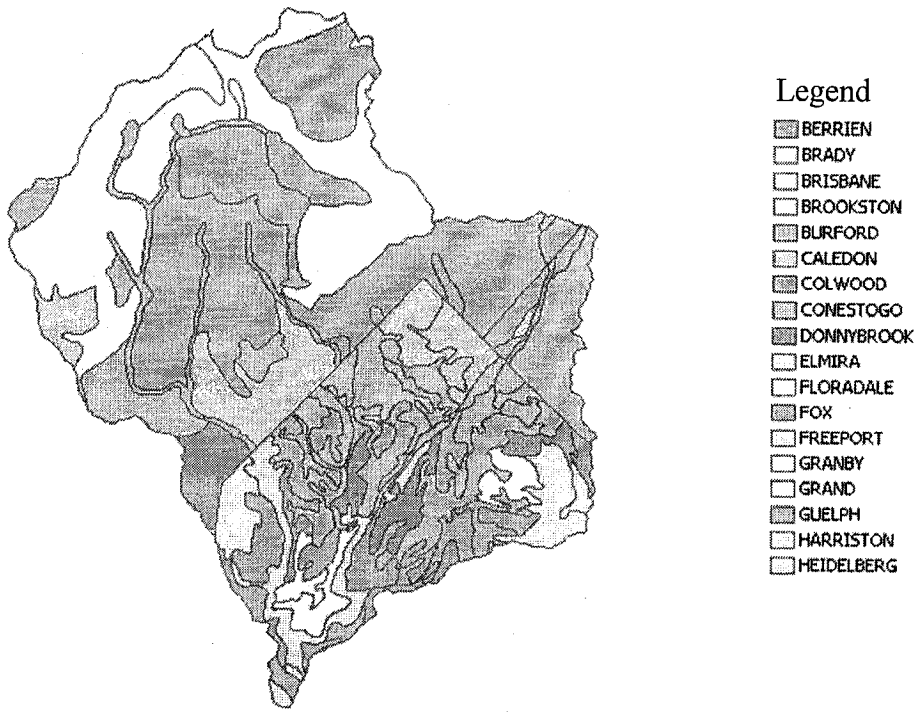

Figure 3.5 Soil map of Canagagigue Creek watershed

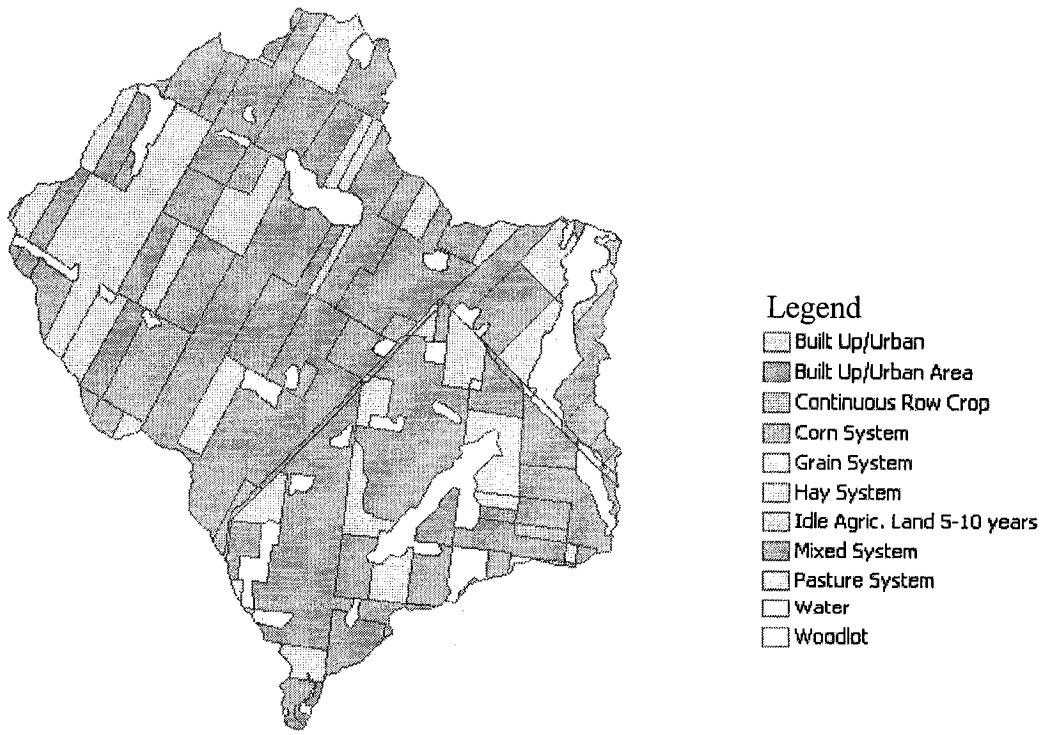

Figure 3.6 Land use map of Canagagigue Creek watershed

θ_{sat}, residual moisture content θ_r, saturated hydraulic conductivity K_s, pressure head at field capacity pF_{fc}, pressure head at wilting point pF_w, α, n and l. Both α (cm^{-1}) and n are curve shape factors; while l (unitless) is an empirical pore tortuosity/connectivity parameter. The van Genuchten parameters were entered into the model. The van Genuchten formula for determining the retention curve is

$$\theta(\psi) = \theta_r + \frac{(\theta_s - \theta_r)}{\left[1 + (\alpha\psi)^n\right]^m} \qquad \{3.26\}$$

The van Genuchten formula for determining Hydraulic conductivity is

$$K(\psi) = K_s \frac{\left(\left(1 + |\alpha\psi|^n\right)^m - |\alpha\psi|^{n-1}\right)^2}{\left(1 + |\alpha\psi|^n\right)^{m(l+2)}} \qquad \{3.27\}$$

Where

ψ is the pressure head,

$k(\psi)$ is the hydraulic conductivity function with respect to pressure head, and

$\theta(\psi)$ is moisture content function with respect to pressure head.

Table 3.1 shows land uses in the watershed by land use category. The continuous row crop is assumed to be corn, the grain system consists of soybean, while the hay and pasture system are alfalfa. The woodlot is assumed to be mostly boreal forest. The mixed system includes crop rotation: two years grain/silage corn, one year soybean, two years alfalfa forage, then back to corn. For each land use type, the model requires the leaf area index (LAI), rooting depth (RD) and crop coefficient (Kc) to be entered into the vegetation property file. Due to lack of data for the study area, appropriate values of RD, LAI and Kc were obtained from the literature.

Table 3.2 shows the values assigned for the different crops and trees on the watershed. The kc values were obtained from the FAO crop coefficient database (Doorenbos and Pruitt, 1977). For each stage, the crop coefficient values were assigned accordingly to the individual cropping system. According to Doorenbos and Pruitt (1977), the crop coefficient value should be 0.55 for the initial crop development stage,

Table 3.1 Percentage of each land use categories within the study area

Description of land cover	**Area (km^2)**	**Percentage of total area (%)**
Built up/urban area	0.1	0.2
Agriculture	46.5	88.6
- Continuous row crop (corn)	2.0	3.8
- Corn system (corn)	12.8	24.4
- Grain system (soybean)	7.7	14.7
- Hay system (alfalfa)	3.8	7.2
-Mixed system (corn/soybean/alfalfa)	19.8	37.7
- Pasture system (alfalfa)	0.4	0.8
Idle Agricultural Land 5-10 yrs	0.07	0.1
Water	0.04	0.08
Woodlot	5.9	11.2
Total	52.5	100

assuming the recurrence interval of significant rainfall (5 mm or more) to be about 7 days and the average ET_o to be 3.9 mm at the beginning of the growing season (May). At mid-season and harvest stages, the crop coefficient values were obtained from Doorenbos and Pruitt (1977), assuming the relative humidity to be greater than 70 % and wind speed to be 0 - 5 m s^{-1}. The values of LAI and RD of pine trees were used for the woodlot.

The geological properties describing the saturated zone are saturated hydraulic conductivity, specific yield, specific storage coefficient, and porosity. A boundary condition of gradient -0.00996 was specified in the lower portion of study area in the model, allowing for groundwater flow out of the watershed. This value is the elevation difference between the cells at the watershed outlet divided by the length between the cells.

Another watershed characteristic required by the model is surface roughness coefficient or Manning's M, the reciprocal of Manning's n*, for the different land covers. The values of Manning's n were taken from the literature (Engman, 1986; Ward and Trimble, 1995). Table 3.3 shows the Manning's M values for the different land uses in

Table 3.2 LAI, RD and Kc for corn, soybean, alfalfa and woodlot

Crops	Corn (grain/silage)				Soybean			
	D.O.G	LAI[a]	RD[b]	Kc[c]	D.O.G	LAI[a]	RD[b]	Kc[c]
Planting	1	0	0	0.55	1	0	0	0.55
Crop development	34	0.72	100	0.55	20	1	100	0.55
Mid-season	78	3.45	900	1.05	55	6.22	800	1
Late-season	132	3.45	900	1.05	115	6.22	800	1
Harvest	166 /141	2.5	900	0.55	143	4.22	800	0.45
Crops	Alfalfa				Woodlot			
	D.O.G	LAI[d]	RD[b]	Kc[c]	LAI[e]		RD[f]	
Planting	1	0	0	0.55	2.9		1200	
Before 1st harvest	69	3.2	500	1.05				
1st harvest	70	0.5	500	0.5				
Before 2nd harvest	161	3.2	500	1.05				
2nd harvest	162	0.5	500	0.5				

LAI - leaf area index (m^2 m^{-2}); RD – rooting depth (mm); Kc – crop coefficient (-); D.O.G – days of growth; a – Goel (2003); b – Jong and MacDonald (2001); c – Doorenbos and Pruitt (1977); d – D'Urso et al. (2004); e – Deblonde et al. (1994); f – Bannan (1940).

Table 3.3 Manning's n* and M for different land use types in the study area

Land use	**Manning's n***	**Manning's M**
Built up/Urban areas	0.011[a]	90.9
Continuous Row crop/Corn system/ Grain system/Mixed system	0.17[b]	5.9
Hay system / Pasture system	0.24[b]	4.2
Agricultural land idle for 5-10 yrs	0.05[b]	20
Water	0.04[b]	25
Woodlot	0.8[b]	1.25

Source: a – Engman (1986); b – Ward and Trimble (2004)

the watershed. For the mixed system, Manning's M was assigned 25 as corn and soybean are the predominating crops, compared to alfalfa, during the simulation period. The detention storage was assumed to be 2 mm, uniformly distributed over the watershed.

3.3.3 Model Simulation Time Step

The time steps used in the model for efficient simulation are: initial unsaturated zone time step (0.01 hr); maximum unsaturated zone time step (2 hrs); maximum saturated zone time step (8 hrs); minimum overland flow time step (0.01 hr); maximum overland flow time step (0.14 hr). The time steps are critical for minimizing overland water balance error which should be less than 1% of the total precipitation.

3.4 PRE-CALIBRATION MODEL SIMULATION

The model was initially run for a nine-year period. Since geological information of the watershed area was not available (depth to impermeable layer, mean water table level, etc.), several runs were done to achieve (i) the approximate base flow percentage encountered in the watershed (about 40%), (ii) the actual evapotranspiration (65 % annually), and (iii) a minimal water balance error (less than 1 %).

3.5 MODEL CALIBRATION, VALIDATION AND PERFORMANCE

Eight years of data were split into two halves for calibration and validation. However, one additional year's run was considered as model initiation for both calibration and validation runs. Statistical tools were used to analyze the results in order to evaluate the model performance for both calibration and validation processes.

3.5.1 Model Calibration

Model parameters represent the physical or hydrologic characteristic of a watershed (Singh, 1995). To adequately represent the system being modeled, during calibration, an iterative process, model parameters are set within an appropriate range.

During this process, each model parameter is varied following a trial and error procedure, with all other parameters being constant. Formal sensitivity analysis was not performed during this study, due to the model's high computational time. Nevertheless, it was found during the calibration process that Manning's M, the snowmelt constant, and the threshold melting temperature were sensitive model outputs. As mentioned by Refsgaard and Storm (1995), "the number of parameters subjected to adjustment during calibration process of a distributed hydrological model like MIKE SHE should be as small as possible". However, given the inability to fully characterise all hydrological processes and the possible difference in scale between the measurement and the model grid square, slight calibration is generally required. Consequently, the model was calibrated by adjusting the snowmelt constant, melting threshold temperature, and Manning's M for the last five years (from hydrologic year 1993-94 to 1997-98). These years were more representative, consisting of all year types, normal, wet, and dry years. Moreover, the data were complete for these years. The first year run was considered as initialization of the model, and was excluded in the model calibration. The results for the last four years were considered for model calibration.

3.5.2 Model Validation

Using parameters fine-tuned in the calibration process, the model was validated with the data from the first five years (from hydrologic year 1989-90 to hydrologic year 1993-94). Like calibration, the first year run was taken as model initiation, and excluded from model performance evaluation.

3.5.3 Model Performance

In addition to qualitative assessment with graphical displays, the model simulation results were evaluated quantitatively using statistical measures. Statistical parameters such as regression coefficients, mean deviation, root mean square error, coefficient of determination, and Nash-Sutcliffe coefficient were used.

The coefficient of determination is a measure of accuracy or the degree to which the measured and predicted values agree. The average deviation suggests whether the model over or under-predicted the values. The root mean square error (RMSE) measures the difference between predicted and observed values. It is sensitive to the extreme values and deals with both systematic and random errors. The Nash and Sutcliffe coefficient (EF%) measures the goodness-of-fit between observed and simulated daily stream flow. A value of 1 represents a perfect model, while a value of zero (0) shows a prediction no better than using the mean of the data. For negative efficiencies, the prediction is worse than simply taking the mean of the measured values.

$$RMSE = \sqrt{\frac{1}{n}\sum_{i=1}^{n}\left[(O_i - P_i)^2\right]} \qquad \{3.28\}$$

$$EF\% = 1 - \frac{\sum_{j=1}^{n}(O_i - P_i)^2}{\sum_{j=1}^{n}\left(O_i - \bar{O}\right)^2} \times 100 \qquad \{3.29\}$$

Where

O_i is the observed flow (mm),

$\bar{O}$ is the mean observed flow (mm),

P_i is the predicted flow (mm), and

n total number of observations.

3.6 MANAGEMENT SCENARIOS ANALYSIS

The MIKE SHE model was used to evaluate the impact of different scenarios on the watershed's hydrologic response. Overall, six scenarios were simulated: (i) urbanization, (ii) deforestation, (iii) conversion of pasture land into agriculture, (iv) diversification of corn system into cash crops, (v) application of tile drainage and (vi) effect of climate change.

Urbanization includes increasing the percentage of urban areas in the watershed by ten fold (from 0.2% to 2%). The areas closer to the existing urban area were chosen for urbanization, as they are more prone to such development.

Deforestation is a common phenomenon occurring in many watersheds around the world. Therefore, for the deforestation scenario, the woodlot areas were replaced by mixed system agriculture.

A general trend all over the world is to bring more area under agriculture to increase food production. While doing so, livestock practices may suffer, and pasture land may be converted to agricultural lands. Thus, the hay/pasture land was converted into mixed system agriculture in the third scenario.

In the scenario of diversification of corn system into cash crops, the areas practicing mono-cropping of corn were shifted to cash crop cultivation. Tomato (*Lycopersicon esculentum* Mill.), being a common cash crop, was considered for this scenario.

The tile drainage scenario was used to evaluate the effect, particularly in terms of stream flow, of installing drainage systems throughout the entire watershed. The model uses a simple drainage method, which considers a time constant and a drain depth. The time constant controls the amount of water being drained out of the soil profile, provided water table is above drain depth. A value of 1e-7 s^{-1} and 1 m were assigned to the time constant and drain depth, respectively.

Studies done on climate change have shown that, besides rising temperatures, there are an increase in rainfall intensity and somewhat more frequent rainfall in certain regions (Clarke, 1993). In this study however, the rainfall was shifted one month forward to study the effect of different rainfall patterns and quantities under different climates and eventually on the stream flow (R. P. Rudra, personal communication, May 2006).

Tables 3.4 and 3.5 show the vegetation properties for tomato crop and the model parameters subjected to adjustment for the multiple scenarios, respectively.

Table 3.4 Vegetative properties of a tomato crop

Crops	Tomato			
	D.O.G	LAI[a]	RD[b]	Kc[c]
Planting	1	0	0	0.55
Crop development	30	0	100	0.55
Mid-season	70	4.5	450	1.05
Late-season	115	4.5	450	1.05
Harvest	145	3.5	450	0.6

D.O.G – days of growth; LAI – leaf area index (m^2 m^{-2}); RD – rooting depth (mm); Kc – crop coefficient (-); a – Scholberg et al. (2000), b – Verhallen and Roddy (2003), c – Doorenbos and Pruitt (1977)

Table 3.5 Model parameters adjustment for multi-scenarios

Scenarios	Model Parameters							
	LAI	RD	Kc	M	DD	tc	PRC	PPT
Urbanization	0	0	-	109.1	-0.6	0	0.75	-
Deforestation	Corn	Corn	Corn	7.1	-	-	-	-
Mixed Agriculture	Corn	Corn	Corn	7.1	-	-	-	-
Cash Crops	Tomato	Tomato	Tomato	7.1	-	-	-	-
Drainage	-	-	-	-	-0.6	1e-7	-	-
Shifting Rainfall	-	-	-	-	-	-	-	1-month shift

LAI – leaf area index (m^2 m^{-2}); RD – rooting depth (mm); Kc – crop coefficient (-); M – Manning's M; DD – drainage depth (m); tc – drainage time constant (s^{-1}); PRC – paved runoff coefficient (-); PPT – precipitation (mm/day).

CHAPTER IV - RESULTS AND DISCUSSION

The nine-year data was divided into two sets, one (1993-94 to 1997-98) used for calibration, and another (1989-90 to 1993-94) for validation. The calibration years were chosen for the completeness of their observed data and their inclusion of representative years (normal, wet and dry). In both sets, the first year was used to initialize the model, and not considered in evaluations of model accuracy. The one-year model initialisation was important because the initial water table depth was estimated on the basis of the season, but might not have been representative of the actual depth, and thus needed to become stabilised. The model, once calibrated, was used to investigate the effect of different management scenarios on the watershed's hydrology. The results obtained in these processes (calibration, validation and management scenarios) are discussed in the following chapter. All the model runs began at the beginning of the hydrologic year (October 1) and ended September 30th of the next year (Schwab et al., 1993).

4.1 PRE-CALIBRATION MODEL SIMULATION

The first of nine years run was considered as model initialization ("warming-up" of model), and was excluded from the analysis of the results. The annual precipitations for the nine-year period were analysed, and those within the range of mean ± one standard deviation were considered 'normal', while years above and below the 'normal' range were considered 'wet' and 'dry', respectively. In the eight-year simulation period, there were two wet years (1990-91 and 1995-96), one dry year (1997-98), the remaining being normal years. The eight-year observed stream flow data had some gaps (d/m/y): 16-21/04/1991, 2-5/01/1992, 6-15/04/1992, 21-26/04/1992, 22-27/09/1992, 27/10/1992 to 1/11/1992, 31/12/1992, 26-31/10/1993, 5-6/07/1994, 8-10/07/1994, 2/01/1996 to 11/02/1996, and 31/12/1996. Missing data are indicated in figures by double-sided arrows. Periods for these missing data were excluded from analysis.

4.1.1 Analysis of Hydrographs

Precipitation hyetographs along with simulated and observed hydrographs for the eight-year period (Figures 4.1 to 4.8) show that the simulated hydrographs generally matched their respective observed hydrographs well. The timing of simulated and observed peaks matched reasonably well; however, in some instances, simulated peak runoffs were slightly over- or under-estimated. These runoff events mostly followed precipitation events, except in the winter/spring period when runoff occurred mainly due to snowmelt.

4.1.2 Statistical Analysis

A year-wise statistical analysis (Table 4.1) showed annual mean deviations (AD) to range from –0.10 to 0.39 mm, negative values indicating a slight over-prediction of runoff in four years (1990-91, 1992-93, 1993-94, and 1997-98), and positive values for the remaining years indicating slight under-prediction. The overall (8-year) AD value of 0.06 mm indicates that the model marginally under-predicted runoff. The coefficients of determination (R^2) were more or less similar for all eight years, with a mean value of 0.43, indicating a fairly close relationship between observed and simulated runoff. The Nash-Sutcliffe coefficient (EF %) varied from 6.6 to 48%, showing a fair performance; however, for 1993-94, the EF% was negative indicating poor performance. Though the overall regression parameters for that year were good (slope – 0.91 and intercept – 0.16), for certain events large discrepancies existed between observed and simulated runoff. As the EF% places greater weight on larger differences, a negative EF% was obtained. Good performance was exhibited for the years 1994-95, 1996-97 and 1997-98, with EF% of 45.7%, 47.5% and 48.0%, respectively. The overall 8-year EF% was 25.5%. Over individual years the root mean square error (RMSE) varied between 1.2 and 2.9 mm, showing the simulation errors were not very high. The t-test results showed that the overall 8-year slope (0.7) and intercept (0.25) were statistically different from their ideal values of 1 and 0, respectively (Table 4.1). This analysis indicates that the results, on the whole, were not very good; however, this test is quite stringent (Bera et al., 2005).

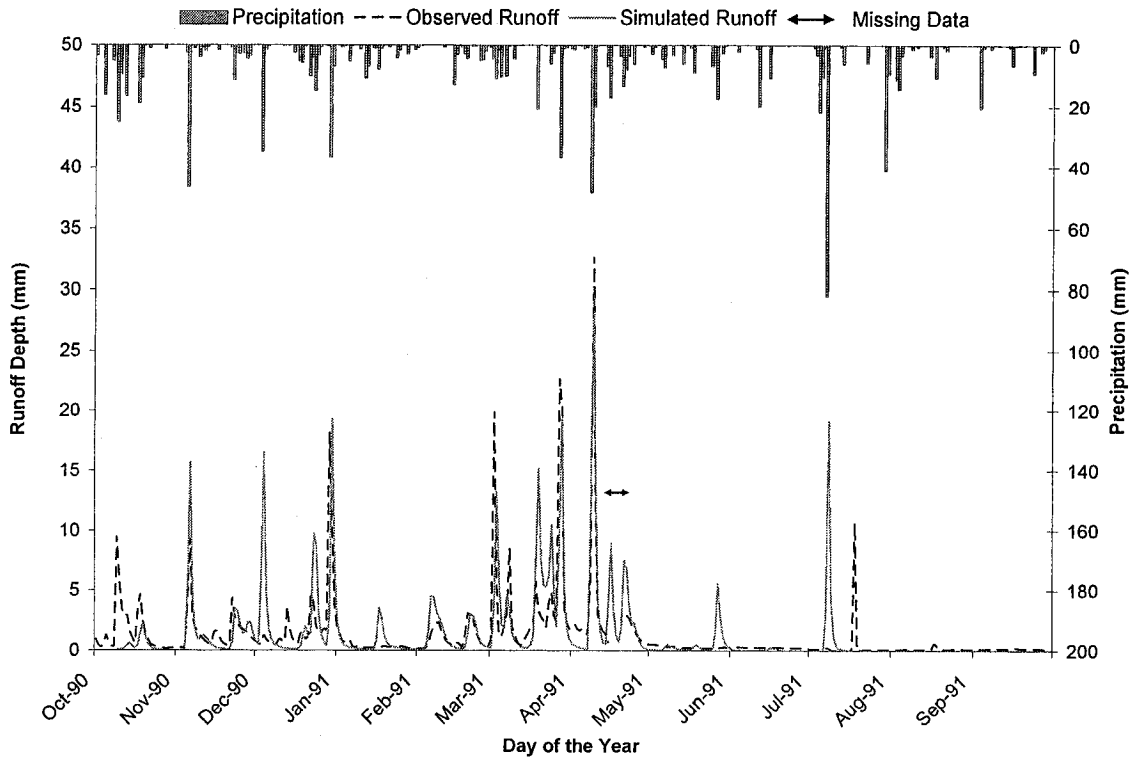

Figure 4.1 Hyetograph and hydrographs for pre-calibration simulation– 1990-91

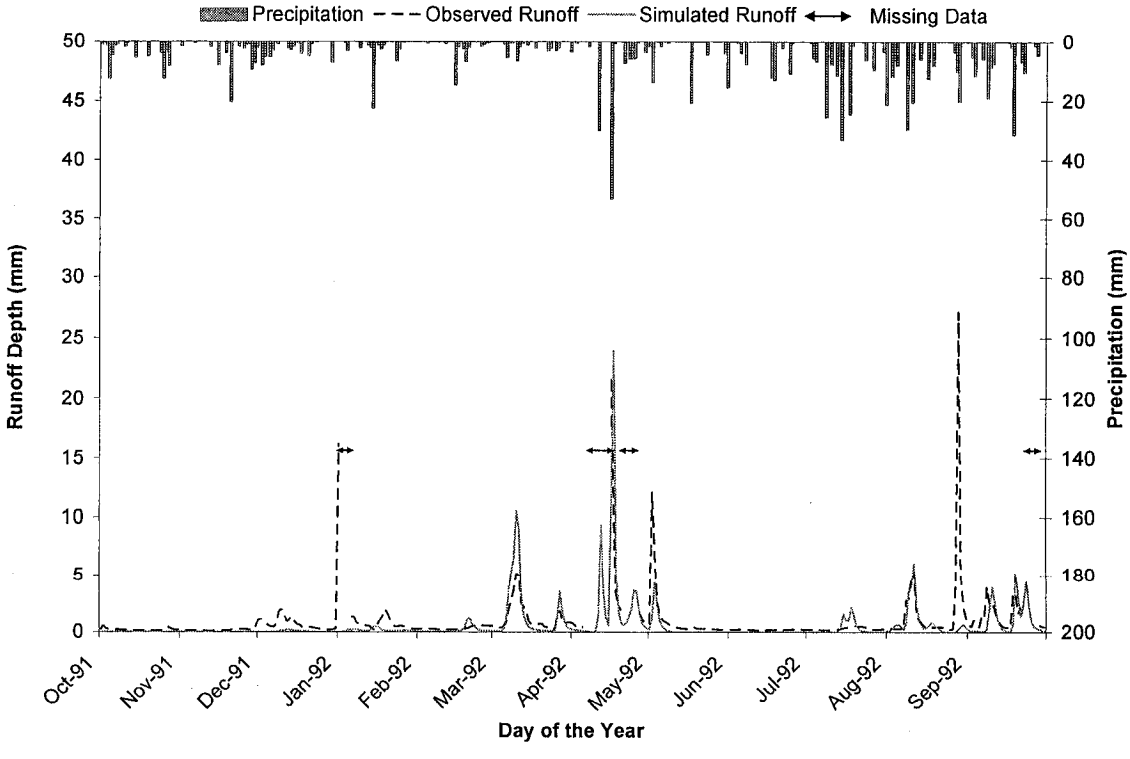

Figure 4.2 Hyetograph and hydrographs for pre-calibration simulation– 1991-92

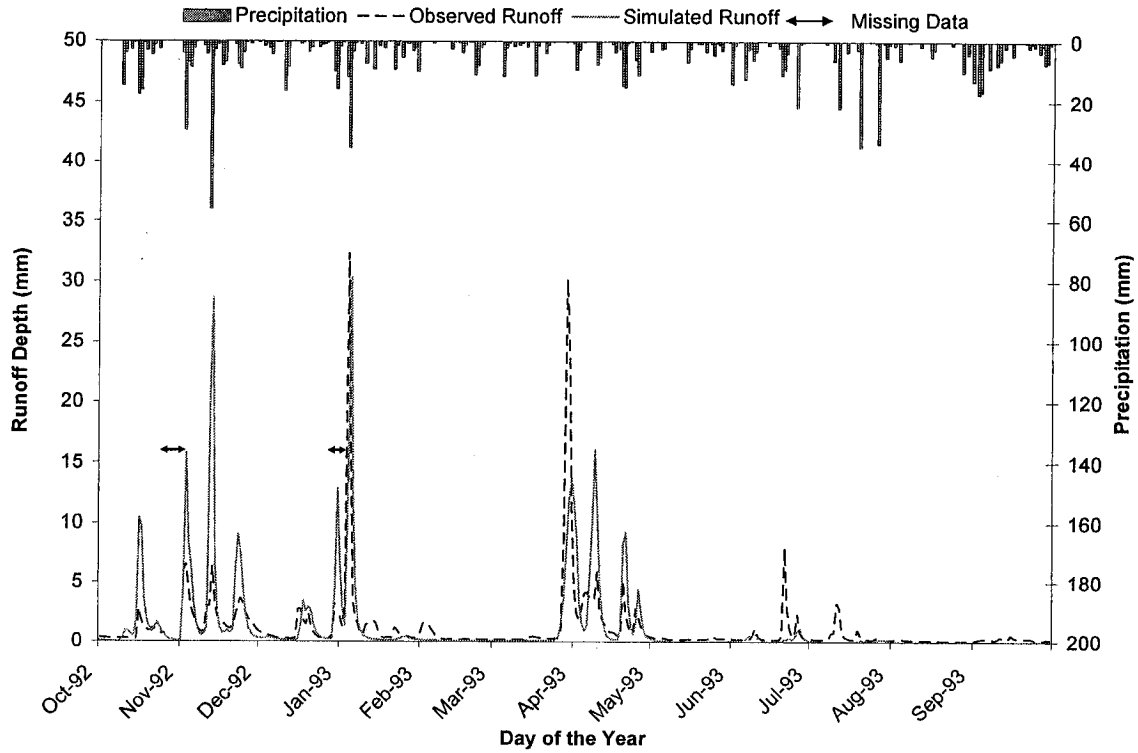

Figure 4.3 Hyetograph and hydrographs for pre-calibration simulation– 1992-93

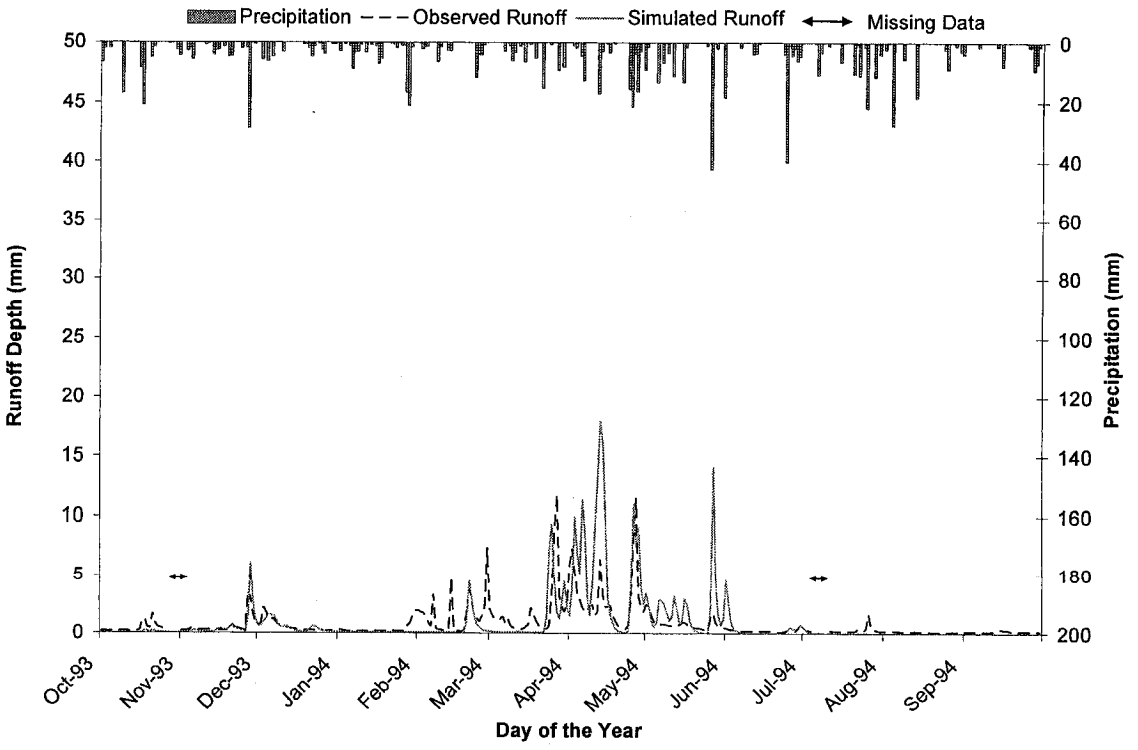

Figure 4.4 Hyetograph and hydrographs for pre-calibration simulation– 1993-94

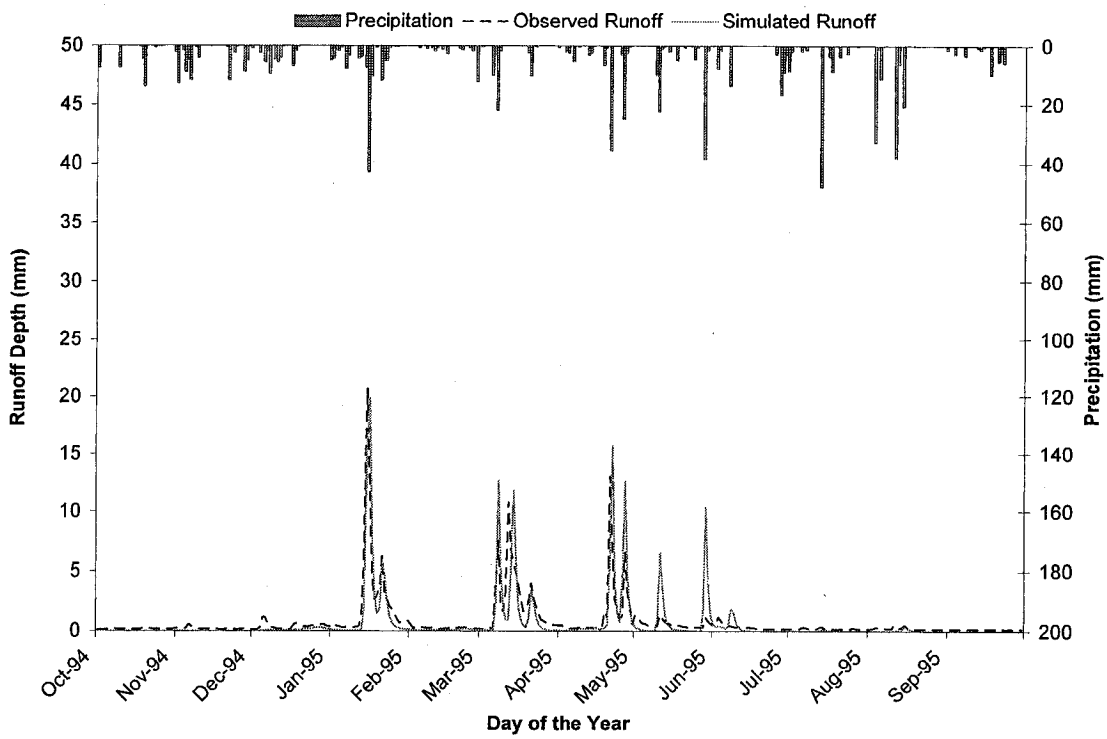

Figure 4.5 Hyetograph and hydrographs for pre-calibration simulation– 1994-95

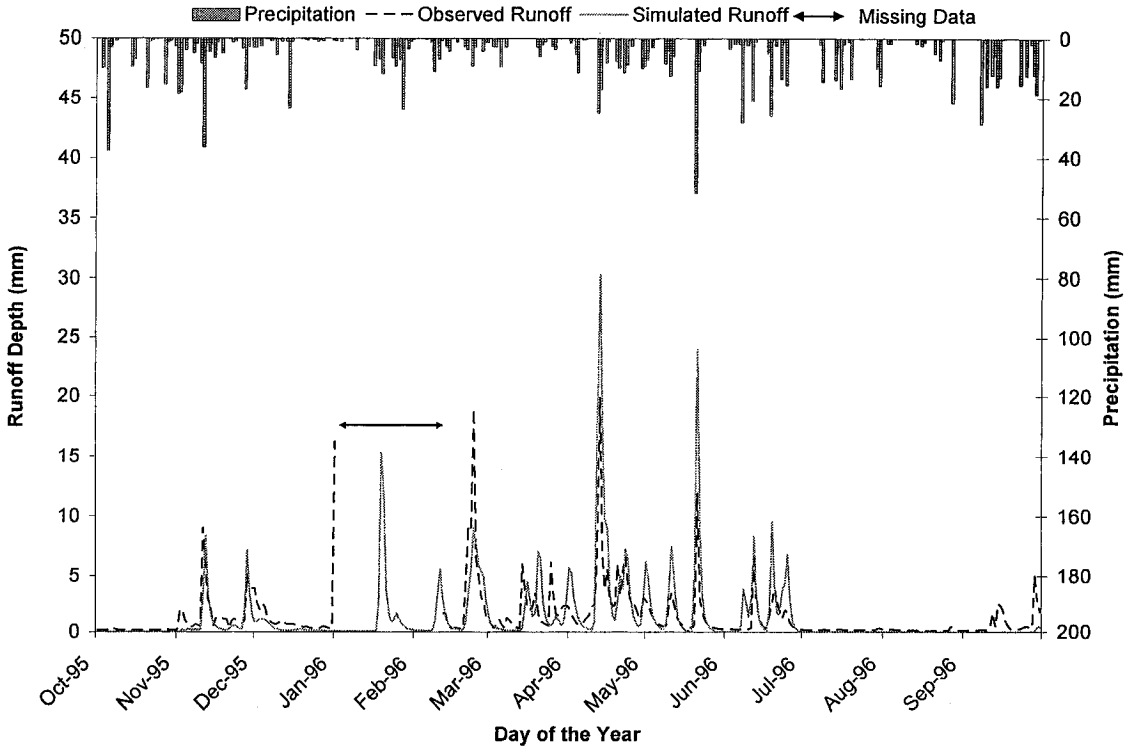

Figure 4.6 Hyetograph and hydrographs for pre-calibration simulation– 1995-96

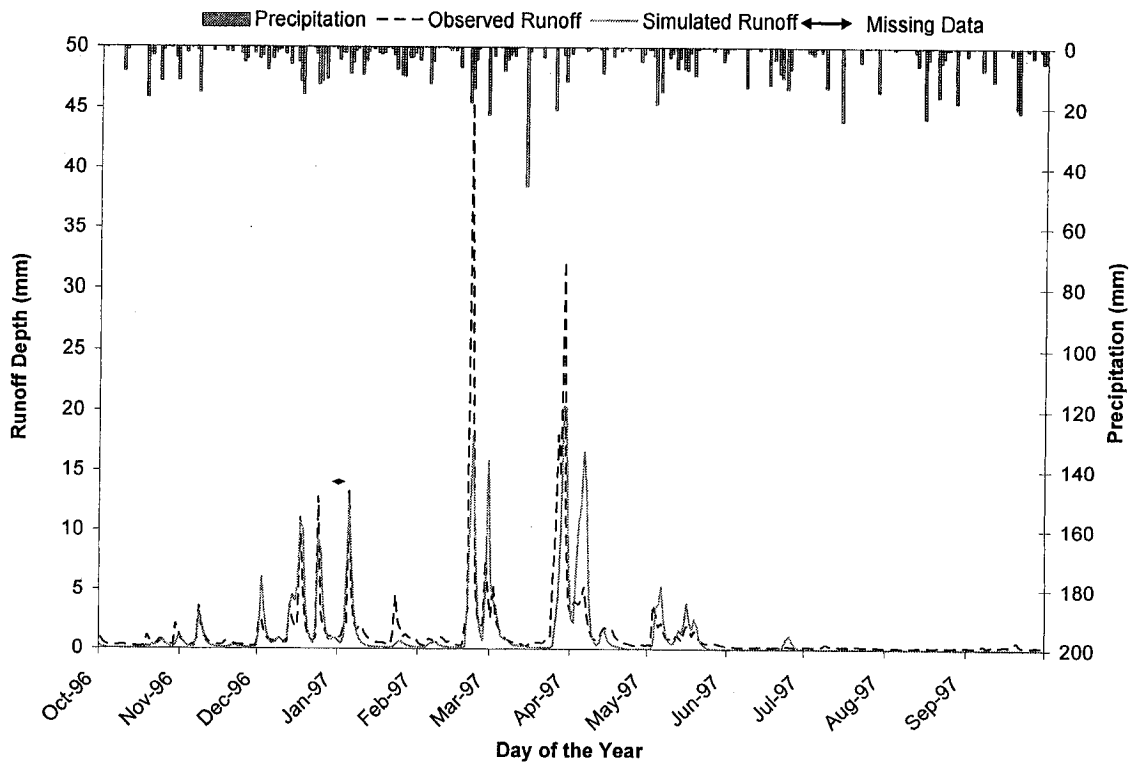

Figure 4.7 Hyetograph and hydrographs for pre-calibration simulation– 1996-97

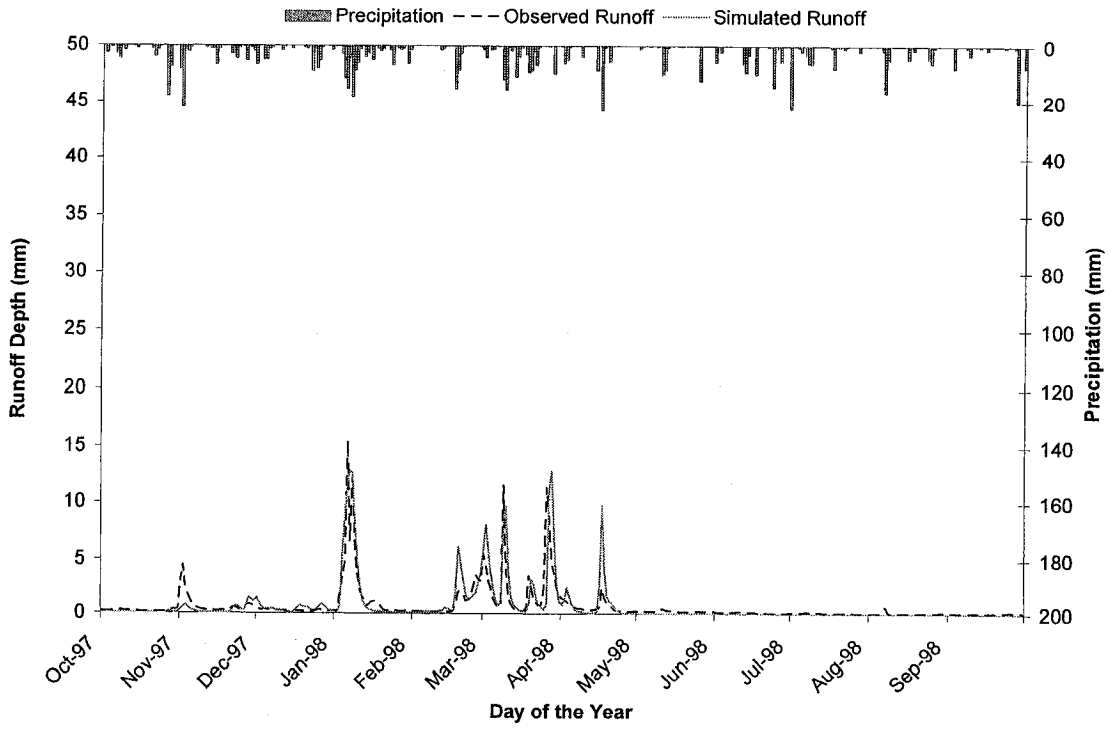

Figure 4.8 Hyetograph and hydrographs for pre-calibration simulation– 1997-98

Overall, statistical analyses showed that the performance of the MIKE SHE model in simulating hydrological processes was average, and further calibration was required.

Table 4.1 Model Evaluation Results for eight years simulation

Hydrologic Year	Observed Runoff (mm)	Simulated Runoff (mm)	AD (mm)	R^2	RMSE (mm)	EF (%)	Regression Parameters	
							Slope	Intercept (mm)
1990-91[a]	475	483	-0.02	0.45	2.6	29.1	0.72*	0.39*
1991-92	311	179	0.39	0.26	2.2	15.3	0.39*	0.17
1992-93	411	449	-0.10	0.36	2.9	6.6	0.69*	0.46*
1993-94	300	329	-0.08	0.31	2.0	-85.4	0.91	0.16
1994-95	282	233	0.13	0.63	1.4	45.7	0.94	-0.09
1995-96[a]	440	431	0.03	0.52	2.2	16.7	0.94	0.05
1996-97	489	428	0.17	0.49	2.6	47.5	0.56*	0.43*
1997-98[b]	254	261	-0.02	0.65	1.2	48.0	0.98	0.04
Total	2963	2793	0.06	0.43	2.2	25.5	0.70*	0.25*

a - wet year; b – dry year; AD – mean deviation; R^2 – coefficient of determination; RMSE – root mean square error; EF (%) – Nash-Sutcliffe coefficient; * - slope and intercept are significantly different ($P \leq 0.05$) from their ideal values of 1 and 0, respectively.

4.2 MODEL CALIBRATION

The model calibration involved adjusting model parameters in such a manner that simulated and measured values showed a better match. The model was calibrated over five years of data (1993-94 to 1997-98). Again, first year of the calibration set was used to initialize the model, and the results for the remaining four years were used to evaluate the calibration process. In this study, the snowmelt constants (degree-day factor and threshold melting temperature) as well as the Mannings' M were adjusted so as to match simulated and observed runoff. At first, a degree-day factor of 2 mm and a threshold melting temperature of $0^{o}C$ were used as suggested in the model. The degree-day factor of 2 mm did not give adequate snowmelt during the snowmelt period, when compared to

observed runoff. Thus, the model was run with a range of degree-day factors (1.5, 2, 2.5, 3, 3.5, and 4) to find the best possible match between observed and predicted. A degree-day factor of 4 mm resulted in greater snowmelt during the winter period, while the 1.5 mm gave rise to greater snowmelt in the late spring. A degree-day factor of 3.5 mm simulated snowmelt events adequately, both in terms of the number of runoff peaks and the timing of runoff peaks, thus giving a better model performance. Though a threshold melting temperature of 0°C is a realistic value, it was varied to determine its impact on surface runoff. It was found that the simulated hydrographs with 0°C matched observed hydrographs. Therefore, it was chosen as the final value. After adjusting the degree-day factor and threshold freezing/melting temperature, the runoff peaks were analyzed.

Table 4.2 Model parameters subjected to calibration

Model Parameters	Initial Simulation	Calibrated parameters	Final Calibration
Degree-day factor (mm snow/day/°C)	2	1.5, 2, 3, 3.5, 4	3.5
Threshold melting temperature (°C)	0	0, 0.8, 1	0
Mannings' M			
-Urban area	90.9	109.1	109.1
-Agricultural crops	5.9	7.1	7.1
-Hay/Pasture	4.2	5.0	5.0
-Fallow land	20	24	24
-Water	25	30	30
-Woodlot	1.25	1.5	1.5

There nonetheless remained some mismatch between the timing of the runoff peaks, simulated peaks generally lagging observed peaks by one or two days. An adjustment in the timing of peaks was attempted by increasing the Mannings' M parameter by 20 % over the entire watershed and thus reducing the surface roughness and increasing the surface runoff velocity. This improved the match between the observed and simulated peaks. Table 4.2 showed the model parameters subjected to calibration.

4.2.1 Water Balance Analysis

The annual water balance summaries for the four years of calibration, and the water table level on October 1st of each water year are presented in Tables 4.3 and 4.4, respectively. Since the model simulated the water table depth for each grid, a mean water table could be calculated by averaging that of all the model's grids. However, to simplify the process, water table depths were taken from five representative grids and averaged. The water balance error was obtained by balancing all the major hydrologic components simulated in the model (precipitation, evapotranspiration, runoff, and changes in storage). This error was then divided by the precipitation and presented as a percent error. The model simulated water balance well, with an acceptable relative error (<1%). From 49 to 88% (mean = 66%) of annual precipitation was simulated as being lost in evapotranspiration across the watershed. In the dry year, evapotranspiration was 599 mm (88%), but only 560 mm in the wet year (49%). This indicates that the model simulated actual evapotranspiration reasonably well.

The change in storage simulated by the model indicated an increase/decrease in water table depths over a given year. For example, the decrease in storage for the hydrologic year 1994-95 implies that the water stored in the soil contributed to surface runoff and evapotranspiration, which overall dropped the water table level from 1.66 m to 1.81 m. While for hydrologic year 1995-96, there was an increase in storage. This can be explained by the precipitation being partly infiltrated into the soil profile as it was a wet year, thus raising the water table depth from 1.81 m to 1.23 m. Although the following year (1996-97) was a normal year and only 230 mm of rainfall fell, the runoff was quite similar (only 30 mm less). Thus the water table dropped by 0.33 m. The last year (1997-98), being a dry year, there was additional decrease in storage, thereby dropping the water table further. In addition, it was found that the model simulated baseflows more or less adequately during the entire year. This was verified by using the WHAT model, which determines baseflow from total streamflow to be 40 % annually for this watershed (Engel et al., 2004).

Table 4.3 Annual Water Balance for Model Calibration

Water Year	PPT (mm)	ET (mm)	RO (mm)	Change in Storage (mm)	Error in mm (%)
1994-95	814	618	244	-46	-2 (0.2)
1995-96[a]	1136	560	444	128	4 (0.4)
1996-97	906	545	414	-50	-3 (0.3)
1997-98[b]	678	599	265	-181	-5 (0.7)
Total	3534	2322	1368	-149	-7 (0.2)

a – wet year; b – dry year; PPT – precipitation; ET – evapotranspiration; RO – runoff

Table 4.4 Simulated Water Table Depths during the calibration Period

Calibration Year	Oct 1994	Oct 1995	Oct 1996	Oct1997	Oct 1997
Mean water table depth (m)	1.66	1.81	1.23	1.56	2.04

The seasonal water balances as well as the seasonal observed runoff are given in Table 4.5. The results indicate that the model simulated the greatest actual evapotranspiration during the summer period. However, the greatest recharge and runoff were found to occur during the winter season, instead of spring. This is explained by the large quantity of recharge and runoff occurring in the March/April months, as shown in the monthly water balance summary (Table A.1 in Appendix A). In this study, April was considered to be in the spring and March in the winter. There was also high runoff and recharge in the month of January. Such high simulated runoff was justified by the high observed runoff which occurred in the same month. The greater recharge simulated by the model was due to its inability to address frozen soil conditions, leading to greater simulated infiltration into the soil and thus greater recharge. Therefore, greater runoff was simulated in the winter months.

Table 4.5 Seasonal Water Balance for the calibrated model

Water Year	**Winter (Dec/Jan/Feb/Mar)**						**Spring (Apr/May)**					
	PPT	ET	BF	Re	S_RO	O_RO	PPT	ET	Bf	Re	S_RO	O_RO
1994-95	241	38	51	9	151	176	178	119	-25	5	59	66
1995-96	230	35	54	12	190	161	237	111	-30	7	130	149
1996-97	392	38	60	15	314	348	114	123	-28	3	39	82
1997-98	276	41	54	13	200	184	94	147	-20	2	24	26
Mean	285	38	55	12	214	217	156	125	25	4	63	81
Water Year	**Summer (Jun/Jul/Aug)**						**Fall (Sep/Oct/Nov)**					
	PPT	ET	Bf	Re	S_RO	O_RO	PPT	ET	Bf	Re	S_RO	O_RO
1994-95	249	351	19	2	14	24	284	106	21	5	59	64
1995-96	263	328	24	4	50	46	254	79	31	5	60	59
1996-97	222	306	19	1	10	17	198	84	26	4	46	35
1997-98	146	320	10	1	2	12	-	-	-	-	-	-
Mean	220	326	18	2	19	25	245	90	26	5	55	53

PPT – precipitation (mm), ET – actual evapotranspiration (mm), BF – baseflow (mm), Re – recharge (mm), S_RO – simulated runoff (mm), O_RO – observed runoff (mm)

4.2.2 Analysis of Hydrographs

While the calibrated model's simulated hydrographs showed a relatively good temporal match to observed hydrographs for the four years' calibration period, the model did at times over- or under-predict surface runoff (Figures 4.9 to 4.12).

In a few cases, anomalies occurred, presumably a result of recording equipment malfunctions: for example, on 1/01/1996 (Figure 4.10), extremely high observed runoff (16.3 mm) was recorded, in spite of the fact that the temperature remained below freezing and little precipitation had fallen during the preceding days. The fact that the equipment failed to record the subsequent period of 02/01/1996—11/02/1996, supports this view. However, the high simulated runoff (17.7 mm) on 19/01/1996 (Figure 4.10) is justified by the important rainfall events on that and preceding days (29.8 mm; ENV CAN, 2005).

4.2.2.1 Summer/Fall Season

Certain runoff events were slightly overestimated (July/August 1995, end June 1996, 25/06/1997, 21/09/1997, and end November 1997) during the summer/fall period. It is suspected that the watershed experienced greater actual evapotranspiration and infiltration compared to what was simulated by the model. Since field data for hydraulic conductivity was not available, it was estimated from the percentage of soil textural classes using the Rosetta software. Furthermore, soil hydraulic conductivity was considered to be uniform throughout the year. In reality, the soil's conductivity can be altered by cultivation operations. Similarly, root development and the enhanced activities of earthworms and other organisms could result in preferential flow through macropores. Therefore, the hydraulic conductivity of the soil might actually have been greater than the value used in the simulation. The model has an option for bypass flow; however it applies to the entire year, so that it is not possible to simulate seasonal variations in hydraulic conductivity (see Jayatilaka et al., 1998).

On 19/06/1996 (Figure 4.10), for example, there was 7.4 mm of simulated runoff compared to 4 mm of observed runoff, arising from a rainfall event of 31.6 mm on the previous day (ENV CAN, 2005). Also, sometimes the lower actual evapotranspiration

and hydraulic conductivity led to the simulation of extra runoff peaks, although very small (e.g. 25/06/1997, Figure 4.11).

Conversely, some simulated runoff peaks were found to be smaller than the observed peaks (12/06/1996, September 1996, 2/11/1997). Greater observed runoff peaks for these events are possibly due to high intensity, short duration storms, usually observed during the summer months. For example, on 28/09/1996 (Figure 4.10), the observed runoff (5.1 mm) was almost twice that simulated (2.4 mm) due to a rainfall depth of 33 mm on that day and those preceding it. These observations indicate that the model had difficulty in simulating runoff for certain events due to (i) the quality of data (daily data) and (ii) spatial and temporal variations in soil and environmental conditions. In cases where hourly rainfall data is considered, the model would likely be better able to simulate the high intensity, short duration rainfall event.

In spite of the over- and under-prediction, the model performed well for the following events: 28/11/1995, 12/06/1996, 8/11/1996, and 2/11/1997. These predicted events matched perfectly with the observed runoff. For example, on 8/11/1996 (Figure 4.11), the simulated and observed runoffs were 4.1 mm and 3.7 mm, respectively, arising from a 15.2 mm rainfall event on the previous day. Although for the same periods, such phenomena were not observed for all the years, this could be explained by spatial and temporal variability in the soil properties and the growth of vegetation. In addition, the time to peaks for the simulated and observed runoff events matched very well during this period (e.g. 12/06/1996, 8/11/1996, and 2/11/1997), possibly because the adjusted Mannings' M was able to represent the watershed surface's roughness coefficient adequately.

4.2.2.2 Winter/Spring Season

Like in the summer/fall season, the model under- or over-estimated the runoff for certain events through the winter/spring period. Though the model was able to use hourly data (air temperature and precipitation, etc.), availability and use of mean daily data was a major drawback during this simulation. The daily air temperature incorporated in the model was unable to consider diurnal variations in temperature. This is most important

during the winter/spring season, especially when the temperature is near the threshold freezing/thawing temperature. During the day, the temperature may rise above freezing, and drop below freezing during night, but when the mean daily temperature is below freezing, the model assumes precipitation to be in the form of snow, even if, when the temperature was above freezing, rain may have fallen and contributed to runoff. Furthermore, the model considers the mean daily temperatures at a specific time of the day and then temperatures are linearly interpolated. Thus, the model is not able to properly partition precipitation into rainfall or snowfall. Also, the model is not able to consider extreme events such as freezing rain or snow pellets, occurring when the temperature is above 0°C, or rain at temperatures below 0°C. Moreover, although the model considers freezing and thawing of snow on the soil surface, it does not consider the effect of temperature on the soil profile. In winter, the soil remains frozen; however the model does not include changes in the physical properties of the soil. Thus, due to the frozen soil conditions, infiltration can be impeded, resulting in greater surface runoff. Apparently, the model does not take into account frozen soil conditions and thus tends to simulate greater infiltration than occurs in the winter/spring period. In addition, snowmelt depends on the number of degree-days, which is calculated based on the mean daily temperature. Furthermore, melting may not occur exactly at a threshold value, e.g. 0°C, while the model considers both the freezing point and melting point as the same temperature (0°C). Therefore, the model may over- or under-estimate the amount of snowfall and rainfall as well as snowmelt.

Therefore for certain events, the model underestimated runoff (15/01/1995, 21/04/1995, 24/02/1996, 13/04/1996, 17/12/1996, 24/12/1996, 5/01/1997, 21/02/1997, 29/03/1997, 6/01/1998, and 8/01/1998). On 21/02/1997 (Figure 4.11), observed runoff (45.5 mm) was over twice the simulated runoff (20 mm), likely as a result of frozen soil conditions and the melting of the previously accumulated snow on the surface. There was a combined rainfall of 32.4 mm on the day and its predecessor, whereas the model considered the rainfall (18.4 mm) on the previous day as snow. This was verified with data from environment Canada. On the runoff day, maximum and minimum temperatures were 12.6°C and 5°C, respectively, whereas the mean recorded temperature was 8.8°C. Based on the degree-day method, mean daily temperatures of 8.8°C and of 12.6°C would

melt a maximum of 30.8 mm and 44.1 mm of snow, respectively, depending on how much snow was available (using a degree-day factor of 3.5 mm snow/day/°C). Therefore, considerable snowmelt would have occurred from the previously accumulated snow with the higher degree-day, resulting in greater runoff compared to the model which had more snow for melting but lower degree-days. In addition, the mean temperature being below the freezing point on almost every other day of that month (February 1997; ENV CAN, 2005) resulted in frozen soil conditions, thus reducing the amount of infiltration.

On the other hand, in certain cases, the model simulated greater runoff than was observed (8/03/1995, 13/03/1995, 23/01/1997, and March 1998). For example on 8/03/1995 (Figure 4.9), the temperature dropped below 0°C (ENV CAN, 2005), causing the rainfall from the previous day to freeze on the ground. However, the model does not consider water freezing on the ground surface, eventually simulating greater runoff. Furthermore, in the following days, there would be less simulated accumulated snow on the ground surface, resulting in less subsequent runoff on 13/03/1995 (Figure 4.9).

For most of the events during the winter/spring period, simulated and observed timing of runoff peaks was found to differ by one day (e.g. 15/01/1995, 21/02/1997, 9/03/1998, and 26/03/1998). This difference is thought to arise due to the quantity of accumulated snow on the soil surface under diurnal temperature variations resulting in differences in the roughness of bare and snow-covered land surfaces. The model considers the same surface roughness coefficient irrespective of the day of the year and the soil surface conditions. In reality, the flow velocity is higher on the snow covered surfaces, thus the time for the runoff to reach the watershed outlet is faster.

Nonetheless, the model performed reasonably well for certain events in this period (e.g. 8/03/1995, 27/04/1995, 11/05/1995, 29/05/1995, 13/04/1996, 21/05/1996, 17/12/1996, and 29/03/1997). On 21/05/1996, the observed and simulated runoffs were 12 mm and 15.9 mm, respectively, from a rainfall event of 62.8 mm on the same and previous day. Peaks' timing matched perfectly for some events, particularly at the beginning of the winter and in the spring (e.g. 27/04/95, 21/05/1996, 17/12/1996, and 24/12/1996), when lesser quantities of snow were accumulated on the soil surface (ENV CAN, 2005).

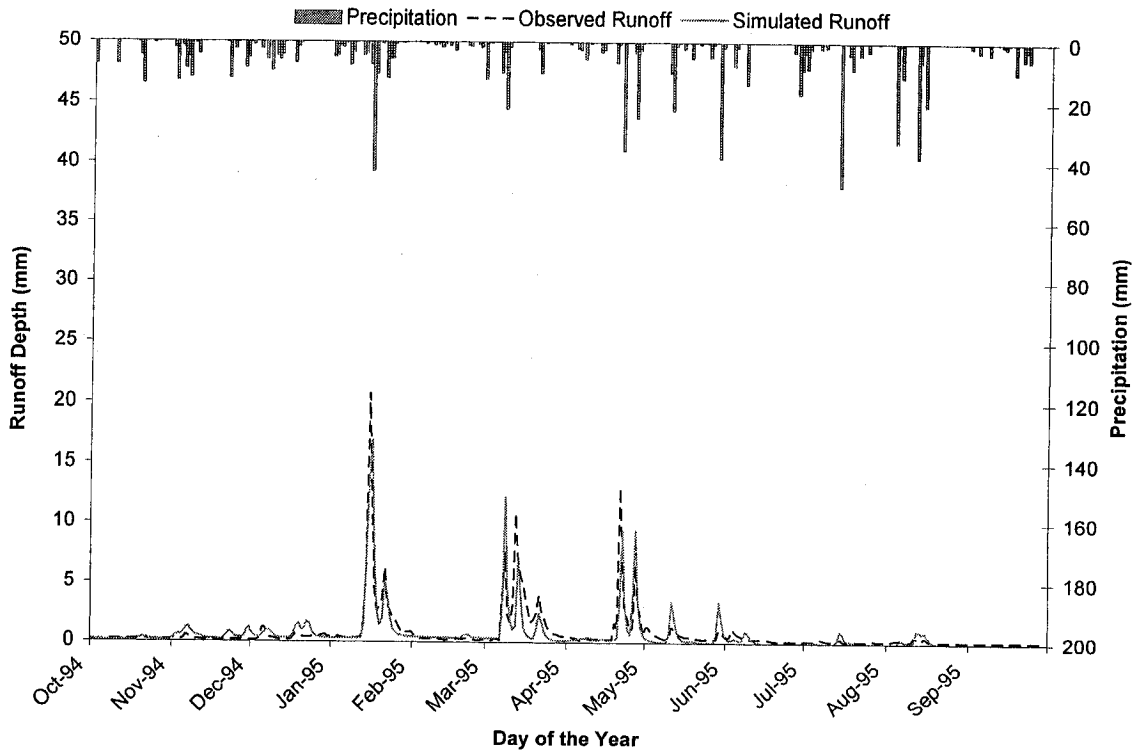

Figure 4.9 Hyetograph and hydrographs for the calibrated model – Year 1994-95

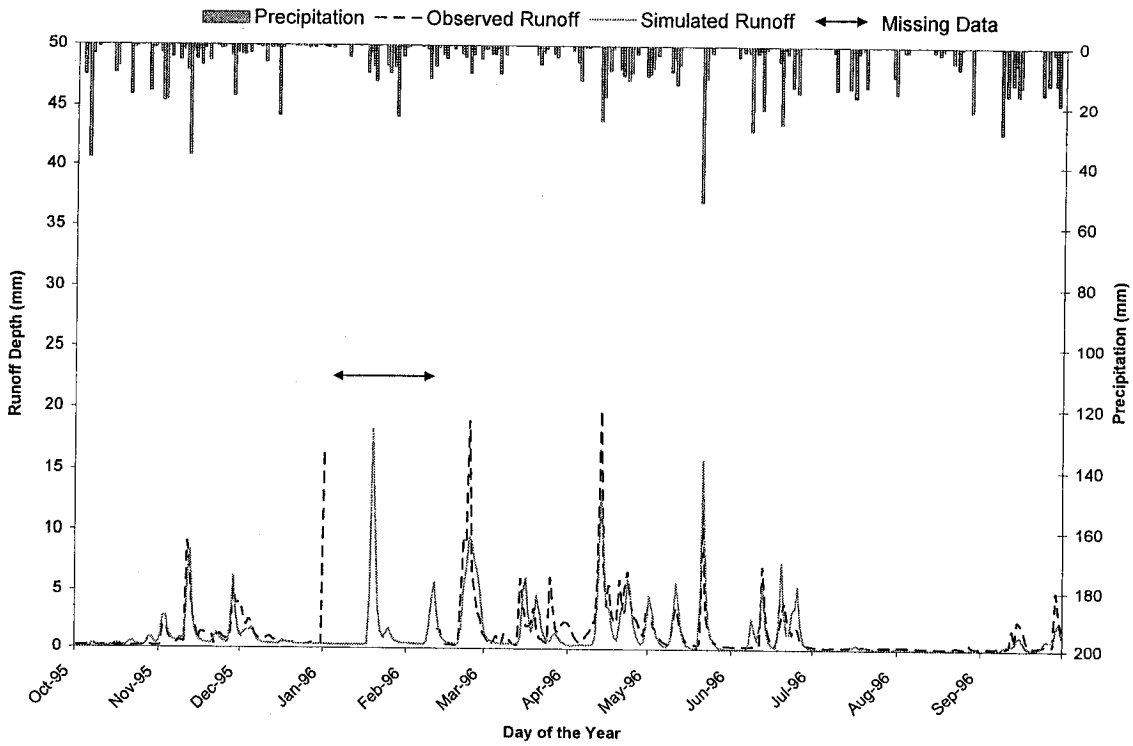

Figure 4.10 Hyetograph and hydrographs for the calibrated model – Year 1995-96

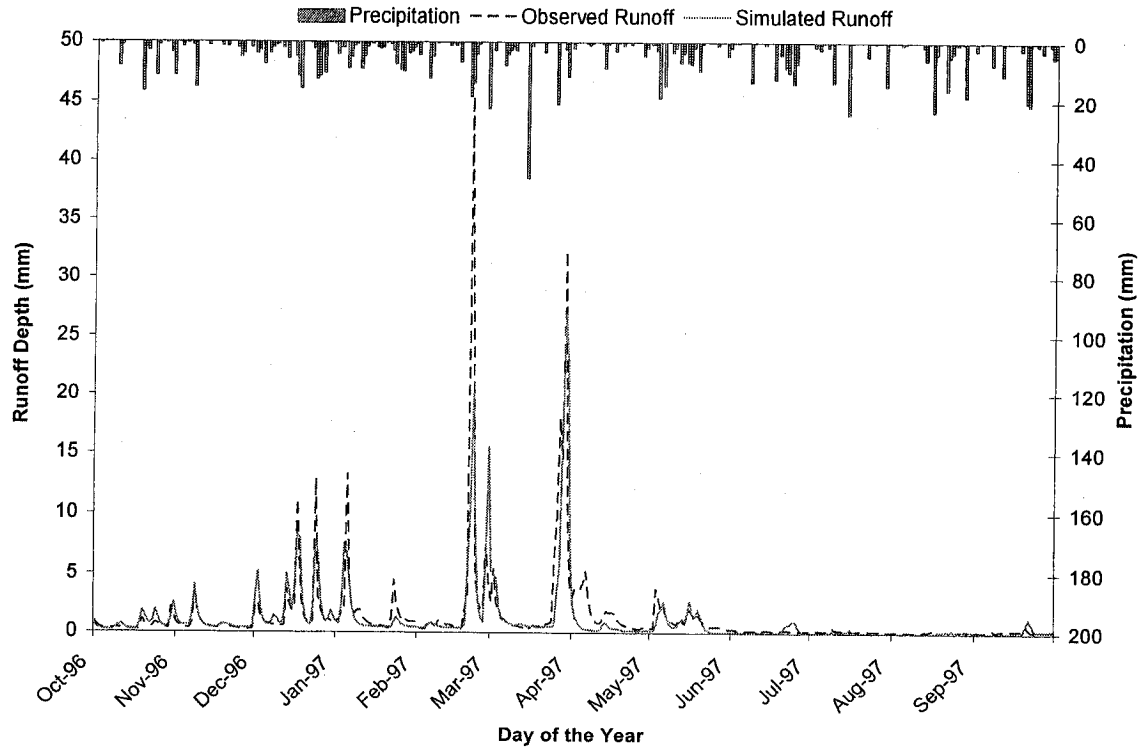

Figure 4.11 Hyetograph and hydrographs for the calibrated model – Year 1996-97

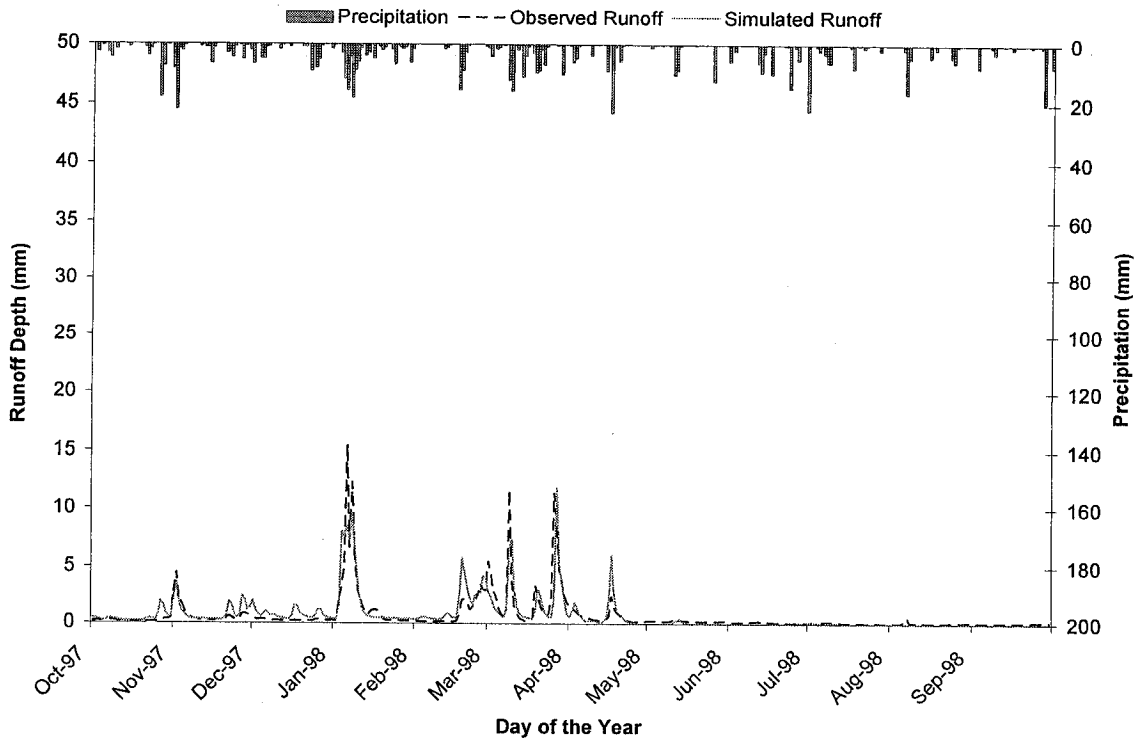

Figure 4.12 Hyetograph and hydrographs for the calibrated model – Year 1997-98

4.2.3 Statistical Analysis

The four-year mean deviation of +0.12 mm between observed and simulated runoff indicates that the model slightly under-predicted runoff (Table 4.6). For the wet year of 1995-96 and the normal years of 1994-95 and 1996-97, the model underestimated runoff, while in the dry year of 1997-98, model predictions were quite accurate. Mean deviation values, ranging from –0.03 to 0.21 mm, indicate that daily over- or under-estimations of runoff were small. The coefficient of determination was above 0.56 for all four calibration years (Table 4.6), showing good correlation between the simulated and observed runoff. The modeling errors were low: the RMSE ranged between 1.0 to 2.4 mm, further indicating a good simulation. The regression parameters, though significantly different from their ideal values (1 and 0) were fair, with the overall slope and intercept values being 0.63 and 0.27 mm, respectively. Ultimately, the model performance was tested by the EF%, which ranged from 55.5 to 66.4%, again corroborating that the observed and predicted runoff volume matched quite well. If one excludes the wet year's apparently erroneous observed runoff of 16.3 mm on 1/01/1996 [2nd paragraph in Section 4.2.2], the EF% for the year rises to 66.6% and that for the overall calibration period to 60.9%.

Table 4.6 Model Performance during Calibration

Hydrologic Year	Observed Runoff (mm)	Simulated Runoff (mm)	AD (mm)	R^2	RMSE (mm)	EF (%)	Regression parameters	
							Slope	Intercept (mm)
1994-95	282	244	0.10	0.67	1.1	66.4	0.75*	0.09
1995-96[a]	440	378	0.20	0.58	1.6	56.8	0.65*	0.29*
1996-97	489	413	0.21	0.56	2.4	55.5	0.56*	0.38*
1997-98[b]	254	265	-0.03	0.67	1.0	65.7	0.75*	0.21*
Total	1465	1300	0.12	0.59	1.6	59.0	0.63*	0.27*

a - wet year; b – dry year; AD – mean deviation; R^2 – coefficient of determination; RMSE – root mean square error; EF (%) – Nash-Sutcliffe coefficient; * - slope and intercept are significantly different ($P \leq 0.05$) from their ideal values of 1 and 0, respectively.

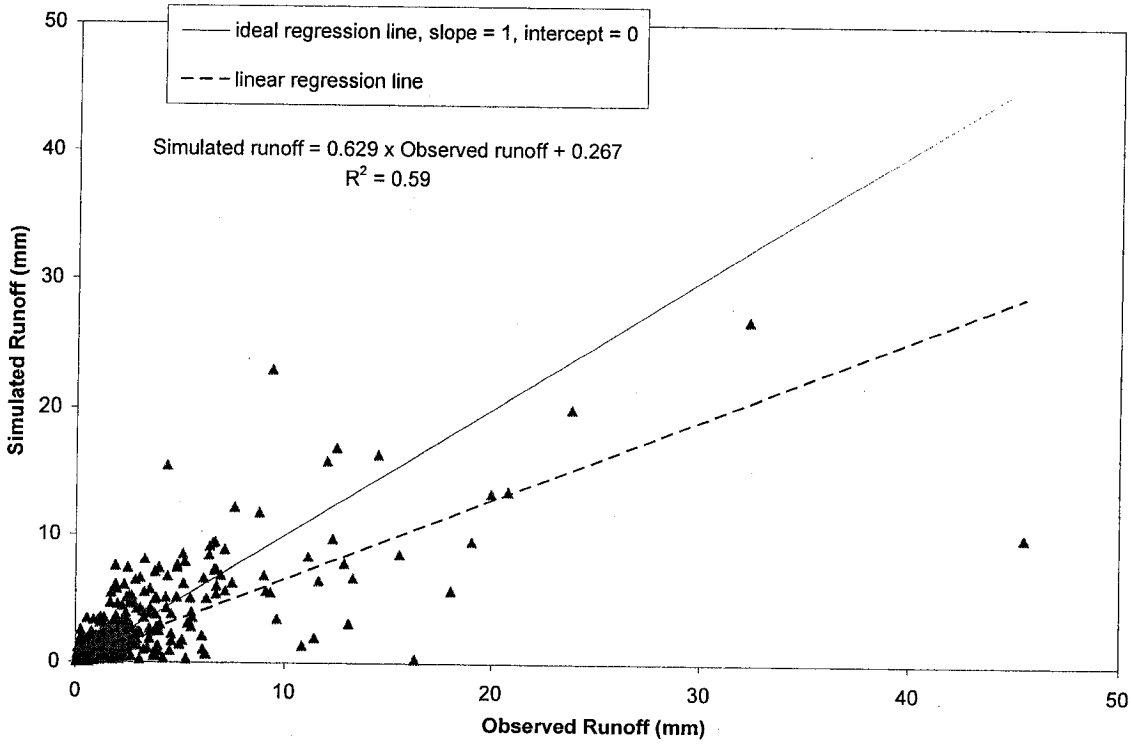

Figure 4.13 A scatter plot of simulated and observed runoff during model calibration

A scatter plot of simulated versus observed runoff for the entire calibration period shows that there was good correspondence between the observed and simulated runoff, and that the model did a good job with a coefficient of determination of 0.59 (Figure 4.13).

4.3 MODEL VALIDATION

The model was validated by running the calibrated model using data from hydrologic years 1989-90 through 1993-94. Like calibration runs, the first year was excluded from the evaluation of model validation performance. The simulated and observed hydrographs together with the precipitation hyetographs for the four years are shown in Figure 4.14 through 4.17.

4.3.1 Water Balance Analysis

The annual water balance for the validation period and the simulated water table levels at the beginning of each water year are shown in Tables 4.7 and 4.8. The mean water table was estimated from the same five representative grids as were used in the calibration period. Similar to the calibration period, the water balance errors for all the hydrologic years during the validation period were <1 % of the total precipitation, showing good model performance. The simulated annual evapotranspiration ranged from 60 to 71% of precipitation, quite close to the mean measured evapotranspiration in the watershed (65%; Das et al., 2004). A decrease in storage was observed in hydrologic year 1990-91, despite it being a wet year. This is because 46 mm of the storage water contributed to runoff and evapotranspiration. However, instead of a drop, the mean water table rose from 1.68 to 1.64 m. Among the five grids, there was a drop in water table in three, but a sharp rise in the other two grids, resulting in a mean rise in water table. When water table levels were checked for other watershed grids, the water table level generally dropped. Thus, it is likely that if all the grids in the watershed were considered, there would be an overall drop in the water table. Some 580 mm and 234 mm of 1991-92 precipitation were respectively contributed to evaporation and surface runoff. The remaining 114 mm of precipitation contributes to the storage, raising the water table from 1.64 to 0.77 m. The last two years (1992-93 and 1993-94) also showed a decrease in storage and the water table was lowered in both years.

Table 4.7 Annual Water Balance for Model — Validation

Hydrologic Year	PPT (mm)	ET (mm)	RO (mm)	Change in Storage (mm)	Error mm (%)
1990-91[a]	1032	620	462	-46	-4 (0.4)
1991-92	932	580	234	114	4 (0.4)
1992-93	925	559	444	-71	-7 (0.8)
1993-94	836	593	302	-54	-5 (0.6)
Total	3725	2353	1443	-57	-14 (0.4)

a – wet year

Table 4.8 Simulated Water Table Level during Validation Period

Validation Year	Oct 1990	Oct 1991	Oct 1992	Oct1993	Oct 1994
Mean water table (m)	1.68	1.64	0.77	1.63	1.75

The seasonal water balances, together with seasonal observed runoffs are shown in Table 4.9. Simulations of all hydrological processes (evapotranspiration, recharge and runoff) during validation were quite similar to those obtained during the calibration period. The summer months experienced the highest actual evapotranspiration, while the greatest recharge and runoff occurred in March and April. The winter months experienced high runoff events due to snowmelt events in March and rainfall events in December (Table A.2 in Appendix A). This was justified by the similar trend in observed runoff data. Overall, the model was able to simulate all the hydrological components adequately.

4.3.2 Analysis of Hydrographs

The model response was more or less similar to that observed in the calibration step. Most simulated runoff peaks matched well with their observed counterparts, both in terms of timing and quantity, though some under- and over-estimations occurred for certain events. During the validation period, the number of missing observed data was greater than during the calibration period, so that the evaluation of some events was not possible. Consequently, these data were excluded from the statistical analysis.

Although runoff was not recorded between April 16th and April 21st 1991 (Figure 4.14), the simulated runoff peak on 16/04/1991 is justified by the rainfall event on the previous day. On the other hand, the observed runoff event on 18/07/1991 (Figure 4.14) appears to be a measurement error as there were no rainfall events in the preceding five days. Another such ambiguity occurred on 1/01/1992 (Figure 4.15), where there was an unusually high observed peak (16.3 mm), and no rainfall or snowfall for the preceding three days. During these days the temperature was below 0°C, thus the possibility of snowmelt was slim. Similarly, on 28/08/1992 (Figure 4.15), though the five days

Table 4.9 Seasonal Water Balance for Model Validation

Water Year	Winter (Dec/Jan/Feb/Mar)						Spring (Apr/May)					
	PPT	ET	BF	Re	S_RO	O_RO	PPT	ET	BF	Re	S_RO	O_RO
1990-91	328	36	65	14	260	250	200	117	32	5	104	96
1991-92	165	37	43	7	90	106	180	139	21	4	62	81
1992-93	251	32	59	10	201	198	126	122	27	3	54	73
1993-94	217	30	44	8	110	128	227	121	29	9	132	119
Mean	240	34	53	10	165	171	183	125	27	5	88	92
Water Year	Summer (Jun/Jul/Aug)						Fall (Sep/Oct/Nov)					
	PPT	ET	BF	Re	S_RO	O_RO	PPT	ET	BF	Re	S_RO	O_RO
1990-91	265	367	22	3	19	26	168	114	18	2	19	16
1991-92	347	312	21	4	33	81	340	75	39	12	203	123
1992-93	236	335	20	1	13	42	222	79	25	4	49	35
1993-94	226	335	22	1	16	20	-	-	-	-	-	-
Mean	269	337	21	2	20	43	244	89	28	6	90	58

PPT – precipitation (mm), ET – actual evapotranspiration (mm), BF – baseflow (mm), Re – recharge (mm), S_RO – simulated runoff (mm), O_RO – observed runoff (mm)

antecedent rainfall was 34.2 mm, the observed runoff, at 27.2 mm, seemed to be very high, where some of the precipitation would have infiltrated the previously dry soil (ENV CAN, 2005). There was runoff peaks observed on (3, 7, 14, 28)/02/1994 (Figure 4.17), but no simulated peaks, though both minimum and maximum temperature in the watershed had remained below 0^{o}C (ENV CAN, 2005). This might be due to the collapse of an ice bridge or erroneous observed data. However, it is apparent from the figures that overall the model simulated runoff reasonably well.

4.3.2.1 Summer/Fall Season

In the summer and fall seasons, some runoffs peaks were overestimated (e.g. 8/07/1991, October/November 1992, 28/11/1993). Despite large rainfall events, observed runoffs were low as a result of the greater actual than predicted evapotranspiration and infiltration. Given the greater hydraulic conductivity during the growing season, actual runoff decreased. For example, on 3/11/1992 (Figure 4.16), a large rainfall event (29.6 mm), was followed by small runoff event of 6.9 mm, whereas simulated runoff was 12.6 mm. Such cases also occurred during the calibration period (e.g. May to September 1995).

On the other hand, some runoff events were under-predicted (e.g. October 1990, 11/08/1992, 8/09/1992, 21/06/1993, and 11/07/1993), possibly due to the high intensity and short duration of the storm events in question. For example, on 9/10/1990 (Figure 4.14), there was 9.6 mm of runoff from a short, high intensity rainfall event of 25.4 mm; however, the model only simulated a negligible runoff depth (2.6 mm). Such event can be compared with that which occurred on 12/06/1996, during the calibration period.

Even though there was some under- and over-prediction, the model did very well most of the time (e.g. 6/11/1990, October 1991, 19/09/1992, and 20/07/1993). For example, on 6/11/1990 (Figure 4.14), the model simulated 10.3 mm of runoff from 49.2 mm of rainfall, very close to the observed runoff of 9.4 mm.

4.3.2.2 Winter/Spring Season

During the winter/spring period, the runoff events occur both due to snowmelt and rainfall, and were either slightly over- or under-predicted by the model. As discussed in the calibration section, this could be due to the use of mean daily temperature which does not consider diurnal temperature variations, linear interpolation of mean daily temperature, extreme events such as freezing rain or snow pellets occurring above 0°C and rain occurring below 0°C, frozen soil conditions, etc. Thus, the model was unable to accurately estimate rainfall and snowfall occurring on a particular day, amount of snowmelt and the runoff as well as the timing of the runoff peaks (e.g. 27/03/1994; Figure 4.17).

The model over-predicted certain observed runoff events (e.g. 4/12/1990, 23/12/1990, and 17/01/1991). For example, the model simulated very high surface runoff (12.7 mm) on 04/12/1990 (Figure 4.14). The mean daily temperatures supplied in the model were 0.7°C and -1.6 °C on eve and day of the event, respectively. The model considered the total precipitation event (35 mm) on the eve as rainfall, while only 18 mm was actually rainfall, and the remaining snowfall. Consequently, the model simulated greater runoff than that observed as a possible result of its not accounting for diurnal variations in temperature, where part of the rainfall might have frozen on the ground.

On the other hand, some simulated runoff events were smaller than those observed (e.g. 2/03/1991, 27/03/1991, 9/04/1991, 16/04/1992, 4/01/1993, and 29/03/1993). Here large observed runoff depths were probably a result of frozen soil conditions, as was observed during the calibration runs (e.g. 21/02/1997). The large observed runoffs on 16/04/1992 (Figure 4.15) and 29/03/1993 (Figure 4.16), the result of rainfall and snowmelt, respectively, were likely attributable to the frozen soil conditions. The temperature was mostly below freezing in these months, resulting in lower infiltration and greater runoff.

Ultimately, the model did perform well for the other events in this period (e.g. 30/12/1990, 19/03/1991, 9/12/1991, and 26/04/1993). On 30/12/1990 (Figure 4.14), the simulated and observed runoffs were 18.3 mm and 18.2 mm, respectively, from a

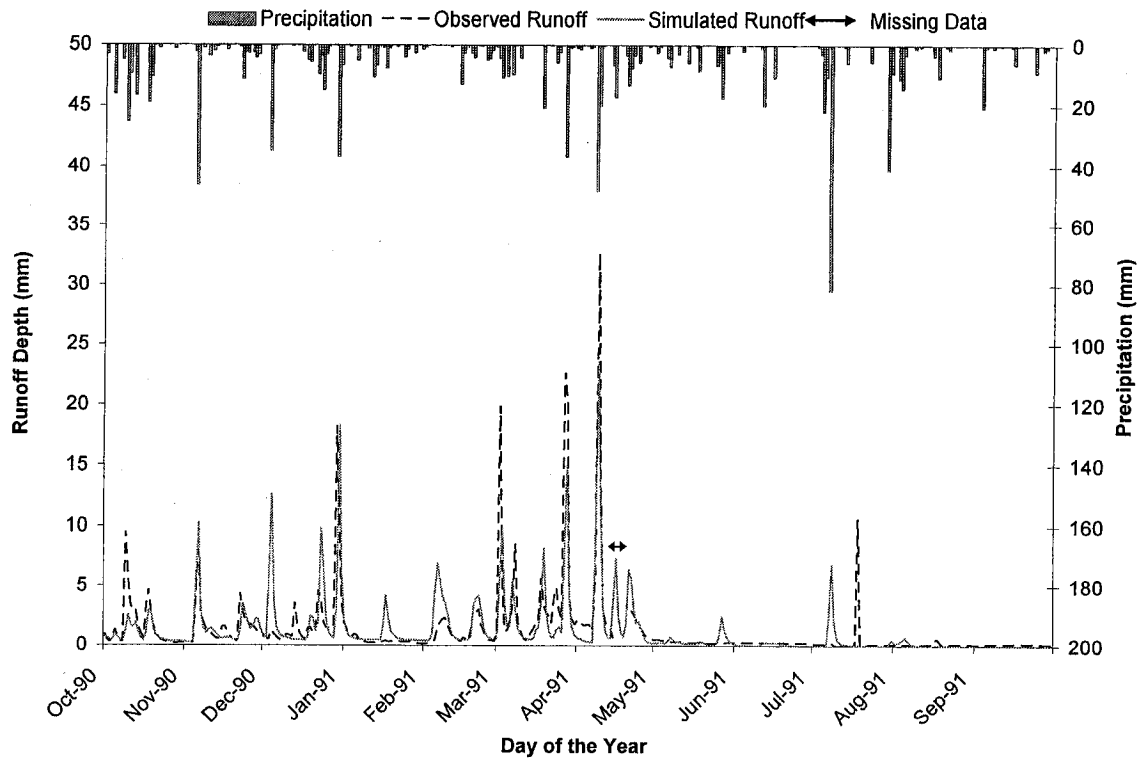

Figure 4.14 Hyetograph and hydrographs for model validation – Year 1990-91

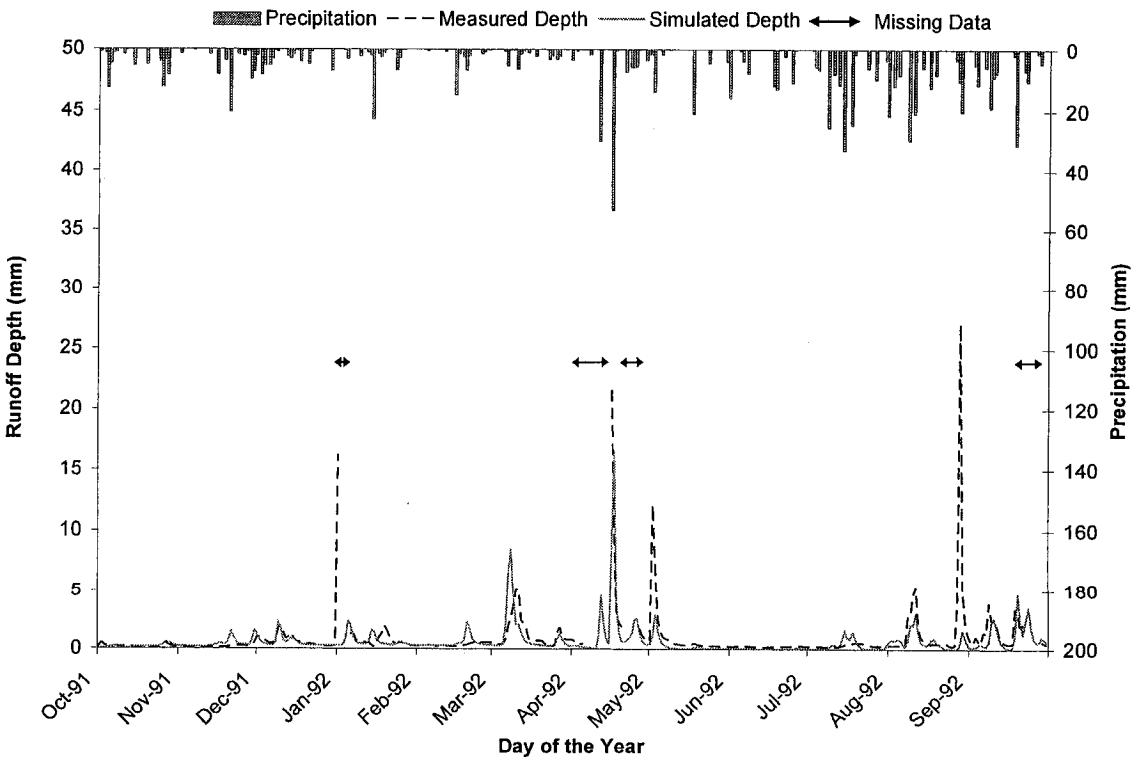

Figure 4.15 Hyetograph and hydrographs for model validation – Year 1991-92

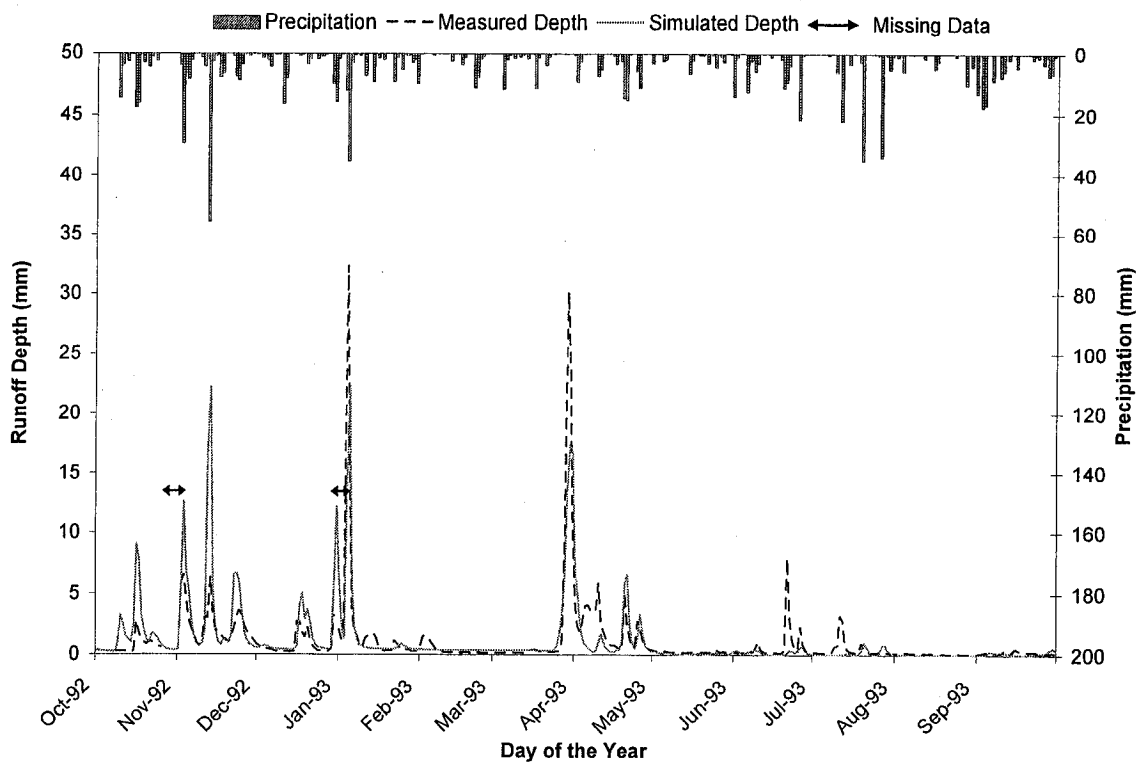

Figure 4.16 Hyetograph and hydrographs for model validation – Year 1992-93

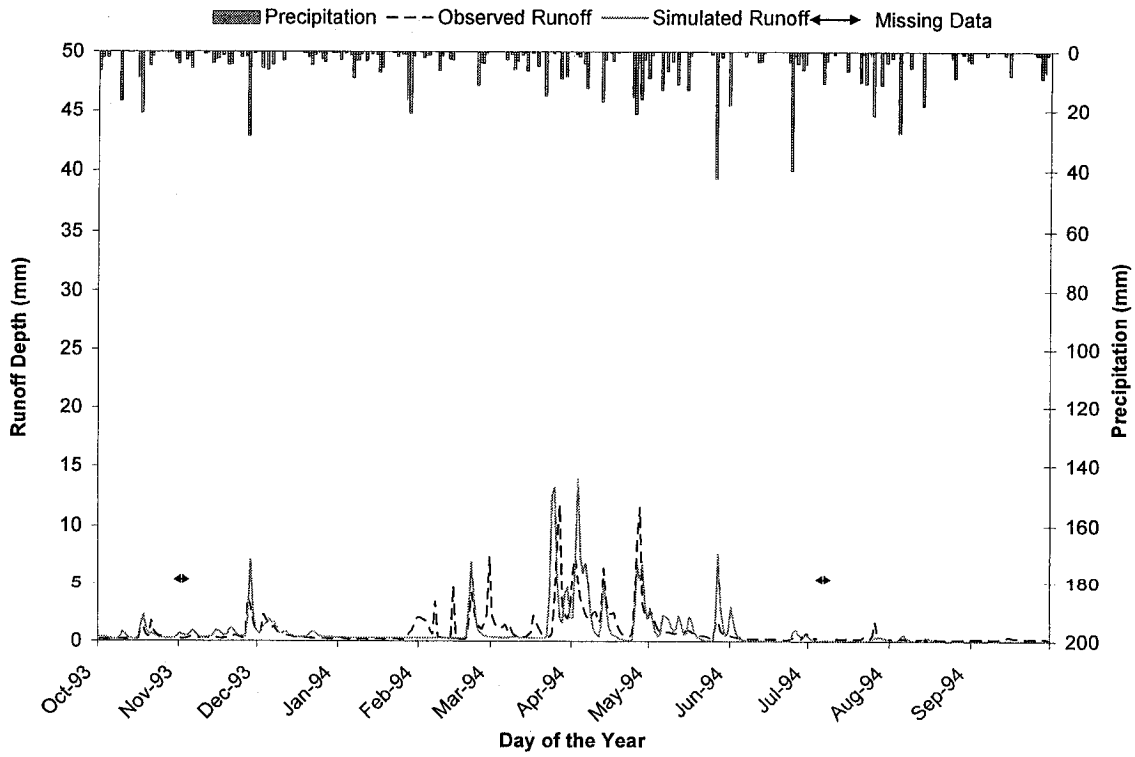

Figure 4.17 Hyetograph and hydrographs for model validation – Year 1993-94

precipitation event totalling 44.4 mm. There was both rainfall and snowfall on that day, together with some snowmelt.

4.3.3 Statistical Analysis

The overall mean deviation (AD) value of 0.09 mm indicates that the model slightly under-predicted runoff (Table 4.10). On a yearly basis, model performance was fair as the AD values ranged from -0.05 to 0.32, with the hydrologic year 1993-94 having a value of zero. The coefficient of determination was high for some years (0.53 in 1990-91 and 1992-93), while other years it was relatively poor (0.22 in 1991-92). For the four-year data, the regressions coefficients, slope (0.56) and intercept (0.38 mm), were poorer than those for the calibration period due to under-prediction of certain extreme events and erroneous data (Figure 4.15). The RMSEs were small (ranging from 1.5 to 2.2 mm), indicating that simulated flows were quite good. Overall, the model performance was slightly poorer than during the calibration period, with the EF% being 39.6% as compared to 59% for calibration. The lower 4-year EF% was mainly attributable to two years (1991-92 and 1993-94), when the simulations were poorer and EF% values were low (19.4% and -7.8%, respectively). The first year (1991-92) had an erroneous observed

Table 4.10 Model performance evaluation for 4 years — validation phase

Hydrologic Year	Observed Runoff (mm)	Simulated Runoff (mm)	AD (mm)	R^2	RMSE (mm)	E (%)	Regression parameters	
							Slope	Intercept (mm)
1990-91[a]	475	442	0.09	0.53	2.1	52.1	0.58*	0.46*
1991-92	311	202	0.32	0.22	2.1	19.4	0.26*	0.36*
1992-93	411	429	-0.05	0.53	2.2	48.2	0.69*	0.41*
1993-94	300	300	0	0.32	1.5	-7.8	0.68*	0.27*
Total	1498	1374	0.09	0.44	2	39.6	0.56*	0.37*

a - wet year; AD – mean deviation; R^2 – coefficient of determination; RMSE – root mean square error; EF (%) – Nash-Sutcliffe coefficient; * - slope and intercept are significantly different ($P \leq 0.05$) from their ideal values of 1 and 0, respectively

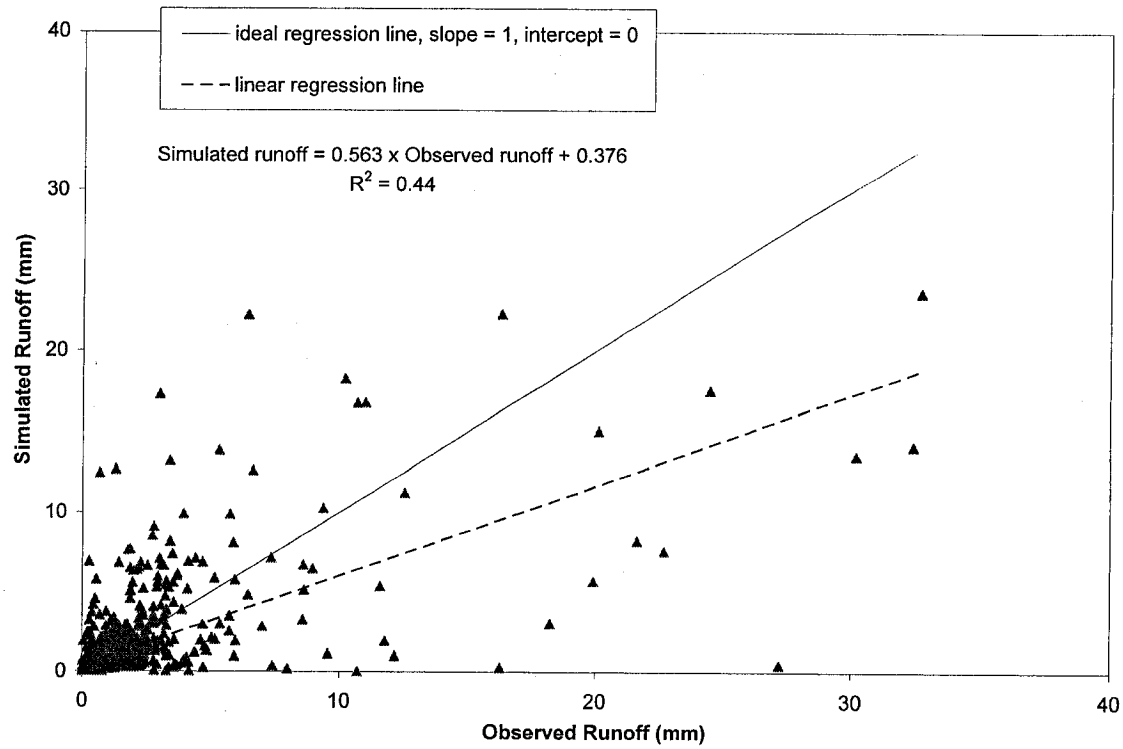

Figure 4.18 A scatter plot of simulated and observed runoff during model validation

runoff data. If excluded, the results improved for the year 1991-92 (EF 42.6 %) and for the entire validation period (EF 44.6%). The other year (1993-94) had several mismatched peaks, perhaps due to the daily mean temperature considered in the model (May 1997) as well as some unexplainable observed runoffs in February 1994, resulting in poorer performance. The best performance was obtained for the hydrologic year 1990-91, with an EF (52.1%). On the basis of visual analysis of the observed and predicted runoff (Figure 4.18), and the values of various statistical parameters judged in light of the malfunction of measuring devices and missing data, the overall simulation appears to be reasonably good.

4.4 SCENARIOS SIMULATIONS

Various watershed management scenarios likely to alter the quantity and timing of water exiting the watershed were simulated with the calibrated model in order to

evaluate their impacts on the watershed's hydrologic response. The scenarios studied were: (i) urbanization, (ii) deforestation, (iii) conversion of pasture land into mono-crop agriculture, (iv) diversification of corn system into cash crops, (v) application of tile drainage over the entire watershed, and (vi) shift in rainfall due to climate change. The hydrographs for all scenarios were compared with the reference hydrograph, developed by running the model using calibrated inputs (Figures 4.20—4.24). Figure 4.19 illustrates a comparison of total annual surface runoff under six scenarios, compared to the original scenario. In this study, the impacts of management scenarios on runoff peaks, P, were rated moderate (5 mm $\leq P <$ 10 mm) or high ($P \geq$10 mm) were also evaluated.

4.4.1 Scenario 1 - Urbanization

In this scenario, the percentage of urban area in the watershed was increased ten-fold, from 0.2 to 2%, to assess the impact of urbanization on surface runoff. The urbanised area was increased by this amount, considering it would far exceed any further increase in development likely to occur over the next 10 years.

Figure 4.20 shows the hydrographs of urbanisation and original scenarios (i.e. 'baseline' in figures). Urbanization had some effect on surface runoff in both the wet and dry years (Figure 4.19, Table 4.11). The surface runoff increased slightly in the wet year (-2.9 %) and decreased in the dry year (1.1 %). The effect was almost negligible in the normal year (-0.2%). Urbanisation normally reduces the amount of pervious areas available for infiltration and thus increases surface runoff velocity and volume. In the long run, it decreases the recharge and base flow as well (Brun and Band, 2000). Because actual evapotranspiration is usually greater in urban areas, where, unlike on vegetated surfaces, rainwater ponds on impervious surfaces, actual evapotranspiration increased for all the years in this scenario (Table 4.12). As shown in Table A.3 in Appendix A, the actual evapotranspiration increased for all the other seasons, except summer. This is because the areas occupied by vegetation were urbanised, consequently reducing the transpiration during the growing season. Compared to the original scenario, the infiltration was decreased in the wet year. However, for both normal and dry years, the infiltration increased due to drier soil conditions. The dryness or wetness can be assessed

from the depth of water table. The increase or decrease in infiltration corresponds very well with the rise and drop in water table level taken at a representative grid in an urban area (Table A.4 in Appendix A). Overall, urbanisation causes a drop in water table in all those years compared to original scenario, due to the lower infiltration in the first year, resulting in a drier soil in the subsequent normal and dry year. Thus, there was more infiltration in the dry year, producing lower surface runoff, respectively.

Overall, this scenario had a trivial impact on surface runoff, perhaps because the urbanised area only represented a small fraction of the total watershed area. However, given that a 1.8% increase in urban area raised surface runoff by 2.9 % in a wet year, there may be a major impact on surface runoff if the urbanisation areas were considerably increased. Such cases are possible in smaller watersheds adjacent to big cities. A study conducted by Brun and Band (2000) showed that significant impacts on surface runoff could be observed when the percentage of impervious cover in the watershed exceeded a certain threshold value (20 % in their case). Urbanisation is also critical as it can cause excessive erosion and flooding in downstream areas.

The impact of urbanization on runoff peaks was also analyzed, where moderate peaks and high peaks were scrutinized. Urbanization increased the peak runoff rate for high peaks to a greater extent than for moderate peaks in the wet year (Table 4.13). In the case of moderate peaks, runoff increased by 2.1% in the mean year. There was a decrease in runoff rates (1.1 %) in the dry year due to the deeper water table.

4.4.2 Scenario 2- Deforestation

Deforestation, a common activity engaged in on many watersheds around the world, is generally intended to provide space for intensive agricultural and urban development. It can adversely affect the natural hydrology of the watershed. For this scenario, the areas occupied by woodlots (11.2 %) were converted into agricultural land, particularly corn (*Zea mays* L.) cultivation. As a result, areas under corn increased from 28.2% to 39.4% of the entire watershed.

The hydrographs for the deforestation and original scenarios are shown in Figure 4.21. A considerable increase (-11%) in runoff was observed throughout the simulation

period (Table 4.11 and Figure 4.19). Previous studies found similar results; for example, Franklin (1992) stated that deforestation in a pristine watershed would increase surface flow by 90%. The removal of trees which have a high leaf area index, great rooting depth and high surface roughness coefficient, reduces both actual evapotranspiration and the amount of infiltration (Table 4.12). Table A.3 in appendix A also showed that the evapotranspiration has increased in all the seasons.

For all the three representative years, runoff rates for both high and moderate peaks under the deforestation scenario increased appreciably compared to the original scenario (Table 4.13). Yuan et al. (2001) reported that a large-scale deforestation affected both the high and low flow regimes in rivers of their watershed. Our simulation results showed that the runoff volume as well as the runoff rates for high and moderate runoff peaks increased under deforestation, suggesting that a certain percentage of increase in deforestation caused a similar percentage increase in surface runoff. Thus, for this watershed, a 1% increased in deforested area led to a 0.98 % increase in surface runoff.

In this scenario, urbanization of certain portion of the deforested area was not considered. It is clear from discussion in section 4.4.1 that urbanization has considerable impact on the runoff volume and rates, based on the percentage area under transformation. If urbanization is considered, there might be a further small increase in runoff.

4.4.3 Scenario 3- Conversion of Pasture Systems into Mono-crop Agriculture

Areas under livestock production or pasture system agriculture are declining over time and being replaced by other forms of agriculture. In this scenario, the areas under pasture and hay (8%) were converted into mono-cropping agriculture (corn cultivation).

The impact of the conversion of the agricultural system was greater in the wet year than the normal or dry year (Figures 4.19 and 4.22). Runoff volume increased considerably (4.1 %) in the wet year (Table 4.11). In general, the change of agricultural system affects both the actual evapotranspiration (leaf area index and rooting depth) and the infiltration (surface roughness coefficient). As a result of the conversion, the actual

evapotranspiration increased slightly in all the three years (Table 4.12). On the other hand, the infiltration decreased in the wet year, but increased in the normal and dry years. However, since the increase in evapotranspiration was minimal, the high surface runoff in the wet year was mostly the result of decreased infiltration, which was, in turn, due to decreased surface roughness leading to a quicker flow of water. Infiltration increased marginally in the normal and dry years, when soil conditions are usually drier.

The runoff rates for both the high and moderate peaks increased under this scenario, particularly in the wet year (Table 4.13), indicating that the change in agricultural systems affected both moderate and high flows. Thus, the impact of changing agricultural system is important and should be considered in watersheds subjected to any management activities.

4.4.4 Scenario 4- Turning Conventional Agriculture into Cash Crops

To increase profits, farmers in many countries around the world have practiced diversifying from mono-cropped agriculture into cash crops. Therefore, in this scenario, the mono-cropping system of corn cultivation was replaced by a cash crop. Tomatoes were chosen as a representative cash crop because it is an important cash crop in the region and it exhibits more or less similar vegetation properties (leaf area index, rooting depth, and surface roughness) as other cash crops (e.g. potato and carrot). Hence, the areas under corn cultivation (28.2 %) were converted into tomato cultivation.

The results showed that the surface runoff increased in all three representative years (Figures 4.19 and 4.23), likely because the change in cropping pattern considerably decreased both actual evapotranspiration (leaf area index and rooting depth) and infiltration (Table 4.12). Though the tomato crop surface roughness coefficient was the same as that of corn, the infiltration was affected because of the different leaf area index, which influenced the interception, and thus net precipitation available for infiltration. The wet year experienced a lower infiltration because of the soil being normally less dry than in a normal or dry year.

Runoff rates for high and moderate peaks, both were increased (Table 4.13), likely because the actual evapotranspiration and infiltration also affected the high flows. Thus, diversification of mono-cropping agriculture into a cash crop affected all the runoff events, including high and moderate runoff events, irrespective of the year type.

4.4.5 Scenario 5- Application of Tile Drainage

Tile drainage is a common practice in North America, especially in humid regions. Although tile drains are installed in certain areas of the watershed, the model does not have a direct option to incorporate an existing, partial tile drainage system on the watershed. Thus, in this scenario, tile drainage is applied over the entire watershed to investigate its impact on surface flow.

The effect of tile drainage on total surface runoff was almost negligible for all the three years of simulation (Figure 4.19 and Table 4.11); however, as expected, the runoff rates for the high and moderate peaks were considerably decreased in all years (Figure 4.24 and Table 4.13). As a result, low flows increased a lot, because there was more infiltration into the soil profile, thereby reducing both the high and moderate runoff peaks (Table 4.12). Also, the actual evapotranspiration decreased slightly as there was less water available on the soil surface for evaporation. Both the baseflow and recharge were increased considerably in all the seasons (Table A.3 in appendix A), showing impact of scenario throughout the year. However, the increase in low flows and decrease in high flows counteracted each other, producing similar overall surface flow. Thus, it is apparent that drainage systems help to alleviate peak runoff rates in the case of heavier rainfall events.

4.4.6 Scenario 6-Climate Change Simulation

Global warming, a serious climatic change phenomenon, more noticeable in recent years, causes more frequent extreme hydrological events such as floods and droughts, increases rainfall intensities, and changes storm patterns. In this study, the

effect of a shift in precipitation on surface runoff was evaluated, where the entire four years' precipitation data was shifted by one month forward.

As shown in Figures 4.19 and 4.25, there was considerable impact on the annual surface runoff for all the three years. Surface runoff increased in the wet year, but decreased in normal and dry years (Table 4.11). Despite the fact that actual evapotranspiration increased and infiltration decreased for all the three years (Table 4.12), the effect was solely because of different precipitation patterns under different climatic condition (air temperature) greatly affecting the overall surface runoff events.

The wet and dry year had a considerable increase in high peak rates, while the normal year had a marked increase in moderate peaks (Table 4.13). Since the change in precipitation pattern is also controlled by other climate variables, the subsequent effects on surface runoff are mostly unpredictable. Overall, this climate change scenario produces more surface runoff in the wet years and less runoff in normal and dry years.

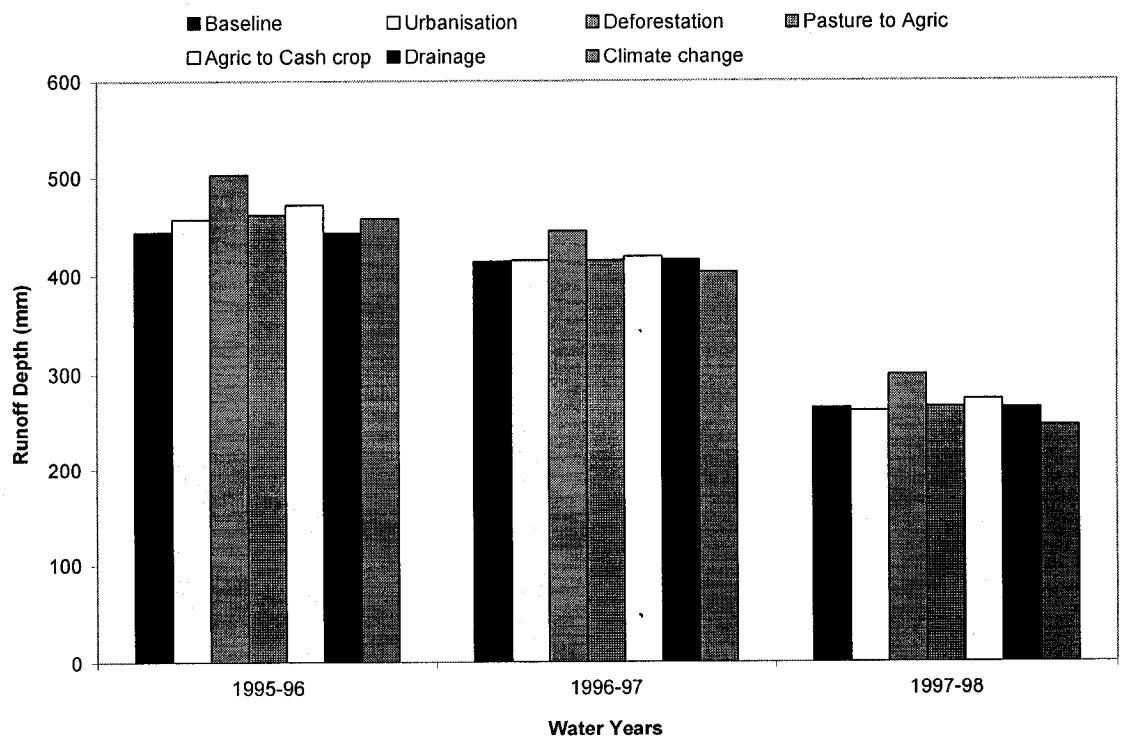

Figure 4.19 Comparison of total annual runoffs for the six scenarios to the original scenario

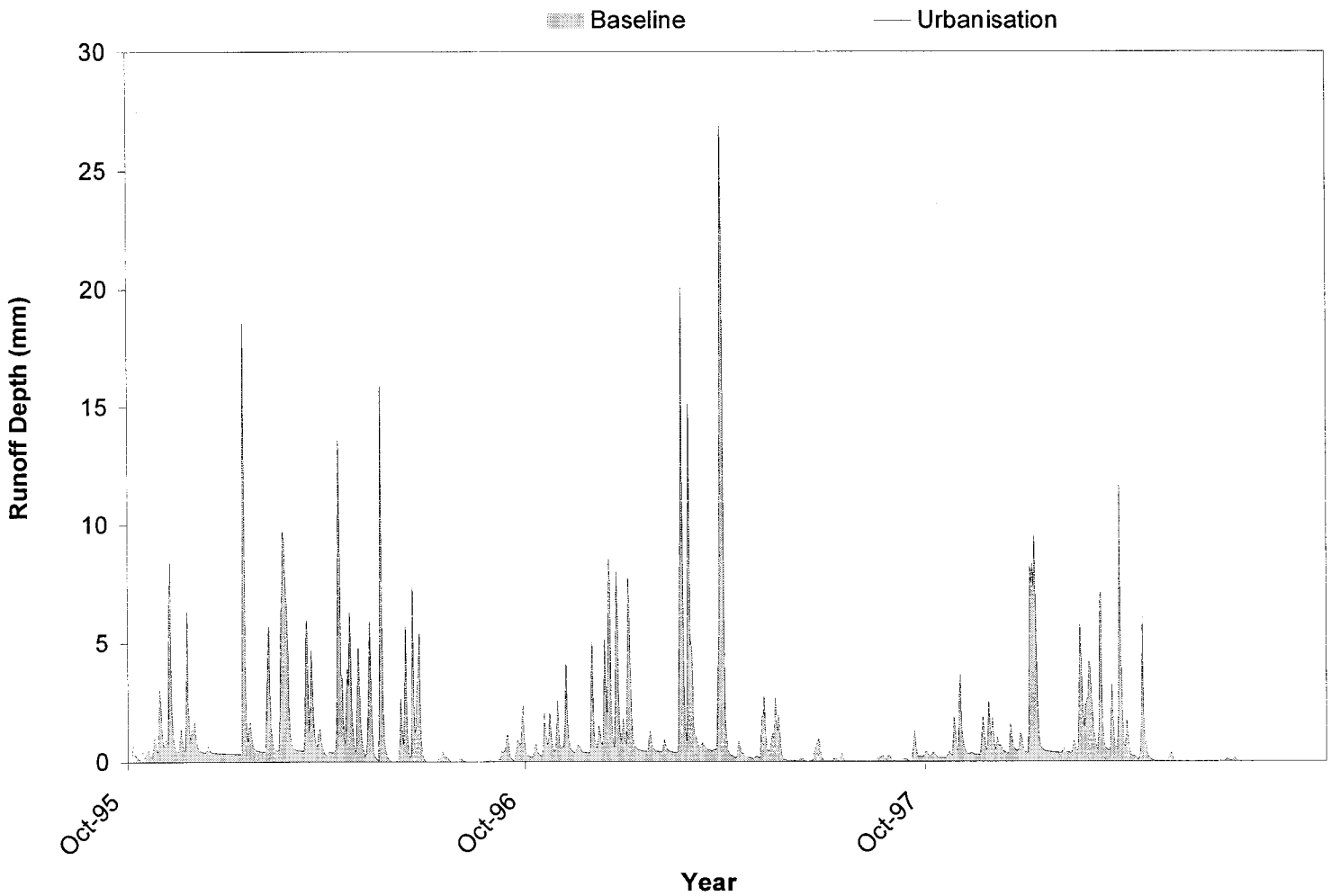

Figure 4.20 Effect of urbanization on surface runoff

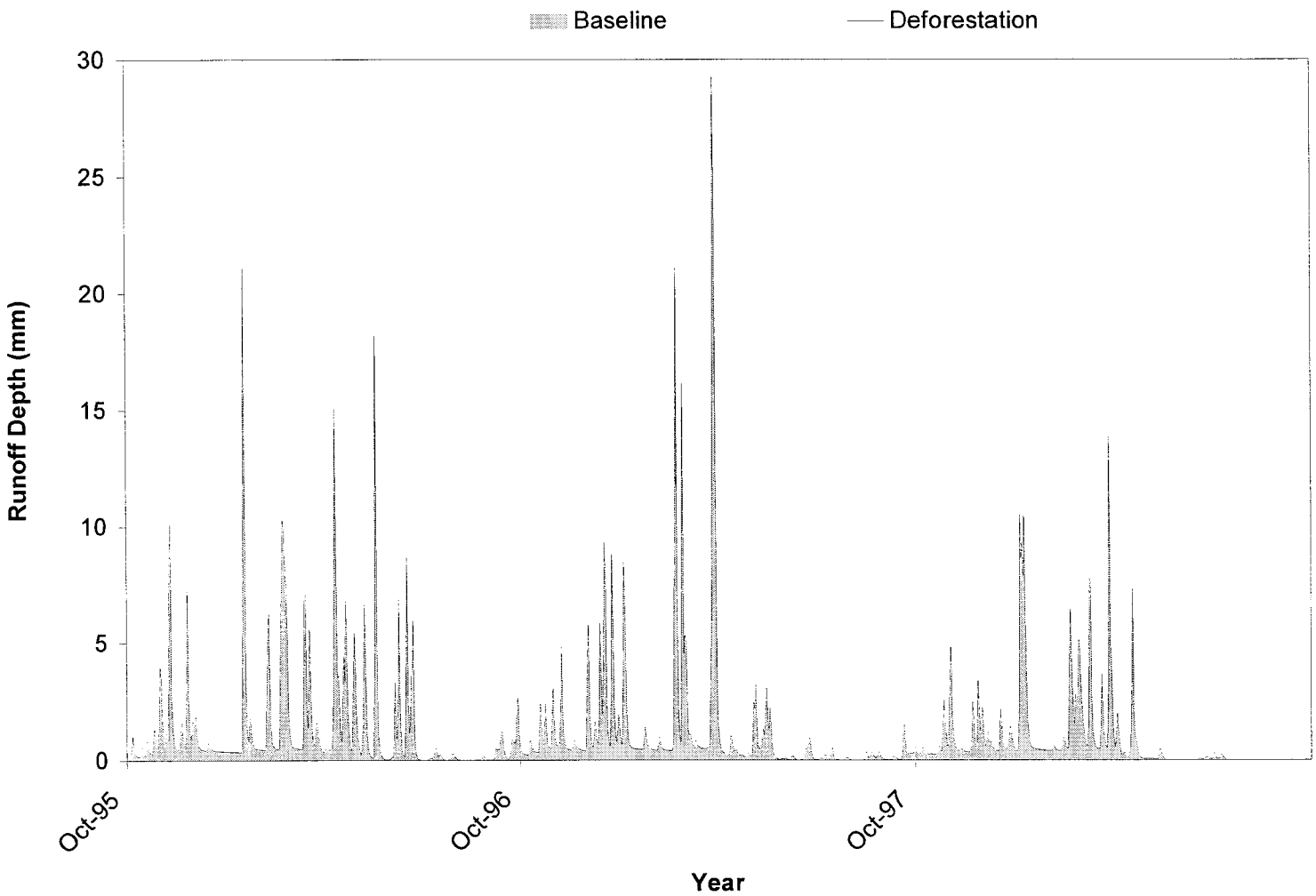

Figure 4.21 Effect of deforestation on surface runoff

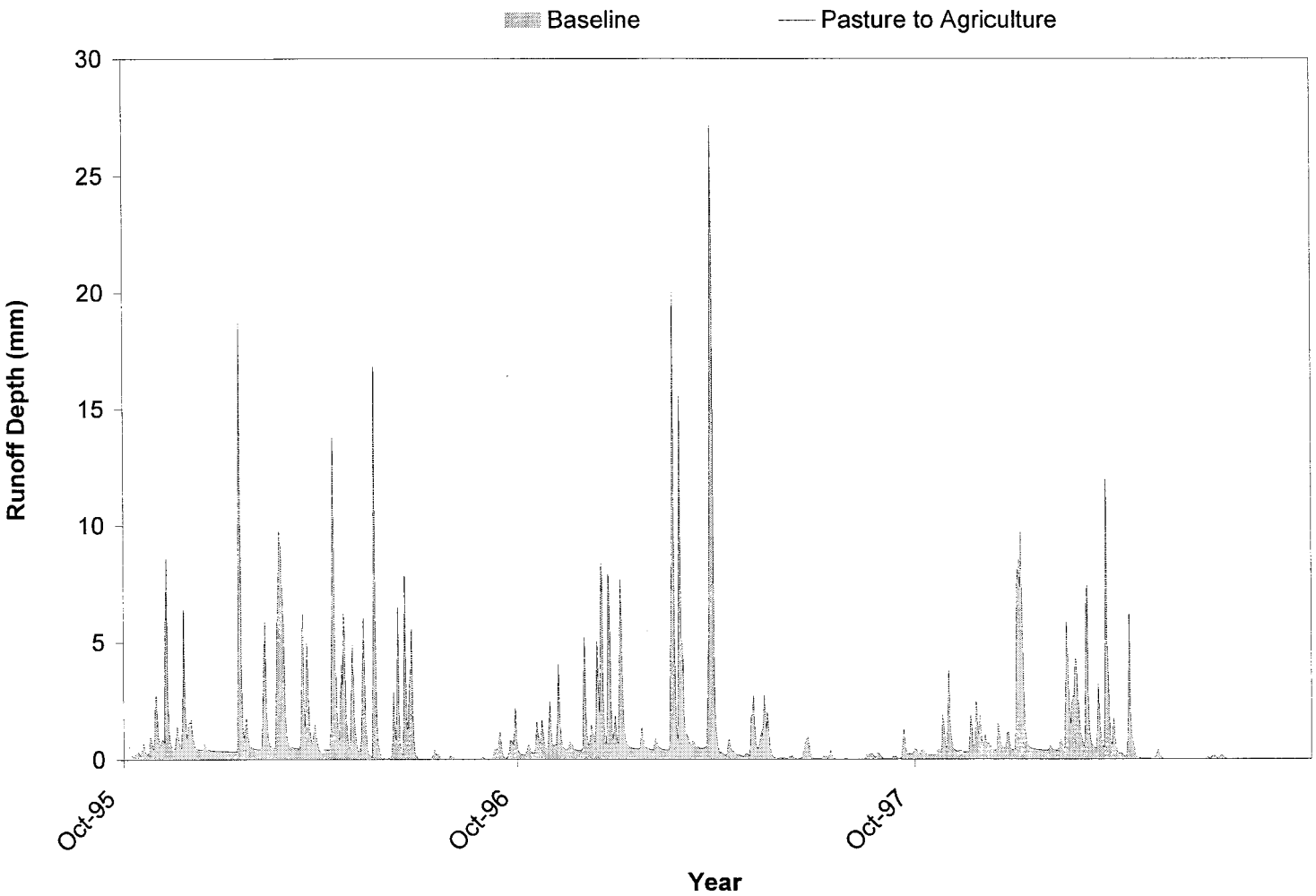

Figure 4.22 Effect of Converting pasture land into agriculture on surface runoff

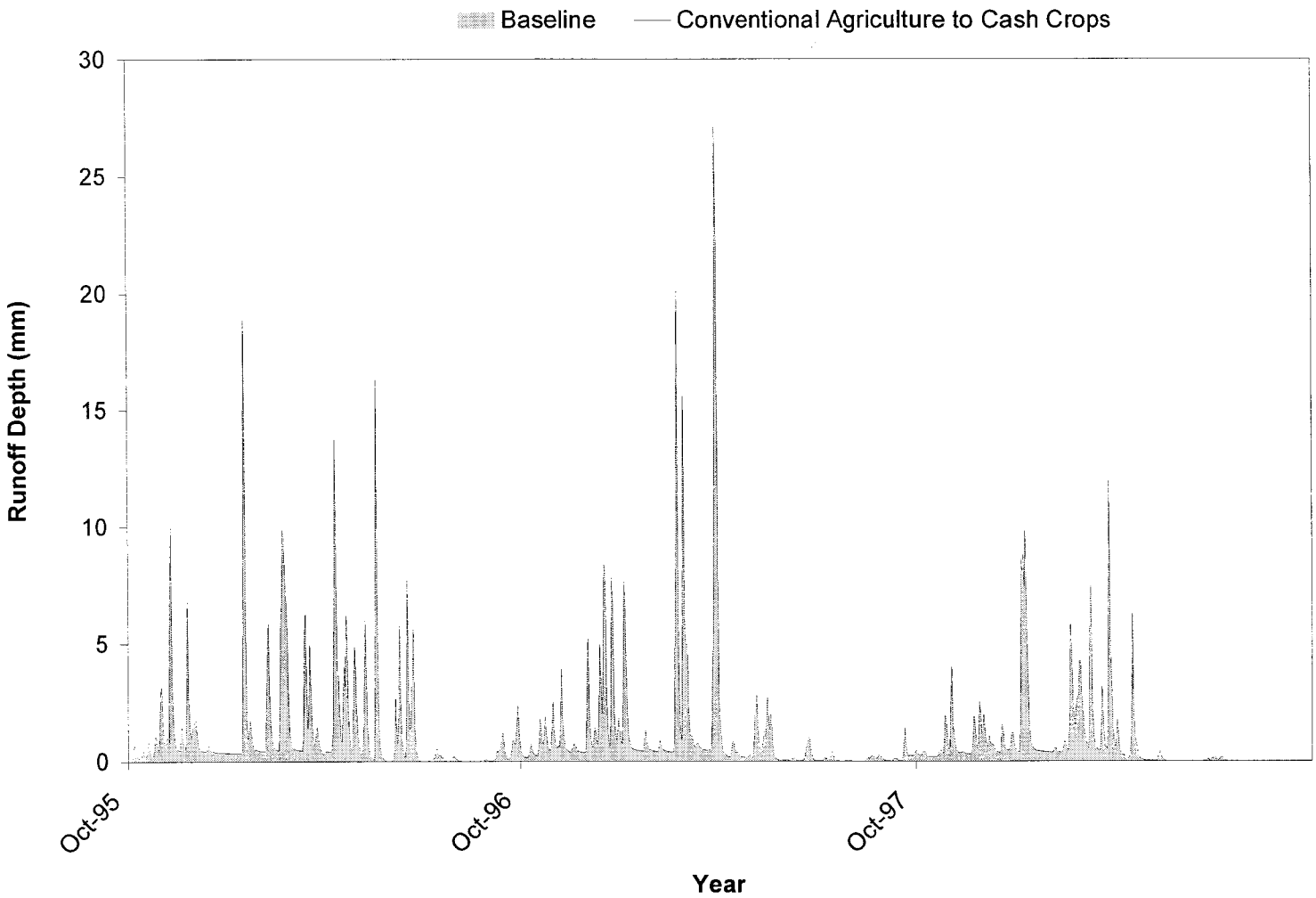

Figure 4.23 Effect of replacing conventional agricultural crop by cash crops on surface runoff

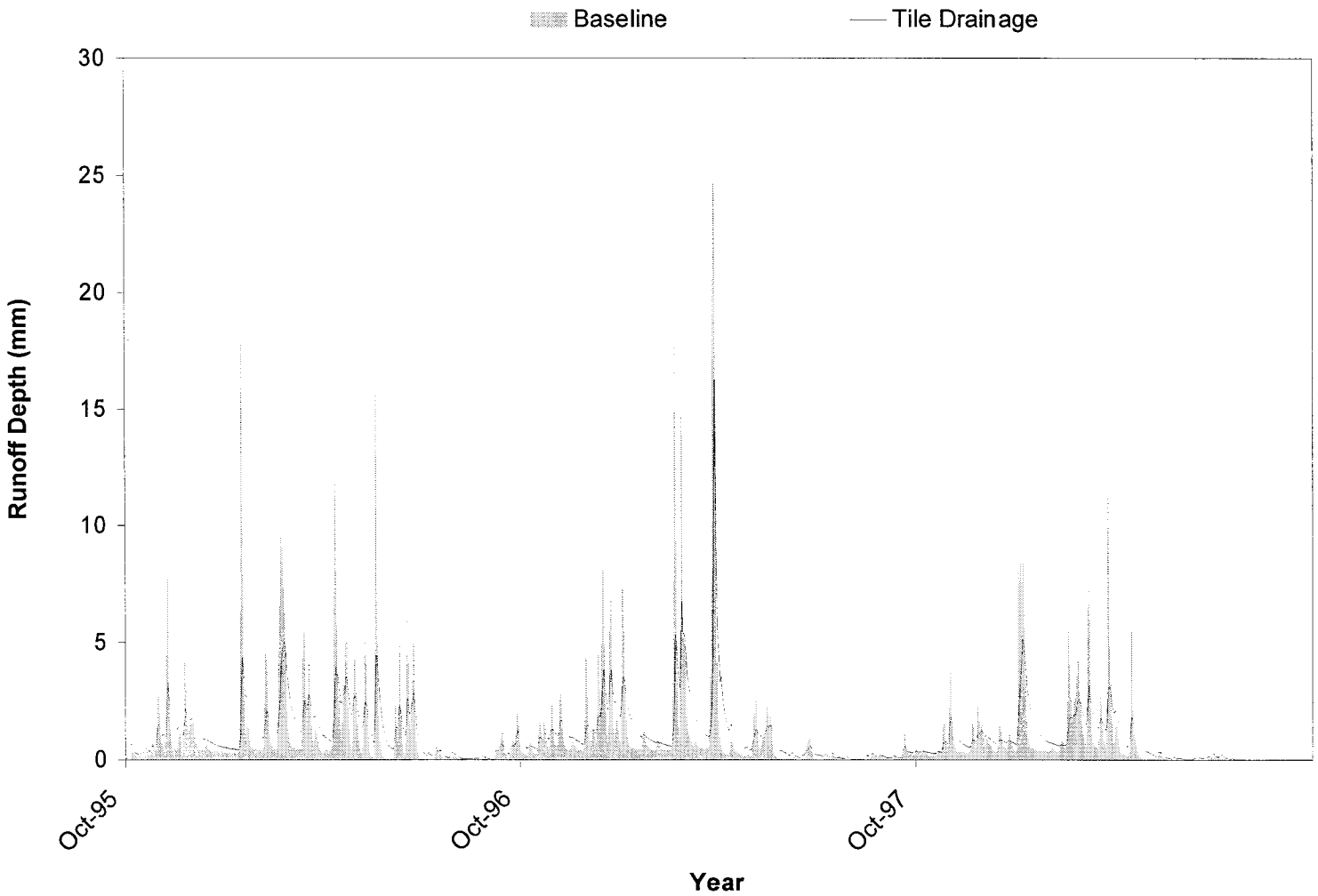

Figure 4.24 Effect of tile drainage on surface runoff

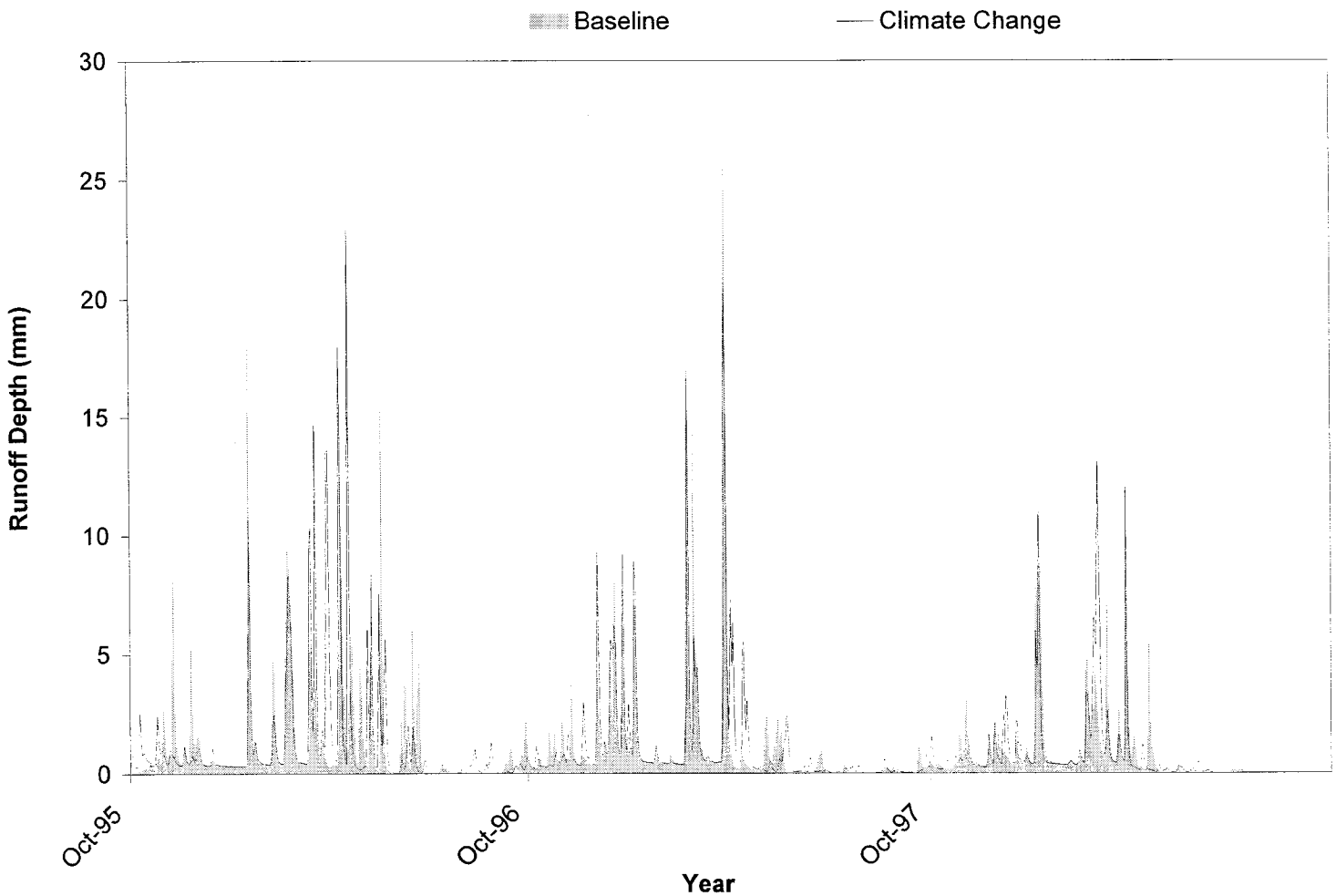

Figure 4.25 Effect of Climate change on surface runoff

Table 4.11 Simulated Surface Runoff for all Scenarios

Scenarios	Runoff in mm			
	Wet Year	Normal Year	Dry Year	Total
Baseline	444	414	265	1123
Urbanization	457	415	262	1134
Deviation (%)	-13 (-2.9)	-1 (-0.2)	3 (1.1)	-11 (-1.0)
Deforestation	503	445	299	1247
Deviation (%)	-59 (-13.3)	-31 (-7.5)	-34 (-12.8)	-124 (-11.0)
Pasture to Agriculture	462	415	266	1143
Deviation (%)	-18 (-4.1)	-1 (-0.2)	-1 (-0.4)	-20 (-1.8)
Agriculture to Cash crop	472	419	274	1165
Deviation (%)	-28 (-6.3)	-5 (-1.2)	-9 (-3.4)	-42 (-3.7)
Application of Drainage	443	416	265	1124
Deviation (%)	1 (0.2)	-2 (-0.5)	0 (0.0)	-1 (-0.1)
Climate Change	458	404	247	1109
Deviation (%)	-14 (-3.2)	10 (2.4)	18 (6.8)	14 (1.2)

Table 4.12 Annual Simulated Hydrologic Components for all scenarios

Scenarios	Evapotranspiration (mm)			Infiltration (mm)		
	Wet Year	Normal Year	Dry Year	Wet Year	Normal Year	Dry Year
Baseline	560	545	599	562	390	329
Urbanization	567	550	604	557	392	336
Deforestation	524	509	561	541	386	326
Pasture to Agriculture	562	546	600	555	392	332
Agriculture to Cash Crop	554	543	593	546	389	328
Application of Drainage	558	537	583	916	668	527
Climate Change	562	546	600	495	378	311
Scenarios	Baseflow (mm)			Recharge (mm)		
	Wet Year	Normal Year	Dry Year	Wet Year	Normal Year	Dry Year
Baseline	134	137	105	29	23	19
Urbanization	144	140	106	29	23	19
Deforestation	152	147	116	30	24	20
Pasture to Agriculture	144	139	106	29	23	19
Agriculture to Cash Crop	146	141	109	30	23	19
Application of Drainage	583	537	391	182	184	141
Climate Change	142	138	103	26	23	17

Table 4.13 Comparison of High and Moderate Surface Runoff Peaks for different Scenarios

Scenarios	Moderate Runoff Peak ($5 \leq P < 10$, mm)			High Runoff Peak ($P \geq 10$, mm)		
	Wet Year	Normal Year	Dry Year	Wet Year	Normal Year	Dry Year
Baseline	66.2	28.9	45.6	47.5	62.4	11.8
Urbanization	66.8	29.5	45.1	48.1	62.1	11.7
Deviation (%)	-0.9	-2.1	1.1	-1.3	0.5	0.8
Deforestation	76.3	32.4	51.6	54.3	66.5	13.8
Deviation (%)	-15.3	-12.1	-13.2	-14.3	-6.6	-16.9
Pasture to Agriculture	69.2	29.3	45.9	49.3	62.8	12
Deviation (%)	-4.5	-1.4	-0.7	-3.8	-0.6	-1.7
Agriculture to Cash Crop	70.4	29	47	48.9	62.8	12
Deviation (%)	-6.3	-0.3	-3.1	-2.9	-0.6	-1.7
Application of Drainage	28.8	12.6	11.8	12.7	28.4	3.1
Deviation (%)	56.5	56.4	74.1	73.3	54.5	73.7
Climate Change	36	64.1	12.6	90.2	37.2	36.2
Deviation (%)	45.6	-121.8	72.4	-89.9	40.4	-206.8

CHAPTER V - SUMMARY AND CONCLUSIONS

MIKE SHE is a flexible modeling system, which can provide solutions to a range of hydrological problems with diverse levels of complexity. Being one of the most versatile, physically-based and fully distributed models, that integrates surface, subsurface and groundwater flow, its applicability under south-central Ontario climatic and soil conditions was tested. The impacts of alternative management practices on the watershed response were also evaluated.

The Canagagigue Creek watershed was selected for this study. Physical properties of soil and land use, meteorological data (such as rainfall, air temperature, and evapotranspiration etc.), and observed runoff were collected for a 9-year period from 1989 to 1998. The data were divided in two sets, one for calibration (1993 to 1998) and the other for validation (1989 to 1994), where the first year in each set was used for initialization. Using the calibration data set, the model was run and calibrated by adjusting snowmelt constants and Mannings' M. Calibration of these parameters improved the model simulation of surface runoff as compared to the initial model run. The calibrated model was applied to the validation data set.

Annual water balance errors were less than 1%. The seasonal water balance showed that the model was able to simulate all the hydrological processes (evapotranspiration, baseflow, recharge and surface runoff) adequately. The maximum actual evapotranspiration was obtained in the summer months (June/July/August) whereas the maximum recharge and runoff were observed for the snowmelt period (March/April). These observations were consistent with field observations (R.P. Rudra, personal communication, May 2006). The baseflow simulated by the model represented about 40% of the total runoff, which is also close to the value obtained by an independent baseflow separation technique. On a daily basis, the model was also able to simulate all the hydrological components well. Although for certain events, the simulated number of runoff events and timing of peaks was mismatched with the observed values, overall the model simulated the hydrology adequately.

Statistical analysis showed that the correlation between observed and simulated daily runoff values was good, as represented by coefficients of determination ranging from 0.22 to 0.53 for the validated model. The mean Nash-Sutcliffe coefficient was 39.6% during validation, with a high value of 66.4 % obtained for the year 1994-95.

The model used mean daily temperature as input. Consequently, it experienced difficulties in simulating watershed hydrology when the temperature was near-freezing. The simplicity of the snowmelt routine used in the model (degree-day based method) also caused some discrepancies between the observed and simulated runoff. Though MIKE SHE is a fully distributed model, use of a finer grid size than 50 km^2 over a watershed required a computational time of several days. In this study, a grid size of 100 m x 100 m was used, which took about 6 hours' computational time to simulate one year's data with a 1 GB memory, 64X2 Processor 3800+ AMD Athlon. Simulation error could be reduced by selecting finer grids, but the model would require a reasonably large amount of data and processing time. Despite such shortfalls, the model simulated runoff with a good accuracy.

Various scenarios simulated by the calibrated model showed that deforestation had the greatest impact on surface runoff, as it considerably increased runoff for all types of years (wet, normal and dry). Urbanisation had negligible effects on surface runoff, which is mainly associated with the small portion of urbanised area in the watershed. Conversion of pasture agriculture into corn cultivation, and diversification of conventional agricultural land into a cash crop showed slight increases in runoff, particularly during the wet year. This showed that change in cropping pattern does affect the surface runoff. Installation of tile drains showed little effect on the total surface runoff volume; however, high flow rates decreased and low flow rates increased significantly. The climate change scenario caused greater flooding in wet years. Although some scenarios had minimal effects on surface runoff, all of them are found to be equally important in determining watershed hydrology based on the area considered.

The study showed that the model performed well in simulating runoff. Furthermore, it can be used to investigate diverse hydrological problems and watershed hydrology in a systematic way.

REFERENCES

Abbott, M.B., J.C. Bathurst, J.A Cunge, P.E. O'Connell, and J. Rasmussen. 1986a. An introduction to the European Hydrological System - Système Hydrologique Européen, "SHE", 1: History and philosophy of a physically-based, distributed modelling system. *Journal of Hydrology*. 87(1): 45-59.

Abbott, M.B., J.C. Bathurst, J.A Cunge, P.E. O'Connell, and J. Rasmussen. 1986b. An Introduction to the European Hydrological System - Système Hydrologique Européen, "SHE", 2: Structure of a physically based, distributed modelling system. *Journal of Hydrology*. 87(1): 61-77.

AGWA (Arana Gulch Watersheds Alliance). 2004. *What is a Watershed.* Santa Cruz, CA: Arana Gulch Watersheds Alliance. Available at:

http://www.aranagulch.org/Watershed/watershed.html. Accessed 28 August 2006.

Albek, M., U.B. Ogutveren, and E. Albek. 2004. Hydrological modelling of Seydi Suyu watershed. *Journal of Hydrology*. 285(1-4): 260-271.

Arnold, J.G., P.M. Allen, and G. Bernhardt. 1993. A comprehensive surface-groundwater flow model. *Journal of Hydrology*. 142(1-4): 47-69.

Baginska, B., W. Milne-Home, and P.S. Cornish. 2003. Modelling nutrient transport in Currency Creek, NSW with AnnAGNPS and PEST. *Environmental Modelling & Software*. 18 (8-9): 801-808.

Bai, H., R.P. Rudra, P.K. Goel, and B. Gharabaghi. 2004. Applicability of ANSWERS-2000 to estimate sediment and runoff from Canagagigue Creek Watershed in Ontario. ASAE/CSAE Paper No. 042060. St. Joseph, Mich.: ASAE.

Bannan, M.W. 1940. The root systems of northern Ontario conifers growing in sand. *American Journal of Botany*. 27(2): 108-114.

Bera, P., S.O. Prasher, A. Madani, J.D. Gaynor, C.S. Tan, R.M. Patel, and S.H. Kim. 2005. Development and field validation of the PESTFATE model in southern Ontario. *Transactions of the ASAE.* 48 (1): 85-100.

Borah, D.K., and M. Bera. 2003. Watershed-scale hydrologic and nonpoint-source pollution models: review of mathematical bases. *Transactions of the ASAE.* 46(6): 1553-1566.

Bosch, D., F. Theurer, R. Bingner, G. Felton, and I. Chaubey. 2001. Evaluation of the AnnAGNPS water quality model. In *Agricultural Non-Point Source Water Quality Models: Their Use and Application.* Southern Cooperative Series Bulletin No. 398. Available at:

http://www3.bae.ncsu.edu/Regional-Bulletins/Modeling-Bulletin/bosch-annagnps-bulletin-manuscript.html#529886. Accessed 28 August 2006.

Bosch, D.D., J.M. Sheridan, H.L. Batten, and J.G. Arnold. 2004. Evaluation of the SWAT model on a coastal plain agricultural watershed. *Transactions of the ASAE.* 47(5):1493-1506.

Boyd, D., A.F. Smith, and B. Veale. 2000. *Flood Management on the Grand River Basin.* Cambridge, ON: Grand River Conservation Authority.

Brooks, K.N., P.F. Ffolliott, H.M. Gregersen, and J.L. Thames. 1991. *Hydrology and the Management of Watersheds.* Ames, IA: Iowa State University Press.

Brun, S.E., and L.E. Band. 2000. Simulating runoff behavior in an urbanizing watershed. *Computers, Environment and Urban Systems.* 24(1): 5-22.

Carey, J.H., M.E. Fox, B.G. Brownlee, J.L. Metcalfe, P.D. Mason, and W.H. Yerex. 1983. *The Fate and Effects of Contaminant in Canagagigue Creek 1. Stream Ecology and Identification of Major Contaminants.* Environment Canada Scientific Series No. 135. Burlington, Ontario: Environment Canada, Inland Waters Directorate.

Chow, V.T, D.R. Maidment, and L.W. Mays. 1988. *Applied Hydrology*. New York: McGraw-Hill.

Christiaens, K., and J. Feyen. 2001. Analysis of uncertainties associated with different methods to determine soil hydraulic properties and their propagation in the distributed hydrological MIKE SHE model. *Journal of Hydrology*. 246(1-4): 63-81.

Chu,T.W., and A. Shirmohammadi. 2004. Evaluation of the SWAT model's hydrology component in the Piedmont physiographic region of Maryland. *Transactions of the ASAE*. (4):1057-1073.

Clarke R. 1993. *Water: The International Crisis*. Cambridge, MA: MIT Press.

Connolly, R.D., D.M. Silburn, and C.A.A. Ciesiolka. 1997. Distributed parameter hydrology model (ANSWERS) applied to a range of catchment scales using rainfall simulator data. III. Application to a spatially complex catchment. *Journal of Hydrology*. 193(1-4): 183-203.

Costantini, E.A.C., F. Castelli, S. Raimondi, and P. Lorenzoni. 2002. Assessing soil moisture regimes with traditional and new methods. *Soil Science Society of America Journal*. 66(6): 1889-1896.

D'Urso G., Dini L., Vuolo F., Alonso L., and Guanter L. 2004. Retrieval of leaf area index by inverting hyper-spectral, multi-angular Chris/Proba data from SPARC 2003. *Proc. of the 2nd CHRIS/Proba Workshop*, ESA/ESRIN, Frascati, Italy, 28-30 April (ESA SP-578, July 2004) Available at:

http://earth.esa.int/symposia/chris_proba_04/papers/15_durso.pdf#search=%22Retrieval%20Of%20Leaf%20Area%20Index%20By%20Inverting%20Hyper-Spectral%2C%20Multi-Angular%20Chris%22. Accessed 28 August 2006.

Das, S., R.P. Rudra, P.K. Goel, N. Gupta, and B. Gharabaghi. 2004. Application of AnnAGNPS model under Ontario conditions. ASAE/CSAE Paper No. 04-2256. St. Joseph, Mich: ASAE.

Deblonde, G., M. Penner, and A. Royer. 1994. Measuring leaf area index with the Li-COR LAI-2000 in pine stands. *Ecology*. 75(5): 1507-1511.

Demetriou, C., and J.F. Punthakey. 1999. Evaluating sustainable groundwater management options using the MIKE SHE integrated hydrogeological modelling package. *Environmental Modelling and Software*. 14(2): 129-140.

DHI. 2004. *MIKE SHE User Manual*. Hørsholm, Denmark: Danish Hydraulic Institute.

Dillaha, T.A., M.L. Wolfe, A. Shirmohammadi, and F.W. Byne. 2004. ANSWERS-2000. In *Agricultural Non-Point Source Water Quality Models: Their Use and Application*. Southern Cooperative Series Bulletin No. 398. Available at: http://www3.bae.ncsu.edu/Regional-Bulletins/Modeling-Bulletin/answers2k-draft0.html. Accessed 28 August 2006.

Dingman, S.L. 2002. *Physical Hydrology*. 2nd ed. Upper Saddle River, N.J.: Prentice Hall.

Donigian A.S. Jr., B.R. Bicknell, and J.C. Imhoff. 1995. Hydrological Simulation Program - Fortran (HSPF). In *Computer Models of Watershed Hydrology*, 395-442. V.P. Singh, ed. Highlands Ranch, CO: Water Resources Publications.

Doorenbos, J., and W.O. Pruitt. 1977. *Guidelines for predicting crop water requirements*. 2nd ed. FAO Irrigation and Drainage Paper 24. Rome: FAO

Du, B., J.G. Arnold, A. Saleh, and D.B. Jaynes. 2005. Development and application of SWAT to landscapes with tiles and potholes. *Transactions of the ASAE*. 48(3):1121-1133.

Duru, J.O., and Jr.A.T. Hjelmfelt. 1994. Investigating prediction capability of HEC-1 and KINEROS kinematic wave runoff models. *Journal of Hydrology*. 157(1-4): 87-103.

Engel, B., Kangwon, Z. Tang, L. Theller, and S. Muthukrishnan. 2004. *WHAT: Web-based Hydrograph Analysis Tool*. Available at:http://pasture.ecn.purdue.edu/~what/ Accessed 28 August 2006.

Engman, E.T. 1986. Roughness coefficients for routing surface runoff. *Journal of Irrigation and Drainage Engineering*. 112(1): 39-53.

Environment Canada (ENV CAN). 2005. *Climate Data for Canada*. Available at: http://climate.weatheroffice.ec.gc.ca/climateData/canada_e.html. Accessed 28 August 2006.

Evers, A.J.M., R.L. Elliott, and E.W. Stevens. 1998. Integrated decision making for reservoir, irrigation, and crop management. *Agricultural Systems*. 58(4): 529-554.

Feldman, A.D. 1995. HEC-1 Flood Hydrograph Package. In *Computer Models of Watershed Hydrology*, 119-150. V.P. Singh, ed. Highlands Ranch, CO: Water Resources Publications.

Franklin, J.F. 1992. Scientific basis for new perspectives in forests and streams. In *Watershed Management*, 25-72. R. J. Naiman, Springer-Verlag, New York.

Gebremeskel, S., R.P. Rudra, B. Gharabaghi, S. Das, A. Singh, H. Bai, and G. Jiang. 2005. Assessing the performance of various hydrological models in the Canadian Great Lakes Basin. In *Proc. Watershed management to meet water quality standards and emerging TMDL (Total Maximum Daily Load)*, 273-282, P.W. Gassmann, ed. ASAE Publication No. 701P0105. Atlanta, GA: ASAE.

Goel, P.K. 2003. Hyper-Spectral Remote Sensing for weed and nitrogen stress detection. PhD thesis. Sainte Anne-de-Bellevue, QC: McGill University, Department of Agricultural and Biosystems Engineering.

GRCA. 2003. Water Quality Issues. In *The Grand Watershed Report*. Cambridge, ON: Grand River Conservation Authority. Available at: http://www.grandriver.ca/WatershedReportCard/pdf/WSReport_Page6.pdf Accessed 28 August 2006.

GRCA. 2004. Water Quality Issues. In *The Grand Watershed Report*. Cambridge, ON: Grand River Conservation Authority. Available at:

http://www.grandriver.ca/WatershedReportCard/2004_Fall_Grand_Pg3.pdf; http://www.grandriver.ca/WatershedReportCard/2004_Fall_Grand_Pg4.pdf http://www.grandriver.ca/WatershedReportCard/2004_Fall_Grand_Pg5.pdf Accessed 28 August 2006.

GRCA. 1997. Description of current forests and wildlife. GRCA – State of the Watershed Report. Cambridge, ON: Grand River Conservation Authority. Available at: http://www.grandriver.ca/.

GRCA. 2005. River level and flow information. Grand River Conservation Authority. Available at: http://www.grandriver.ca/WaterData/flowmaps/can_500.gif. Accessed October 2005.

Heatwole, C.D., K.L. Campbell, and A.B. Bottcher. 1987. Modified CREAMS hydrology model for coastal plain flatwoods. *Transactions of the ASAE* 30(4): 1014-1022.

Jaber, F.H., and S. Shukla. 2005. Hydrodynamic modelling approaches for agricultural storm water impoundments. *Journal of Irrigation and Drainage Engineering.* 131 (4): 307-315.

Jayatilaka, C.J, B. Storm, and L.B Mudgway. 1998. Simulation of water flow on irrigation bay scale with MIKE SHE. *Journal of Hydrology.* 208(2): 108-130.

Johnson, M.S, W.F. Coon, V.K. Mehta, T.S. Steenhuis, E.S. Brooks, and J. Boll. 2003. Application of two hydrologic models with different runoff mechanisms to a hillslope dominated watershed in the northeastern US: a comparison of HSPF and SMR. *Journal of Hydrology.* 284(1): 57-76.

Jong, R.D, and K.B. MacDonald. 2001. Water balance components in the Canadian mixed wood ecozone. In: *Sustaining the Global Farm. (10th International Soil Conservation Organization Conference*), 1144-1151. D.E. Stott, R.H. Mohtar, and G.C. Steinhardt, eds. West Lafayette, IN: International Soil Conservation Organization, USDA-ARS National Soil Erosion Research Laboratory, and Purdue University. Available at:

http://www.tucson.ars.ag.gov/isco/isco10/SustainingTheGlobalFarm/P255-DeJong.pdf#search=%22Water%20Balance%20Components%20In%20The%20Canadian%20Mixed%20Wood%20Ecozone%22 Accessed 28 August 2006.

Kang, M.S., S.W. Park, J.J. Lee, and K.H. Yoo. 2005. Applying SWAT for TMDL programs to a small watershed containing rice paddy fields. *Agricultural Water Management*. 79(10): 72-92.

Karakoc, G., F.U. Erkoc, and H. Katircioglu. 2003. Water quality and impacts of pollution sources for Eymir and Mogan lakes (Turkey). *Environment International*. 29(1): 21-27.

King, K.W., J.G. Arnold, and R.L. Bingner. 1999. Comparison of Green-Ampt and Curve Number methods on Goodwin Creek watershed using SWAT. *Transactions of the ASAE*. 42(4): 919-925.

Knisel, W.G., and J.R. Williams. 1995. Hydrology Components of CREAMS and GLEAMS Models. In *Computer Models of Watershed Hydrology*, 1069-1114. V.P. Singh, ed. Highlands Ranch, CO: Water Resources Publications.

Mishra, A., R. Singh, and N.S. Raghuwanshi. 2005. Development and application of an integrated optimization-simulation model for major irrigation projects. *Journal of Irrigation and Drainage Engineering*. 131(6): 504-513.

Muttiah, R.S., and R.A. Wurbs. 2002. Scale-dependent soil and climate variability effects on watershed water balance of the SWAT model. *Journal of Hydrology*. 256(3/4): 264-285.

Parsons, J.E., D.L. Thomas, and R.L. Huffman. 2004. Model Summary Tables. Southern Cooperative Series Bulletin No. 398. Available at:

http://www3.bae.ncsu.edu/Regional-Bulletins/Modeling-Bulletin/ModelSummaryTables.html. Accessed 28 August 2006.

Punthakey J.F., R. Cooke, N.M. Somaratne, R.S. Carr, and K.K. Watson. 1993. Large-scale catchment simulation using the MIKE-SHE model: 2. Modelling the Berrigin irrigation district. In: *Environmental Management Geo-water and Engineering Aspects: Proceedings of the International Conference on Environmental Geo-water and Engineering Aspects*, 467-472. Robin N. Chowdhury, S.M. Sivakumar, eds. Leiden, The Netherlands: A.A. Balkema

Refsgaard, J.C, and B. Storm. 1995. MIKE SHE. In *Computer Models of Watershed Hydrology*, 809-846. V.P. Singh, ed. Highlands Ranch, CO: Water Resources Publications.

Rogers, G.O, and B.B. DeFee. 2005. Long-term impact of development on a watershed: early indicators of future problems. *Landscape and Urban Planning*. 73(2-3): 215-233.

Rudra, R.P., W.T. Dickinson, and G.J. Wall. 1985. Application of the CREAMS model in southern Ontario conditions. *Transactions of the ASAE*. 28 (4): 1233-1240.

Sahoo, G.B, C. Ray, and E.H. De Carlo. 2006. Calibration and validation of a physically distributed hydrological model, MIKE SHE, to predict streamflow at high frequency in a flashy mountainous Hawaii stream. *Journal of Contaminant Hydrology*. In Press.

Scholberg, J., B.L. McNeal, J.W. Jones, K.J. Boote, C.D. Stanley, and T.A. Obreza. 2000. Growth and canopy characteristics of field-grown tomato. *Agronomy Journal*. 92(1): 152-159.

Schwab, G.O, D.D. Fangmeier, W.J. Elliot, and R.K. Frevert. 1993. *Soil and Water Conservation Engineering*. 4th ed. New York: Wiley.

Shrestha, S., M.S. Babel, A.D. Gupta, and F. Kazama. 2005. Evaluation of annualized agricultural nonpoint source model for a watershed in the Siwalik Hills of Nepal. *Environmental Modelling and Software*. 21(7): 961-975.

Singh, R., J.C. Refsgaard, L. Yde, G.H. Jorgensen, and M. Thorsen. 1997. Hydraulic-hydrological simulations of canal-command for irrigation water management. *Irrigation and Drainage Systems*. 11(3): 185-213.

Singh, R., K. Subramanian, and J.C. Refsgaard. 1999. Hydrological modelling of a small watershed using MIKE SHE for irrigation planning. *Agricultural Water Management*. 41(3): 149-166.

Singh,V.P. 1995. *Computer Models of Watershed Hydrology*. Rev. ed. Highlands Ranch, CO: Water Resources Publications.

Sorooshian, S., and V.K. Gupta. 1995. Model Calibration. In *Computer Models of Watershed Hydrology*, 23-68. V.P Singh, ed. Highlands Ranch, CO: Water Resources Publications.

Spruill, C.A., S.R. Workman, and J.L. Taraba. 2000. Simulation of daily and monthly stream discharge from small watersheds using the SWAT model. *Transactions of the ASAE*. 43(6): 1431-1439.

Sui, J. 2005. Estimation of design flood hydrograph for an ungauged watershed. *Water Resources Management*. 19: 813-830.

Suttles, J.B., G. Vellidis, D.D. Bosch, R. Lowrance, J.M. Sheridan, and E.L. Usery. 2003. Watershed-scale simulation of sediment and nutrient loads in Georgia coastal plain streams using the annualized AGNPS model. *Transactions of the ASAE*. 46(5): 1325-1335.

Thompson, J.R., H.R. Sorenson, H. Gavin, and A. Refsgaard. 2004. Application of the coupled MIKE SHE/MIKE 11 modelling system to a lowland wet grassland in southeast England. *Journal of Hydrology*. 293(2): 151-179.

Vázquez, R.F. and J. Feyen. 2001. Effect of potential evapotranspiration estimates on the performance of the MIKE SHE code applied to a medium sized catchment. *ASAE/CSAE Paper No*. 01-2037. St. Joseph, Mich: ASAE.

Verhallen, A., and E. Roddy. 2003. *Irrigating Vegetable Crops*. Toronto, ON: Ontario Ministry of Agriculture, Food and Rural Affairs (OMAFRA). Available at: http://www.omafra.gov.on.ca/english/crops/facts/info_irrigation.htm. Accessed 28 August 2006.

Ward, A.D., and S.W. Trimble. 2004. *Environmental Hydrology*. Boca Raton, Fl.: Lewis Publishers.

Warren, V.Jr., and L.L. Gary. 2003. *Introduction to Hydrology*. 5th ed. Upper Saddle River, NJ: Prentice Hall.

Williams, J.R. 1995. The EPIC model. In *Computer Models of Watershed Hydrology*, 909-1000. V.P. Singh, ed. Highlands Ranch, CO: Water Resources Publications.

Young, R.A., C.A. Onstad, and D.D. Bosch. 1995. AGNPS: An agricultural nonpoint source model. In *Computer Models of Watershed Hydrology*, 1001-1020. V.P. Singh, ed. Highlands Ranch, CO: Water Resources Publications.

Yuan, Y., R.L. Bingner, and R.A. Rebich. 2001. Evaluation of AnnAGNPS on Mississippi Delta MSEA watersheds. *Transactions of the ASAE*. 44(5): 1183-1190.

Yuan, Y., R.L. Bingner, and R.A. Rebich. 2002. Application of AnnAGNPS for analysis of nitrogen loadings from a small agricultural watershed in the Mississippi Delta. Total maximum daily load (TMDL) environmental regulations, In *Proc. Watershed management to meet water quality standards and emerging TMDL (Total Maximum Daily Load)*, 268-279. P.W. Gassmann, ed. ASAE Publication No. 701P0102. Forth Worth, Texas, USA: ASAE.

Appendix A

Table A.1 Monthly Water Balance for Calibration Period (Hydrologic Year 1994-95 to 1997-98)

Water Year	PPT (mm)	ET (mm)	BF (mm)	Re (mm)	S_RO (mm)	O_RO (mm)
Oct	37, 107, 59, 55	21, 19, 11, 17	6, 7, 12, 9	0, 1, 2, 1	5, 8, 22, 13	5, 6, 16, 6
Nov	76, 144, 40, 64	5, 4, 3, 3	9, 12, 13, 11	1, 4, 2, 2	16, 50, 23, 27	6, 54, 19, 22
Dec	49, 45, 104, 43	2, 3, 2, 3	11, 12, 15, 12	2, 2, 4, 3	20, 18, 82, 23	13, 27, 67*, 8
Jan	114, 92, 89, 106	3, 3, 3, 4	14, 13, 15, 14	4, 3, 3, 3	71, 51, 39, 66	81, 16*, 54, 67
Feb	26, 55, 88, 32	8, 8, 12, 9	12, 13, 13, 12	1, 4, 3, 3	11, 77, 80, 44	8, 66*, 108, 26
Mar	51, 38, 112, 95	24, 21, 21, 26	14, 15, 17, 16	2, 3, 4, 4	48, 43, 113, 67	75, 52, 119, 83
Apr	90, 131, 26, 54	38, 37, 51, 55	13, 15, 14, 13	2, 4, 1, 2	42, 71, 12, 22	47, 104, 48, 18
May	87, 107, 89, 40	81, 73, 72, 92	12, 15, 13, 7	3, 3, 2, 0	17, 59, 26, 2	19, 45, 34, 8
Jun	64, 128, 72, 75	96, 82, 93, 92	8, 13, 8, 4	1, 3, 0, 0	5, 47, 6, 0	11, 35, 6, 4
Jul	73, 92, 66, 30	126, 130, 114, 109	6, 6, 6, 4	0, 0, 0, 0	4, 2, 2, 1	6, 6, 7, 4
Aug	112, 43, 85, 40	130, 116, 98, 120	5, 4, 5, 2	1, 0, 0, 0	6, 1, 2, 0	7, 5, 5, 4
Sep	33, 155, 78, 43	84, 64, 64, 71	3, 7, 6, 2	0, 1, 0, 0	0, 15, 6, 0	5, 24, 7, 4

In each cell's four values are for the years 1994-95, 1995-96, 1996-97, 1997-98, respectively; * - missing observed runoff data

Table A.2 Monthly Water Balance for Validation Period (Hydrologic Year 1990-91 to 1993-94)

Water Year	PPT (mm)	ET (mm)	BF (mm)	Re (mm)	S_RO (mm)	O_RO (mm)
Oct	109, 64, 68, 71	10, 25, 8, 17	12, 6, 13, 9	3, 1, 5, 2	29, 6, 49, 15	48, 6, 17*, 10*
Nov	87, 62, 158, 64	4, 4, 3, 3	14, 8, 16, 10	5, 1, 7, 3	50, 13, 122, 28	49, 5, 74*, 17
Dec	129, 49, 74, 36	3, 2, 2, 2	16, 11, 16, 12	6, 2, 5, 3	88, 18, 50, 23	70, 21, 25*, 18
Jan	48, 48, 107, 82	4, 3, 5, 3	16, 11, 18, 11	4, 2, 5, 2	27, 20, 71, 9	14, 35*, 79, 10
Feb	39, 33, 32, 39	8, 8, 7, 7	15, 10, 13, 10	5, 2, 2, 2	54, 15, 12, 23	31, 10, 12, 43
Mar	112, 34, 39, 60	22, 25, 18, 18	18, 12, 14, 12	6, 3, 3, 4	90, 38, 67, 55	135, 41, 82, 56
Apr	132, 117, 83, 112	42, 46, 47, 52	19, 13, 17, 15	6, 4, 5, 6	92, 53, 52, 91	86*, 47*, 65, 92
May	68, 63, 42, 115	76, 93, 76, 70	15, 10, 12, 15	2, 1, 1, 5	13, 8, 4, 42	10, 34, 8, 27
Jun	35, 51, 79, 71	107, 104, 94, 93	10, 6, 9, 11	0, 0, 1, 1	3, 1, 7, 10	8, 6, 23, 8
Jul	183, 158, 112, 83	133, 100, 117, 126	9, 8, 8, 8	3, 1, 1, 0	14, 10, 6, 3	14, 9, 15, 8*
Aug	48, 138, 46, 73	127, 108, 125, 115	8, 11, 6, 7	0, 3, 0, 0	3, 21, 0, 3	5, 65, 4, 5
Sep	42, 115, 87, 31	86, 64, 58, 86	4, 11, 7, 4	0, 3, 1, 0	0, 33, 5, 0	5, 32*, 7, 6

In each cell's four values are for years 1990-91, 1991-92, 1992-93, 1993-94, respectively; * - missing observed data

Table A.3 Seasonal Runoff, Actual Evapotranspiration, Baseflow and Recharge for all Scenarios

Scenarios	Runoff (mm)				Actual Evapotranspiration (mm)			
	Winter	Spring	Summer	Fall	Winter	Spring	Summer	Fall
Baseline	186, 311, 197	129, 40, 24	51, 11, 2	60, 46	35, 38, 41	111, 123, 148	330, 308, 322	79, 84
1	195, 315, 198	132, 38, 23	51, 10, 1	61, 46	37, 39, 43	113, 125, 148	329, 306, 320	81, 85
2	211, 331, 218	143, 42, 27	58, 13, 3	68, 58	24, 28, 30	100, 117, 141	324, 296, 311	71, 71
3	197, 316, 201	136, 39, 24	53, 10, 2	57, 46	34, 38, 41	107, 123, 147	332, 306, 321	82, 84
4	199, 317, 205	135, 41, 24	53, 11, 2	59, 49	35, 37, 40	110, 121, 145	324, 302, 316	86, 80
5	193, 265, 182	124, 75, 39	55, 16, 4	67, 46	35, 38, 41	110, 122, 141	327, 300, 312	79, 84
6	203, 283, 200	184, 70, 11	25, 10, 2	43, 38	35, 38, 41	112, 123, 148	329, 307, 318	79, 84
Scenarios	Baseflow (mm)				Recharge (mm)			
	Winter	Spring	Summer	Fall	Winter	Spring	Summer	Fall
Baseline	52, 61, 54	30, 29, 20	25, 20, 11	31, 26	12, 15, 13	7, 3, 2	4, 1, 1	5, 4
1	58, 62, 54	32, 28, 20	26, 19, 11	33, 26	12, 15, 12	7, 3, 2	4, 1, 1	5, 4
2	60, 64, 58	33, 29, 21	27, 21, 13	34, 29	12, 15, 13	7, 3, 2	4, 1, 1	5, 5
3	58, 62, 54	32, 28, 20	26, 19, 11	32, 26	12, 15, 13	7, 3, 2	4, 1, 1	5, 4
4	59, 62, 55	32, 28, 20	26, 19, 11	32, 27	12, 15, 13	7, 3, 2	4, 1, 1	5, 4
5	245, 295, 234	151, 102, 64	89, 45, 28	101, 77	76, 93, 74	39, 31, 24	32, 23, 16	38, 32
6	54, 61, 53	34, 29, 19	25, 21, 10	29, 25	12, 14, 12	8, 4, 1	2, 1, 1	4, 3

In each cell's three values are for wet, normal, and dry years, respectively

1: Urbanization; 2: Deforestation; 3: Conversion of Pasture to Mono-crop Agriculture; 4: Turning Conventional Agriculture into Cash Crops; 5: Application of Tile Drainage; 6: Climate Change

Table A.4 Comparison of Water Table Elevation in Urbanisation Scenario

Scenarios | Year	Oct 1995	Oct 1996	Oct 1997	Oct 1998
Baseline (m)	370.85	372.00	371.10	370.30
Urbanisation (m)	371.30	372.80	371.88	370.33

Appendix B

B.1 Data Preparation for MIKE SHE

i. Shape Format File

All the shape files imported directly into MIKE SHE (the land use, soil and study area boundary polygons) or converted into other format (dfs, such as Mannings' M, paved runoff coefficient, geological unit distribution) had to be defined initially by the coordinate system specific for that region. This was done in ArcToolbox, in the Data Management Tools/Projections/Define Projection Wizard (shapefiles, geodatabase). The coordinate system used is WGS 1984 UTM zone 17 N.

ii. Topography

The original elevation data (digital elevation model - DEM), was converted into a point shape file using ArcGIS 8.2. The DEM file had a resolution of 100 × 100 m. The DEM is imported into ArcMap. Regular points at a spacing of 100 × 100 m were generated in Analysis tools/Generate Regular Points. These generated points were converted into a 3-dimensional array using 3D Analyst/convert/Features to 3D. Finally, the DEM elevation attributes were assigned to the 3D point shape file using XToolsPro/Table Operations/Add x, y, z coordinates.

iii. Soil and land use

The soil and land use maps were already available in polygon shape format for the entire province of Ontario, and so were clipped to the specific study area, namely the upper portion of the Canagagigue creek watershed, using the Tools/Geoprocessing Wizard/clip on layer based on another.

iv. Mannings' M

Surface roughness coefficient, the reciprocal of Mannings' M, depends on land cover type. The land use polygon shape file was imported into ArcMap of ArcGIS 8.2. A new field was added in its attribute table using options/add field. The field type chosen

was long integer with precision 7. In the attribute table, the Mannings' M field was edited with values obtained from literature for each land use type. This Mannings' M polygon shape file was converted into MIKE SHE dfs format. In ArcGIS 8.2, the polygon shape file was converted into raster format using Spatial Analyst/convert/Features to Raster. The raster file obtained was then converted into ASCII format in ArcGIS 9.0 ArcToolbox using Conversion Tools/Raster to ASCII. Finally, this ASCII file was imported into MIKE Zero/MIKE Zero Toolbox, where it is converted into dfs format using GIS/Grd2Mike.

v. Paved Runoff Coefficient

This parameter was also dependent on land use types: paved/urban areas were assigned a value of 0.75 while other land use types were assigned a value of zero. The paved runoff coefficient is the fraction of the surface flow that is removed through the drainage network, where it goes directly to the specified boundary of the saturated zone drainage network (DHI, 2004). The Mannings' grid file (.dfs) was opened in MIKE SHE. The grids having values equal to 109.1 (paved/runoff land use) were selected in Tools/select/values and changed to 0.75 in Tools/Set value. This was repeated for the other land uses, where the values were changed to zero.

vi. Geological Unit Distribution

The geological unit distribution is a soil code that is dependent on soil types, which is distributed both over the watershed (horizontal) and along the soil profile (vertical). In the polygon soil shape file, new fields were added in the attribute table to edit the soil code assigned to each soil type for the geological layers. The soil profile was divided into four geological layers. Then the polygon shape file having the soil codes attribute was converted into raster format in ArcGIS 8.2, then to ASCII format in ArcGIS 9.0. Eventually, the ASCII file was converted into MIKE SHE grid format (dfs). The same procedure was applied as in the Mannings' M section (Appendix B).

B.2 MIKE SHE Model Set-up

i. Climate Data Files

The precipitation, air temperature, and reference evapotranspiration file were originally prepared in MS-Excel, consisting of two columns only (date and climate variable). These files are imported into MIKE SHE, where time series dfs files are created using the function create on the display dialog for each variable in MIKE SHE. Then, the created time series files are open and the unit are verified or changed accordingly in the edit/items function. The files names are Precipitation, Air Temperature, and Reference Evapotranspiration.

ii. Vegetation Property File

A new vegetation property file is opened using MIKE SHE/vegetation property file and the file is saved. All the vegetations to be considered in the study are entered in the file with all the following information: stage of growth, leaf area index at each stage, rooting depth at each stage, crop coefficient at each stage. In this study, irrigation was not considered and the default ET parameters were used. The file name was Vegetation.

iii. Unsaturated Zone Soil Properties

A new unsaturated zone soil property file was opened using the MIKE SHE/UZ soil property and the file was saved. The van Genuchten methods were used for both the retention curve and hydraulic conductivity functions. One file was created for each soil series, where that file had the information of all the layers for that particular series. In all, there were 9 UZ soil property files. For each file, information about the saturated soil moisture content, residual soil moisture content, saturated hydraulic conductivity, alpha, n, and l parameters were entered for each layer of that soil series. These van Genuchten soil parameters were obtained from the Rosetta model.

These data were entered directly into MIKE SHE/Unsaturated zone for each soil polygon (one polygon representing a soil series). Thus, for each soil polygon, all the soil existing layers were entered. In addition to the van Genuchten parameters entered via the unsaturated zone soil properties files, the depth of each soil layer was required.

iv. Saturated Zone Geologic Properties

The soil properties (horizontal and vertical saturated hydraulic conductivities, specific yield, specific storage coefficient, and porosity) were required for all the soil layer of all the soil series. In this study, the vertical and horizontal saturated hydraulic conductivities were assumed to be equal. Porosity is considered equivalent to the saturated soil moisture content. The specific yield and specific storage coefficients were obtained from literature.